

DISSERTATION

SUBMITTED TO THE
COMBINED FACULTY OF NATURAL SCIENCES AND MATHEMATICS
OF HEIDELBERG UNIVERSITY, GERMANY
FOR THE DEGREE OF
DOCTOR OF NATURAL SCIENCES

PUT FORWARD BY
FELIX ARJUN KUHN
BORN IN OCHSENHAUSEN

ORAL EXAMINATION: 14 APRIL 2021

UNDERSTANDING COSMIC STRUCTURE
A NEW PREDICTION FOR THE GRAVITATIONAL
LENSING POWER SPECTRUM

REFEREES: MATTHIAS BARTELMANN
 BJÖRN MALTE SCHÄFER

Felix Arjun Kuhn : *Understanding cosmic structure*
A new prediction for the gravitational lensing power spectrum , PhD
Thesis , in die festo Don Ioannis Bosco, 2021

*So hilf uns, Gott, zu dieser Frist,
weil unsre Weisheit Einfalt ist.*

Heinrich der Vogler; König, Bass
(R. Wagner: Lohengrin)

ABSTRACT

The nonlinear evolution of large scale structure has long been poorly understood as it has not been possible to thoroughly describe the physics of the underlying processes by means of theoretical physics until recent years.

This lack of understanding not only has hampered progress in the understanding of cosmic history but also of the constituents of the universe as most of them are of a still unknown nature and cannot be observed directly.

We calculate a new theoretical and model-independent prediction for the weak lensing power spectrum using both model-independent cosmology, a newly invented method to circumvent the need of a cosmological model, as well as Kinetic Field Theory, a recent technique to analytically describe the nonlinear stages of structure formation.

Thus, by adding a nearly parameter-free prediction of the central statistical quantity of gravitational lensing – a well established method to analyse the distribution of cosmic matter density – to the framework of Kinetic Field Theory we provide another possibility in order to verify, calibrate and improve the successful analytic approach to nonlinear cosmic structure formation.

ZUSAMMENFASSUNG

Die Entwicklung großer kosmischer Strukturen ließ sich lange Zeit unter anderem deshalb nicht vollständig durchdringen, weil die Analyse dieser nichtlinearen Prozesse mit Mitteln der theoretischen Physik erst in den letzten Jahren durch die Entwicklung mathematisch konsistenter Theorien möglich wurde.

Dieses fehlende Verständnis von kosmischer Strukturbildung hemmte nicht nur die Erforschung der Geschichte des Universums, sondern auch die der verschiedenen, größtenteils unbekannt, Formen von Materie und Energie, die zwar das Universum in seiner heutigen Zusammensetzung dominieren, sich jedoch nicht direkt beobachten lassen.

In dieser Arbeit berechnen wir eine neue, theoretische und modellunabhängige Vorhersage für das Leistungsspektrum des Gravitationslinseneffekts, mit dem sich auch die unbekannte Materieform indirekt beobachten lässt. Hierzu nutzen wir sowohl modellunabhängige Kosmologie, eine jüngst eingeführte Methode, mit der sich ein großer Teil physikalischer Annahmen über das Universum ersetzen lässt, als auch die Kinetische Feldtheorie, mit welcher man die nichtlineare Entwicklung kosmischer Strukturen analytisch beschreiben kann.

Indem wir die zentrale, statistische Größe des Gravitationslinseneffekts mit Hilfe dieser Theorien neu und nahezu parameterfrei berechnen, fügen wir dem breiten Spektrum möglicher Anwendungen der Kinetischen Feldtheorie eine weitere hinzu. Damit soll es in Zukunft möglich sein, die erfolgreiche Theorie mithilfe von Daten aus neuen Durchmusterungen zu verifizieren, zu kalibrieren und zu verbessern, um schließlich auch die Strukturbildung im nichtlinearen Bereich vollständig erfassen und begreifen zu können.

ABSTRACTUM

Vastae structurae universi quomodo non lineariter evolutae sint, diu percognita non erat, cum processus huius rei physice, si theoretica physice uteris, describi non poterant usque ad exitum decenni exacti.

Qua ignorantia impedimur, quominus complectamur cum historiam universi, tum omnia, ex quibus universum constitutum est, quia plurimarum partium naturam nondum perspicimus neque ea ipsas observare possumus.

Fecimus novam theoreticam neque ab exemplis pendentem praedictionem spectri potentiae lentium lenium utentes et nuper inventa via, qua exempla aliter necessaria evitari possunt, cosmologiae non ab exemplis pendentis et theoria camporum cineticorum, qua via nova mathematice describuntur gradus formationis structurarum.

Cum addamus compagi theoriae camporum cineticorum praedictionem quantitatis statisticae summae lentium gravitationis minimis exemplaribus utentes— via consuetissima, qua, quomodo massa in universe distributa sit, investigatur —, providemus aliam facultatem probandi, adaequandi, meliorem faciendi adiutum analyticum, quo ad formationem non linearem structurae universi adire possumus.

CONTENTS

INTRODUCTION	1
I COSMOLOGY	
1 COSMOLOGICAL FOUNDATIONS	7
1.1 The Cosmological Principle	7
1.2 Describing the Dynamics of the Universe	7
1.3 Einstein’s Field Equations	8
1.4 The Mass Density ρ	11
1.5 Redshift	13
1.6 Cosmic Distances	14
2 COSMIC STRUCTURE	19
2.1 Linear Structure Formation	20
2.2 The Linear Growth Function D_+	22
2.3 Statistical Measures of Density Fluctuations	24
3 GRAVITATIONAL LENSING	27
3.1 Jacobi Equation	28
3.2 The Tidal Matrix	29
3.3 Lensing Potential and Lensing Equation	33
3.4 Cosmic Shear and Convergence	34
3.5 The Weak Lensing Power Spectrum	37
3.6 Measurement and Uncertainty	40
4 MODEL INDEPENDENT COSMOLOGY	43
4.1 Deriving the Expansion Function $E(a)$	44
4.2 The Linear Growth Function $D_+(a)$	46
4.3 Results from Haude et al. [21]	48
5 KINETIC FIELD THEORY	53
5.1 The Generating Functional	53
5.2 Equations of Motion	55
5.3 Density	56
5.4 Cosmological Applications	58
5.5 Initial Probability Distribution	60
5.6 Simplifying Z_0	61
5.7 The Factorised $Z_0[\mathbf{L}]$	63
5.8 The KFT Matter Density Fluctuation Power Spectrum	64
5.9 A Note on Interactions	65

II WEAK LENSING POWER SPECTRA	
6	THE PARAMETER-FREE WEAK LENSING POWER SPECTRUM 71
6.1	Analysing the Ingredients with Schmidt and Bartelmann [38] 72
6.2	A New P_δ for the Lensing Power Spectrum 77
6.3	A Model-Independent weak lensing spectrum 81
7	INTERMISSION: OBSERVING C_ℓ 87
7.1	From Observations to Shear Data 87
7.2	From Real-Space Shear to the Lensing Power Spectrum 88
8	UNCERTAINTIES 93
8.1	A Naive Approach to the Variance 93
8.2	A 4th-Order Correlator with KFT 94
8.3	Finding an Approximation 98
	CONCLUSION 103
	ACKNOWLEDGEMENTS 105
	BIBLIOGRAPHY 107

INTRODUCTION

Throughout history the search for the origin of the world has been one of the central questions of humanity. Scientists of all disciplines ranging from astronomy to theology and philosophy provided different perspectives to the debate.

As our knowledge of the cosmos evolved, we developed not only a clearly defined vocabulary, classifying different objects in space, made observable by modern techniques, but were also able to ask better and more precise questions. While the question *why* the universe came into existence at all, mostly remained with philosophers and theologians, physicists and astronomers started to develop theories in order to determine *how* the universe and its constituents evolved. The latter question then gave rise to the discipline of cosmology, which investigates the history of the universe and the nature and evolution of its components by applying fundamental laws of physics to the observable universe. Especially during the last century much progress was achieved by remarkable findings both in theory (the most influential, presumably, being the theory of general relativity in 1915 invented by [19]) and by observation (e.g. the heroic measurements of the cosmic microwave background of Penzias & Wilson in 1965) leading to the establishment of the so-called *standard model* of cosmology, which is able to explain most of the universe's history, beginning at the time shortly after the so-called *Big Bang*. In fact, the model, as improved and updated from day to day is able to plausibly explain the evolution of the universe and its characteristic features during different epochs.

Among those features are the universe's constituents, energy and matter in different manifestations, which are investigated in order to get linked to the standard model of particle physics, allowing for a connection of cosmology with a field of physics where actual experiments can be performed.

Although the modern standard model can explain most of the observed phenomena, there is still a number of unresolved questions in cosmology - one of them being the question of how structures (e.g. galaxies, galaxy clusters or the observed filaments forming the cosmic web) formed and evolved in the cosmos' history. Although the early stages of structure formation

are understood quite well, the understanding of the nonlinear evolution of structure has proven to be challenging.

This issue is addressed by the recently invented *Kinetic Field Theory*, which allows to investigate structure formation deep into the nonlinear domain of structure formation, making use of statistical methods invented for quantum field theory. This new method at hand, it is possible to calculate a closed, analytic form of the matter density power spectrum, the most central quantity for a statistical analysis of cosmic structure.

Apart from the investigation of cosmic structure with the means of theoretical and statistical physics the second, complementary part of cosmology was able to make remarkable progress with observational methods, contributing to our knowledge of the universe and its history. It is however still difficult to actually *measure* some of the central quantities. The density fluctuation power spectrum, for example, is typically measured with the help of biased tracers, e.g. bright galaxies. There is strong evidence for the existence of a form of matter which can *not* be observed directly. This so-called *dark matter* is actually assumed to account for more than 80% of the matter content of the universe. Therefore, the measurement of the matter density with the help of biased tracers cannot be a satisfactory state of measuring quantities like the power spectrum.

A well-established method to map the distribution of both dark and ordinary matter which we can directly observe arises from the theory of general relativity [19]. One of its consequences is an effect called *gravitational lensing* which describes the deflection of light by matter overdensities along the line of sight. A systematic analysis of those deviations allows to analyse the distribution of matter and to calculate a power spectrum for the gravitational lensing effect, a statistical correlator closely related to the density fluctuation power spectrum.

One of the improvements in theoretical cosmology was the invention of model-independent cosmology. This method allows to replace cosmological models which are needed to calculate, e.g. distances in the universe, with a set of functions which are based on observations only. As this allows to omit most of the assumptions on parameters and cosmic evolution this provides for better analyses of complex observables like the power spectrum.

In the scope of this thesis we will make use of both this method and the Kinetic Field Theory in order to predict a weak lensing power spectrum which relies on as little assumptions about the

universe and cosmological models as possible. This result will allow for a thorough analysis of structure formation theory, comparing the spectrum to spectra obtained from observations or numerical simulations and analysing the observed differences. In chapter 1 we introduce the basic principles of physical cosmology (1.1) describing the physics of the universe (1.2, 1.3) and the most important quantities (1.4, 1.5, 1.6) for our analysis.

In the next chapter, we discuss the physics of structure formation in the early universe starting with linear structure formation (2.1), introducing the linear growth function $D_+(a)$ (2.2) and the power spectrum, our way to discuss the statistics of matter density in the universe (2.3).

The following chapter presents the theory of gravitational lensing starting from the statements of general relativity 3.1. We investigate the lensing contributions by local overdensities (3.2) and introduce the fundamental quantities of gravitational lensing (3.3,3.4) as well as a statistical measure of the lensing effect (3.5, 3.6).

We discuss a novel method of deriving two essential functions describing the evolution of the cosmos (4.1) and structures therein (4.2) only with observational methods and with as little assumptions as possible in chapter 4. We compare those functions to their counterparts in classically modelled cosmologies (4.3).

Chapter 5 discusses the Kinetic Field Theory, a recently introduced technique to derive a cosmic density power spectrum with path integral methods, starting from an initial power spectrum. There, we introduce the fundamental quantity, a generating functional (5.1), discuss the physical operators and equations needed (5.11, 5.3) and continue to apply the general theory to cosmology (5.4-5.7) in order to derive a matter density power spectrum (5.8).

We present our own results in chapter 6, where we use the tools discussed so far in order to derive the model-independent weak lensing spectrum (6.3). We continue with a short discussion on how to actually derive a weak lensing power spectrum from observations in chapter 7 and discuss our approach to calculate an analytic form for the weak lensing spectrum uncertainty in 8 as well as our approximation (8.3).

We finally conclude our analysis in the last chapter discussing our findings and outlining future tasks which are needed to improve our results.

Part I

COSMOLOGY

COSMOLOGICAL FOUNDATIONS

Cosmology is the science of describing the history and the evolution of the universe (from ancient greek $\delta\ \kappa\acute{o}\sigma\mu\omicron\varsigma$ = order, world; $\delta\ \lambda\acute{o}\gamma\omicron\varsigma$ = law, rule). To describe the fundamentals of cosmology as a discipline of physics (while the subject is studied by philosophers and theologians as well) we will introduce the fundamental assumptions of cosmology as well as a very brief overview of today's knowledge about the physics of the universe.

1.1 THE COSMOLOGICAL PRINCIPLE

The most important assumption in cosmology is called the *cosmological principle*, stating

- i) that we are at no preferred position in space compared to another observer, meaning that someone at a far distant place in another part of the universe, must, considering large scales, observe structures very similar to the structure we observe,
- ii) and *isotropy*: the structure of matter distribution of the universe looks approximately the same, independently of the direction the observer is looking in.

Both principles combined imply *spatial homogeneity*, meaning that the universe as observed today is approximately a spatially homogeneous system if considered at large scales.

1.2 DESCRIBING THE DYNAMICS OF THE UNIVERSE

For the description of the laws of physics in the large-scale universe where gravity is the dominating force we use the theory of General Relativity which was first presented by [19]. In our presentation of this theory, we describe spacetime as $(3 + 1)$ -dimensional manifold, equipped with a metric tensor g with components $g_{\mu\nu}$.

The differential line element to measure a distance between

two *events*, i.e. two different coordinate tuples in space-time, is defined as:

$$ds^2 = g_{\mu\nu} dx^\mu dx^\nu, \quad (1.1)$$

with $dx^{\mu,\nu}$ being the coordinate differences. We furthermore introduce the scalar product of two vectors x, y :

$$x_\mu y^\mu = \langle x, y \rangle = g_{\mu\nu} x^\nu y^\mu. \quad (1.2)$$

In both equations we already used the Einstein convention, which we will continue to use for the rest of the chapter unless stated otherwise:

$$g_{\mu\nu} a^\nu b^\mu := \sum_{\mu,\nu=0}^3 g_{\mu\nu} a^\nu b^\mu, \quad (1.3)$$

i.e. we drop the summation sign Σ and imply summation over indices which are repeated on different levels (i.e. on the sub- and superscript-level). Furthermore, we state that greek letter indices imply summation over four-dimensional spacetime, whereas latin letter indices,

$$g_{ij} a^i b^j := \sum_{i,j=1}^3 g_{ij} a^i b^j, \quad (1.4)$$

imply the summation over spatial dimensions only. Moreover, we silently made use of the metric tensor's property of converting vectors to 1-forms and vice versa:

$$x^\mu = g^{\mu\nu} x_\nu, \quad (1.5)$$

$$x_\mu = g_{\mu\nu} x^\nu. \quad (1.6)$$

Due to the notation convention chosen here, this is also referred to as *raising* and *lowering* indices.

1.3 EINSTEIN'S FIELD EQUATIONS

The perhaps most important conclusion from Einstein's theory of general relativity is the equivalence of the geometry of the universe described as a function of the metric $g_{\mu\nu}$ to the content (both matter and energy) of the same:

$$G_{\mu\nu} = \frac{8\pi G}{c^4} T_{\mu\nu}, \quad (1.7)$$

where we introduce the Einstein tensor:

$$G_{\mu\nu} = R_{\mu\nu} - \frac{1}{2} R g_{\mu\nu}, \quad (1.8)$$

and the stress-energy tensor $T_{\mu\nu}$ which we will specify for certain cases later on. In general terms, $T_{\mu\nu}$ describes the matter and energy-content of the considered system. The Ricci tensor $R_{\mu\nu}$ is a contraction of the Riemann tensor

$$R_{\mu\nu} := R^{\lambda}{}_{\mu\lambda\nu}, \quad (1.9)$$

which itself, characterising the curvature, is defined as a mapping of three vector fields into another vector field $R : V \times V \times V \rightarrow V$ in a way that [e.g. 45, eq. 15.27]:

$$R(X, Y)Z = \nabla_X(\nabla_Y Z) - \nabla_Y(\nabla_X Z) - \nabla_{[X, Y]}Z. \quad (1.10)$$

1.3.1 A Possible Solution: The FLRW Metric

In order to simplify Einstein's field equations (1.7) one applies the cosmological principle (section 1.1) to the metric. As $g_{\mu\nu}$ is required to be symmetric, $g_{\mu\nu} = g_{\nu\mu}$, only ten of its 4×4 elements can be independent. We can then further reduce the number of independent elements by:

- i) considering the coordinates of freely falling observers called *comoving coordinates*. In their frames, the spatial coordinates are $dx^i = 0$, implying:

$$ds^2 = g_{00}dt^2 = -c^2dt^2. \quad (1.11)$$

- ii) If it is not possible to synchronise clocks in a way that $g_{0i} = 0$, a preferred direction in space would arise from that nonvanishing three-vector. This would violate isotropy. Thus, g_{0i} must vanish:

$$g_{0i} = 0, \quad (1.12)$$

in order to introduce coordinates that are time-orthogonal.

This transforms the line element into:

$$ds^2 = -c^2dt^2 + g_{ij}dx^i dx^j. \quad (1.13)$$

The possibility to write the line element like this in fact separates space and time, allowing to foliate spacetime into hypersurfaces of the four-dimensional manifold which are, at constant time, of spatial nature. Allowing the spatial part of the metric to be scaled with time we write:

$$ds^2 = -cdt^2 + a^2(t)dl^2. \quad (1.14)$$

Demanding isotropy, i.e., spherical symmetry in the spatial line element dl^2 , we can transform this part of the metric to spherical polar coordinates (w, θ, ϕ) :

$$dl^2 = dw^2 + f_K^2(w) \left[d\theta^2 + \sin^2 d\phi^2 \right]. \quad (1.15)$$

$f_K(w)$ is called *comoving angular diameter distance* and depends on the curvature parameter K :

$$f_K(w) = \begin{cases} \sin(K^{1/2}w) K^{-1/2} & (K > 0) \\ w & (K = 0) \\ \sinh(|K|^{1/2}w) |K|^{-1/2} & (K < 0). \end{cases} \quad (1.16)$$

By combining all information we arrive at the Friedmann-Lemaître-Robertson-Walker (FLRW) metric:

$$ds^2 = -cdt^2 + a(t) \left[dw^2 + f_K^2(w) d\Omega^2 \right]. \quad (1.17)$$

This is the metric describing a spatially homogeneous and isotropic universe. By using this metric we can now compute the components of the Einstein tensor $G_{\mu\nu}$ on the basis of eq. 1.8. The components of the stress-energy tensor T are set to

$$T^{\mu\nu} = (\rho c^2 + p)u^\mu u^\nu + pg^{\mu\nu}, \quad (1.18)$$

which corresponds to the tensor of an ideal fluid with mass density ρ and pressure p as seen by an observer who looks at an isotropic surrounding on his spatial hypersurface. Putting everything together in the field equations then leads us to the two differential equations describing the dynamics of the so-called scale factor $a(t)$, introduced for the first time in 1.14. These are the *Friedmann equations*:

$$\left(\frac{\dot{a}}{a} \right)^2 = \frac{8\pi G}{3} \rho + \frac{\Lambda c^2}{3} - \frac{Kc^2}{a^2}, \quad (1.19)$$

$$\frac{\ddot{a}}{a} = -\frac{4\pi G}{3} \left(\rho + \frac{3p}{c^2} \right) + \frac{\Lambda c^2}{3}. \quad (1.20)$$

The \dot{a} refers to the scale factor's time derivative, Λ describes a cosmological constant which is usually related to the so-called *dark energy* introduced to describe the observed acceleration of the cosmic expansion. For the remainder of this chapter, we normalise the scale factor $a(t)$ with $a_0 := a(t_0) = 1$ first, unless stated otherwise. We furthermore define the *Hubble parameter*:

$$H(t) := \frac{\dot{a}}{a} =: h(t) \cdot 100 \frac{km}{s \cdot Mpc}. \quad (1.21)$$

The measured values for the current value H_0 range from ~ 67 to $\sim 77 \frac{\text{km}}{\text{s}\cdot\text{Mpc}}$ [e.g. 26, 29, 34, 37]. We will in the scope of this thesis mainly adapt a current-day value for h of $h_0 = 0.7$. This Hubble parameter automatically provides us with a time $t_H = H^{-1}$ and a length scale $l_H = ct_H$.

1.4 THE MASS DENSITY ρ

There are different elements contributing to the density parameter ρ in the Friedmann equation. Each of its constituents behaves differently during the universe's expansion. We relate energy density ρ and pressure p by the equation of state

$$p = wc^2\rho, \quad (1.22)$$

where w now is the specific equation-of-state parameter ($w = 0$ for non-relativistic matter; $w = \frac{1}{3}$ for relativistic matter and $w = -1$ for a cosmological constant). One can now combine both Friedmann equations 1.19 and 1.20 and obtain a conservation equation for the energy density:

$$\dot{\rho} + \frac{\dot{a}}{a} \left(3\rho + \frac{p}{c^2} \right) = 0. \quad (1.23)$$

Plugging in the equations of state for different types of matter leads to:

$$\begin{aligned} \rho_m &\propto a^{-3}, \\ \rho_r &\propto a^{-4}, \\ \rho_\Lambda &\propto \text{const.}, \\ \rho_K &\propto a^{-2}, \end{aligned}$$

where for the first time we used the scale parameter as a parameter of cosmic evolution instead of time. We further define a *critical density*:

$$\rho_{\text{crit}} = \frac{3H^2}{8\pi G}, \quad (1.24)$$

which is defined as *critical closure parameter* [28, p. 116], meaning this parameter is equal to the total matter density of the universe, if and only if the universe is spatially flat. We indeed assume this flatness ($K = 0$) for the universe today. The critical density then gives rise to the important *density parameters*:

$$\Omega_i := \frac{\rho_i}{\rho_{\text{crit}}} \quad (i = m, r, \Lambda, K). \quad (1.25)$$

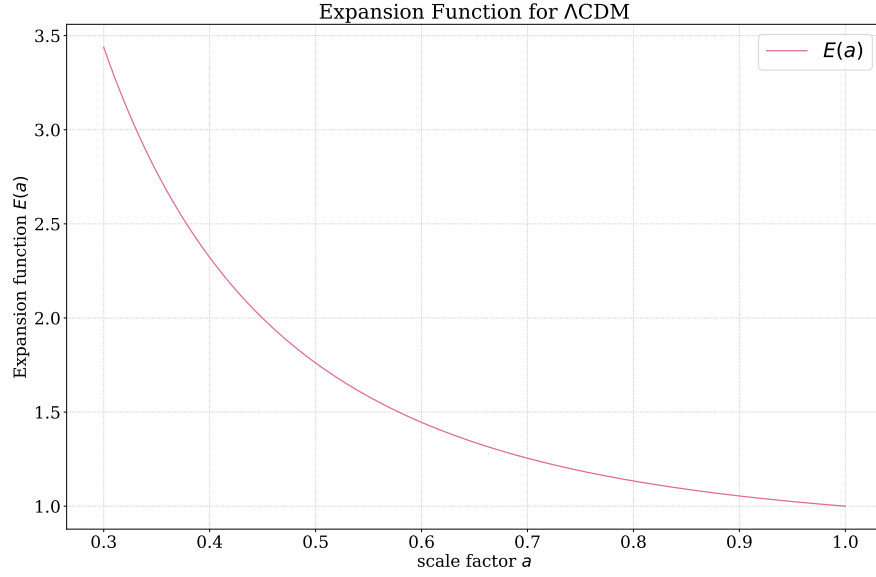


Figure 1.1: Expansion function for a Λ CDM cosmology (cf. eq. 1.27) with density parameters $\Omega_{m0} = 0.3, \Omega_{\Lambda0} = 0.7, \Omega_{b0} = 0.04$ and Hubble factor $h = 0.7$ as described in eq. 1.27. In order to provide an expression for the expansion function $E(a)$ a specific cosmological model is needed. It is convenient to normalise this particular function to unity at present-day scale factor, $E(1) = 1$.

A present day value for ρ_{crit} is $\rho_{\text{crit},0} = 9.20 \cdot 10^{-30} \text{ g cm}^{-3}$ [e.g. 6], assuming $h_0 \approx 0.7$. It is convenient not to explicitly write down ρ_K and Ω_K but simply set $\Omega_K = 1 - \sum \Omega_i$ with Ω_i being all other density parameters.

By using these expressions the first Friedmann equation 1.19 can be abbreviated:

$$H^2(t) = H_0^2 \left(\Omega_{m0} a^{-3} + \Omega_{r0} a^{-4} + \Omega_{\Lambda0} + \Omega_{K0} a^{-2} \right). \quad (1.26)$$

By introducing the expansion function $E(a)$ one can further simplify and write:

$$H^2(a) =: H_0^2 E^2(a). \quad (1.27)$$

It is worth mentioning that this form of $E(a)$ is specific for the cosmological model we just discussed. We will discuss a more general approach for a definition of $E(a)$ in chapter 4. Nevertheless, we want to show the form of the expansion function $E(a)$ for a specific Λ CDM cosmology with $\Omega_{m0} = 0.3, \Omega_{\Lambda0} = 0.7, \Omega_{b0} = 0.04$ and Hubble factor $h = 0.7$ in Fig. 1.1.

1.5 REDSHIFT

In the next section, we introduce cosmic redshift as a measure of an object's velocity and relate it to cosmic expansion. We consider a photon moving in radial direction in the expanding universe. The FLRW metric (eq. 1.17) then implies together with $ds^2 = 0$:

$$cdt = -a(t)dw, \quad (1.28)$$

where without loss of generality we choose dt to be positive. It is furthermore worth mentioning that neglecting angular coordinates only corresponds to our choice of the coordinate system being centred at the observer. Since both the observer and the source of light are comoving in the coordinate frame considered we know the distance between the source (emitter e) and observer (o) to be constant:

$$w_{eo} = \int_{t_e}^{t_o} dw = \int_{t_e}^{t_o} dt \frac{c}{a(t)}. \quad (1.29)$$

As a direct consequence its time derivative vanishes:

$$\frac{dw_{eo}}{dt_o} = 0 = \frac{c}{a(t_o)} \frac{dt_o}{dt_e} - \frac{c}{a(t_e)}, \quad (1.30)$$

leading to:

$$\frac{dt_o}{dt_e} = \frac{a(t_o)}{a(t_e)}. \quad (1.31)$$

Fixing now $dt = \nu^{-1}$ to the periodic time of a light wave with frequency ν we get:

$$\frac{\nu_e}{\nu_o} = \frac{a(t_o)}{a(t_e)} = \frac{\lambda_o}{\lambda_e} = 1 + \frac{\lambda_o - \lambda_e}{\lambda_e} =: 1 + z, \quad (1.32)$$

where we added 0 in the penultimate step and defined the *redshift* of light z in the last step. By fixing $a_0 = 1$ and renaming $a_e =: a$ we get to the relation of redshift and scale factor:

$$a = \frac{1}{1 + z}, \quad (1.33)$$

$$z = \frac{1}{a} - 1. \quad (1.34)$$

These relations describe how light is redshifted (or inversely blueshifted) with the scale factor by which the universe expanded in between emission time and time of observation.

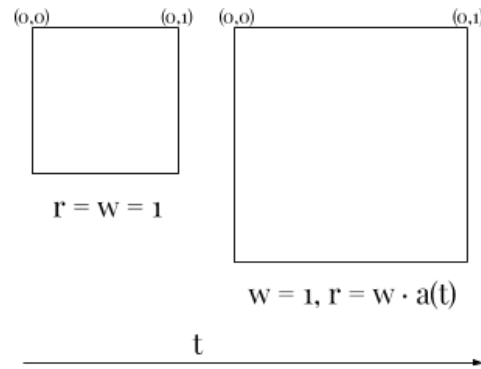


Figure 1.2: Comoving and physical distances. While the comoving distance w symbolised by the difference between grid points here stays constant the physical distance r between the grid points increases with the scale factor $a(t)$. Image scheme taken from [17].

1.6 COSMIC DISTANCES

Having discussed the redshift we now turn to distances. In this section, we introduce different measures of distance used in cosmology which will become important when discussing measurements later on. For the discussion of this subject we closely follow [17].

1.6.1 Comoving Distance

Although we already used the comoving distance without naming it in 1.29 we want to formally introduce this distance measure as well as explain its physical meaning.

Considering the universe's expansion characterised by the scale factor $a = a(t)$ one can picture space like a three-dimensional hypersurface with a grid (cf. Fig. 1.2). Whereas, the *physical distance* changes during expansion – the grid points' names, i.e. the coordinates, do *not*. This fact gives rise to *comoving* coordinates. While the physical distances, i.e. the distance between two points, increase with the cosmic expansion the comoving distance, e.g. the distance between the two points described in comoving coordinates, stays constant. While there are several interesting comoving distances we however want to introduce only one of them and refer to [28] for further examples. The co-

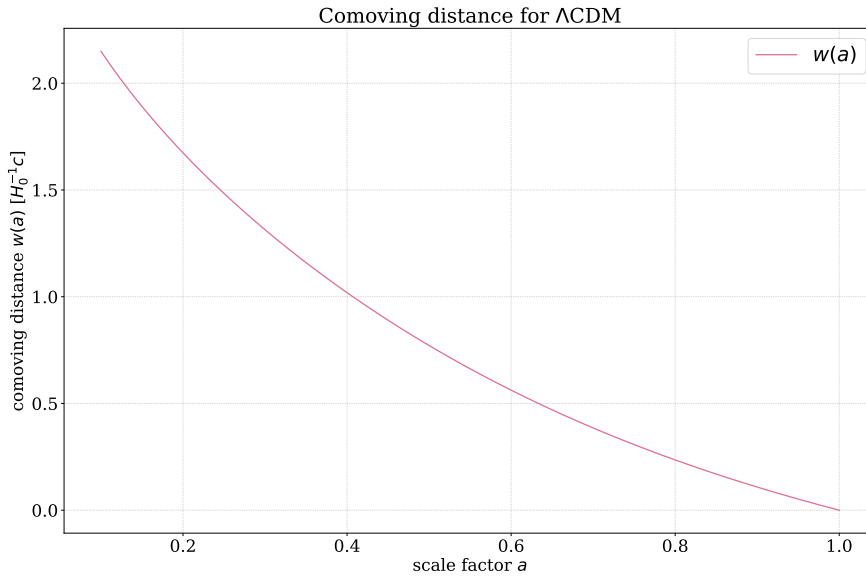


Figure 1.3: Comoving distance. The comoving distance as given in eq. 1.35 is shown as a function of scale factor a . The variable refers to the scale factor or time the signal was emitted, whereas the comoving distance then describes the distance between the source of emission and an observer at redshift $z = 0$ or scale factor $a = 1$. For $a = 1$ when the position of the source and the observer is the same the comoving distance vanishes. The earlier the signal was emitted, the farther away is the source due to cosmic expansion, measured in units of comoving distance.

moving distance between a distant light source and an observer is given by

$$w(a) = \int_{t(a)}^{t_0} \frac{dt}{a(t)} = \int_a^1 \frac{da'}{a'^2 H(a')}, \quad (1.35)$$

and illustrated in Fig. 1.3 as a function of the scale factor a .

1.6.2 Angular Diameter Distance

Another important distance measure is the angular diameter distance which is abbreviated by d_A and introduced as it is convenient in astronomy to measure angles θ of objects of known physical size l . In fact, measuring distances differently often proves impossible. Assuming small angles one can calculate

$$d_A = \frac{l}{\theta}. \quad (1.36)$$

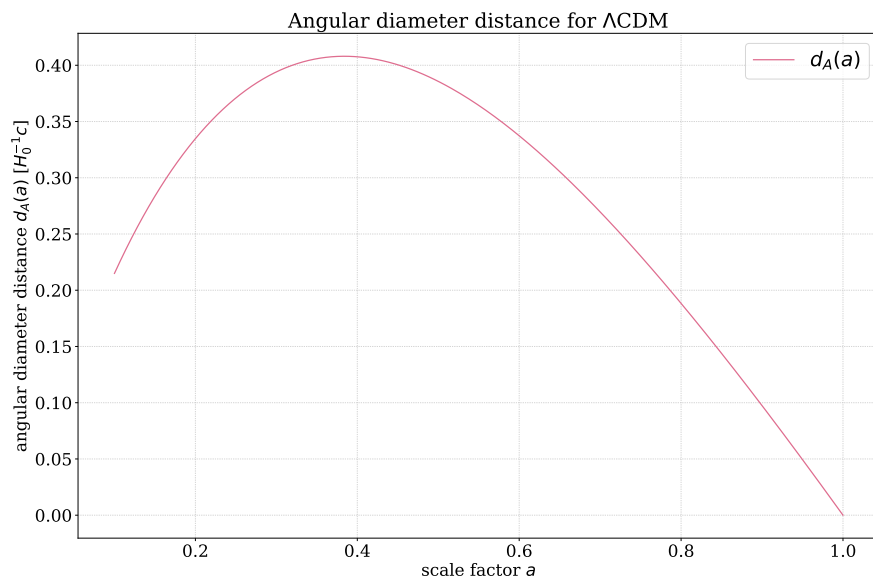


Figure 1.4: Angular diameter distance. The angular diameter distance as given in eq. 1.37 is shown as a function of scale factor a . The variable refers to the scale factor or time the signal was emitted, whereas d_A describes a distance between the source of emission and an observer at redshift $z = 0$ or scale factor $a = 1$. In a flat universe which we assume here objects at a smaller scale factor appear larger as they would at a higher scale factor. This effect can be explained by the interplay of the expansion of the universe and the finite speed of light.

As the comoving length of the object is given by $l_c = l/a$ and the comoving distance to the object considered is given by $w(a)$ we obtain the angle $\theta = (l/a)/w(a)$. This can then be used in order to obtain for a flat universe:

$$d_A^{flat} = aw(a) = \frac{w(a)}{1+z}. \quad (1.37)$$

We show an illustration of the angular diameter distance in Fig. 1.4.

1.6.3 Luminosity Distance

One can also measure the flux from an object whose luminosity is already known. An object at distance d and luminosity L gives rise to the observed flux:

$$F = \frac{L}{4\pi d^2}. \quad (1.38)$$

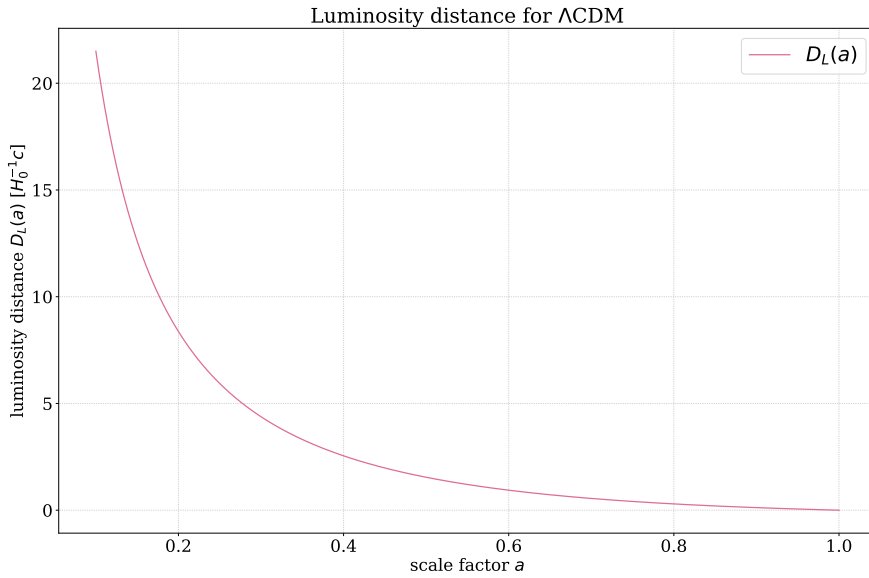


Figure 1.5: Luminosity distance. The luminosity distance as discussed in eq. 1.6.3 is shown as a function of scale factor a . The variable refers to the scale factor when the signal was emitted. The luminosity distance D_L describes the distance between the source of emission and an observer at redshift $z = 0$ or scale factor $a = 1$. For $a = 1$, when the position of the source and the observer is the same the comoving distance vanishes. The earlier the signal was emitted, the farther away is the source due to cosmic expansion.

If we do assume a static universe this flux is constant. Generalising, however, to a dynamic and expanding universe we find depending on the scale factor a that the flux is

$$F = \frac{L(w)}{4\pi w^2}, \quad (1.39)$$

where $L(w)$ is the luminosity through a sphere of comoving radius w . The energy per unit time passing the sphere at w will be reduced by a^{-2} due to redshift and space expansion. We therefore observe:

$$F = \frac{La^2}{4\pi w^2}, \quad (1.40)$$

and can still write the flux as before if we define $D_L = w/a$. We show the luminosity distance in Fig. 1.5. In all Figures illustrating the different distance measures (1.3, 1.4, 1.5) we used a flat Λ CDM cosmology with $\Omega_{m0} = 0.3, \Omega_{\Lambda 0} = 0.7, h = 0.7$ and $\Omega_{b0} = 0.04$.

COSMIC STRUCTURE

The first statement within the cosmological principle (1.1) is to notice that the distribution of matter in the universe is mainly homogeneous. Performing surveys in the neighbourhood of the Earth or simulating the evolution of the universe, however, we observe massive structures and find large voids in between the filament-like structured matter. It is therefore essential to recall that the principle of homogeneity only holds on sufficiently large scales.

In order to understand the evolution of those structures, in this chapter, we address the gravitational instability which cumulates mass on scales which are small compared to the Hubble radius. We operate in the expanding universe with a FLRW metric and introduce classical ways in order to investigate the formation of structures in the universe and their main complications which in turn lead to the development of a new theory of structure formation invented by [8, 10, 11].

In the description of this, we loosely follow [6, 17, 32] describing the evolution of matter within the frame of ideal fluid dynamics. We shall however stick to the conventions used in [6]. We recall that the concept of the ideal fluid implies that one assumes a negligible mean free path of the particles implying vanishing friction. Although this description is both easy and commonly used, it cannot be sufficient to describe the behaviour of dark matter not only because of the obvious limitations of the concept of an ideal fluid, but also because the concept implies and requires a unique velocity field assigning a unique velocity vector to every spatial point considered. With only weakly interacting (or non-interacting) dark matter, however, there can be multiple crossing streams and the concept cannot account for a sophisticated description of the evolution of dark matter structures. Nevertheless, it is a common and easy illustration of the evolution of cosmic structures in the linear regime.

2.1 LINEAR STRUCTURE FORMATION

The analysis of structure formation in the linear regime builds on the description of mass conservation in the *continuity equation*:

$$\dot{\rho} + \nabla \cdot (\rho \vec{v}) = 0, \quad (2.1)$$

the conservation of momenta in the *Euler equation*:

$$\dot{\vec{v}} + (\vec{v} \cdot \nabla) \vec{v} = \frac{-\nabla P}{\rho} - \nabla \Phi, \quad (2.2)$$

and the *Poisson equation* describing the Newtonian gravitational potential:

$$\nabla^2 \Phi = 4\pi G \rho. \quad (2.3)$$

Here, we introduced the mass density $\rho = \rho(\vec{r}, t)$ and a velocity field $\vec{v} = \vec{v}(\vec{r}, t)$. At this point, we describe all quantities in terms of the *physical* coordinates \vec{r} as opposed to comoving coordinates. The gradient of the pressure P exerts a force as well as the gradient of the gravitational potential Φ does.

The next step is to change into a comoving coordinate system and replace \vec{r} by:

$$\vec{x} = \vec{r}/a. \quad (2.4)$$

Calculating the derivative:

$$\vec{v} = \partial_t \vec{r} = \dot{a} \vec{x} + a \dot{\vec{x}}, \quad (2.5)$$

we notice that there are two components of the velocity. We name the first part:

$$\dot{a} \vec{x} = H \vec{r}, \quad (2.6)$$

the *Hubble velocity*, as it is the velocity caused by the expansion of the universe only. The latter part, $a \dot{\vec{x}} =: a \vec{u}$ is called *peculiar velocity* and describes the motion of the objects themselves, relative to the Hubble expansion.

Also transforming the temporal and spatial derivatives to the comoving system with:

$$\begin{aligned} \partial_t &\rightarrow \partial_t - H \vec{x} \cdot \nabla, \\ \nabla &\rightarrow \frac{1}{a} \cdot \nabla, \end{aligned} \quad (2.7)$$

we arrive at new expressions for the continuity, Euler and Poisson equation in comoving coordinates:

$$\dot{\rho} - H \vec{x} \cdot \nabla \rho + \frac{1}{a} \nabla \cdot (\rho \vec{v}) = 0, \quad (2.8)$$

$$\dot{\vec{v}} - H (\vec{x} \cdot \nabla) \vec{v} + \frac{1}{a} (\vec{v} \cdot \nabla) \vec{v} = \frac{-\nabla P}{a \rho} - \frac{\nabla \Phi}{a}, \quad (2.9)$$

$$\nabla^2 \Phi = 4\pi G \rho a^2. \quad (2.10)$$

It is convenient to split both the density and the velocity into homogeneous background contributions and deviations from that background:

$$\rho = \rho_0(1 + \delta), \quad (2.11)$$

$$\vec{v} = \vec{v}_0 + a\vec{u}. \quad (2.12)$$

Here, we introduce the density contrast:

$$\delta = \frac{\rho - \rho_0}{\rho_0}. \quad (2.13)$$

The equation system (2.11-2.12) above must hold for the background contribution independently. Then we can derive equations for the evolution of the two perturbation quantities δ and \vec{u} :

$$\dot{\delta} + \frac{1}{a} \nabla \cdot [(1 + \delta)\vec{u}] = 0 \quad (2.14)$$

$$\dot{\vec{u}} + 2H\vec{u} + (\vec{u} \cdot \nabla) \vec{u} = \frac{-c_s^2 \nabla \delta}{a^2(1 + \delta)} - \frac{\nabla \phi}{a^2}, \quad (2.15)$$

where we introduce the speed of sound c_s defined as:

$$c_s^2 \rho_0 \delta := \left(\frac{\partial P}{\partial \rho} \right) \delta \rho, \quad (2.16)$$

and a modified Newtonian potential:

$$\phi = \Phi - \frac{2}{3} \pi G \rho_0 a^2 x^2, \quad (2.17)$$

satisfying the Poisson equation for the density contrast alone:

$$\nabla^2 \phi = 4\pi G \rho_0 a^2 \delta. \quad (2.18)$$

In order to further simplify the problem we start to drop any terms quadratic in either the density contrast or the velocity or mixed terms. This reduces the equation system to the linearised equation system

$$\dot{\delta} + \nabla \cdot \vec{u} = 0, \quad (2.19)$$

$$\dot{\vec{u}} + 2H\vec{u} = \frac{-1}{a^2} \left(c_s^2 \nabla \delta + \nabla \phi \right). \quad (2.20)$$

The Poisson equation for the density contrast, 2.18, still holds additionally. We can combine the temporal derivative of the linearised, comoving continuity equation with the spatial divergence of the linearised, comoving Euler equation 2.20 in order

to eliminate the divergence of \vec{u} . Then a second-order differential equation emerges describing the time development of the density contrast :

$$\ddot{\delta} + 2H\dot{\delta} = 4\pi G\rho_0\delta + \frac{c_s^2\nabla^2\delta}{a^2}. \quad (2.21)$$

This equation is linear and homogeneous which is why we choose to expand the density contrast into Fourier modes:

$$\hat{\delta}_k(t) := \hat{\delta}(t, \vec{k}) = \int d^3x \delta(t, \vec{x}) e^{-i\vec{k}\vec{x}}, \quad (2.22)$$

$$\delta(t, \vec{x}) = \int \frac{d^3k}{(2\pi)^3} \hat{\delta}(t, \vec{k}) e^{i\vec{k}\vec{x}}. \quad (2.23)$$

This transformation makes the Laplace-operator in the right-hand-side of 2.21 easy to evaluate and results in a factor of $-k^2$. The evolution equation of the density contrast in Fourier space then reads:

$$\ddot{\delta}_k + 2H\dot{\delta}_k = \left(4\pi G\rho_0 - \frac{c_s^2 k^2}{a^2}\right) \hat{\delta}_k. \quad (2.24)$$

The right hand side of this equation vanishes for wave numbers $k_J^2 := \frac{4\pi G\rho_0 a^2}{c_s^2}$ which is referred to as *Jeans wave number*.

Analysing the differential equation 2.24 for vanishing H , $H = 0$, i.e. for a static universe, we can see that for $k \geq k_J$ the density contrast must oscillate, whereas for $k \leq k_J$ density modes start to grow. By translating this wave number into a length scale we obtain the *Jeans length*:

$$\lambda_J := \frac{2\pi}{k_J} = \frac{c_s}{a} \sqrt{\frac{\pi}{G\rho_0}} \quad (2.25)$$

and realise that only density perturbations larger than this length can grow. Evaluating the equation with $H \neq 0$ for a dynamic universe we find that the formerly neglected term $+2H\dot{\delta}$ leads to a damping of both the oscillating and the exponentially increasing solutions.

2.2 THE LINEAR GROWTH FUNCTION D_+

In linear theory modes are uncoupled allowing them to evolve independently of another, but with the same rate. Thus, we can write the solutions as:

$$\hat{\delta}_k(t) = \hat{\delta}_k(t_0) \cdot D(t). \quad (2.26)$$

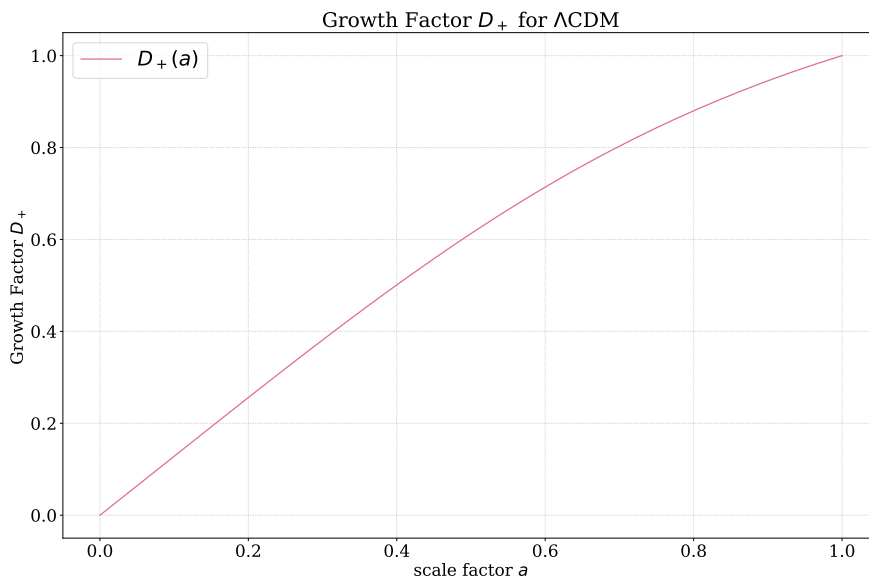


Figure 2.1: The linear growth factor $D_+(a)$ (eq. 2.27) for a standard cosmology with $\Omega_{\Lambda 0} = 0.7, \Omega_{m0} = 0.3, h = 0.7$.

Analysing 2.24 we find two independent solutions for D . For the case of nonrelativistic matter after the radiation-dominated era we find a growing solution with $D_+ \propto a$ and a solution decaying with $D_- \propto a^{-3/2}$. Analysing the differential equation for different kinds of matter in different stages of the cosmic evolution we find that we can describe the growth of the density contrast in the Λ -dominated era with $D_+(a)$ approximated by:

$$D_+(a) = \frac{5a}{2} \Omega_m \left[\Omega_m^{4/7} - \Omega_\Lambda + \left(1 + \frac{1}{2} \Omega_m\right) \left(1 + \frac{1}{70} \Omega_\Lambda\right) \right]^{-1}. \quad (2.27)$$

This is shown for a standard cosmological model with $\Omega_{\Lambda 0} = 0.7, \Omega_{m0} = 0.3, h = 0.7$ in Figure 2.1 This description requires a cosmological model with $\Omega_m < 1$ and $\Omega_\Lambda > 0$. The most prominent example of such a cosmology is the standard model of cosmology: Λ CDM. This model is named after its main components, cosmological constant Λ and cold dark matter CDM. The *cold* refers to the property of moving slowly compared with the speed of light whereas *dark* refers to the matter not interacting with light. The major component is often modeled as *cosmological constant* with a negative equation of state parameter (cf. eq. 1.22).

2.3 STATISTICAL MEASURES OF DENSITY FLUCTUATIONS

One of the central quantities of structure formation is the *matter density power spectrum* defined either as:

$$\langle \delta_k(t) \delta_{k'}^*(t) \rangle := (2\pi)^3 \delta_D(\vec{k} - \vec{k}') P_\delta(k), \quad (2.28)$$

or

$$\langle \delta_k(t) \delta_{k'}(t) \rangle := (2\pi)^3 \delta_D(\vec{k} + \vec{k}') P_\delta(k), \quad (2.29)$$

where we used the Dirac delta distribution δ_D and the complex conjugate of the Fourier mode $\delta_k^*(t)$ in the first definition. The density power spectrum P_δ depends on the wave number k only because isotropy prohibits this quantity to depend on a direction. Looking at its definition we realise that the power spectrum is simply the variance of the Fourier transformed k -dependent density contrast. We could also calculate the variance of the real-space density contrast:

$$\langle \delta(\vec{x}, t) \delta(\vec{x} + \vec{r}, t) \rangle =: \zeta(t, r). \quad (2.30)$$

This quantity is called *correlation function* and turns out to be the Fourier transform of the power spectrum as its constituents are the Fourier transform of the constituents of the power spectrum:

$$\zeta(t, r) = \int \frac{d^3k}{(2\pi)^3} P(k) e^{-i\vec{k}\vec{r}}. \quad (2.31)$$

In this thesis, however, we will concentrate on the treatment of the power spectrum. It is easy to describe the evolution of the power spectrum in the linear phase when the description of the linear evolution of the density contrast is given by eq. 2.26. Considering the definition of the power spectrum we immediately can derive:

$$P_\delta^{lin}(k, t) = P_\delta^0(k) \cdot D_+^2(t). \quad (2.32)$$

We will choose an *initial* power spectrum P_δ^0 at an initial time of approximately recombination for structure formation is assumed to be linear at that point in time and we can determine the power spectrum of that phase with CMB measurements.

From the analysis of the density contrast's evolution during different phases in the evolution of the universe (i.e. radiation-, matter- and Λ -dominated epochs) we can derive the behaviour of the power spectrum. For a detailed calculation we refer the reader to [e.g. 6, 17, 32] and give the result of these calculations directly:

During the expansion of the universe the Hubble radius $r_H = c/H(t)$ increases. This means that modes that were larger than the horizon before now enter the horizon and evolve differently than before. In fact, density perturbations of relativistic matter grow only as long as they have not entered the horizon. Entering the horizon, however, these modes start to oscillate instead of growing – their growth ends. When the universe starts to be dominated by nonrelativistic matter (the time of the transition from matter- to radiation-domination is marked by the expansion parameter a_{eq}) modes grow independently of their length scale. This implies that those modes which enter the horizon earlier are suppressed with respect to those entering the horizon at a later stage. Detailed calculations of the physical processes lead to the following behaviour of the power spectrum for cold dark matter:

$$P(k) \propto \begin{cases} k & (k < k_{eq}) \\ k^{-3} & (k > k_{eq}) \end{cases}, \quad (2.33)$$

where the parameter k_{eq} is defined as:

$$k_{eq} = a_{eq} \frac{2\pi}{r_{H,eq}}, \quad (2.34)$$

and the Hubble radius at equality time is given by:

$$r_{H,eq} = \frac{c}{H(a)} = \frac{c}{H_0 E(a)} \Big|_{a=a_{eq}} = \frac{c}{H_0} \frac{a_{eq}^{3/2}}{\sqrt{2\Omega_{m,0}}}. \quad (2.35)$$

We show the form of the linear power spectrum of cold dark matter in Fig. 2.2.

The possibility of a linear description of the density contrast evolution that we sketched so far ceases as soon as δ approaches unity. Analytic investigation of density evolution would require further strong assumptions on the system itself. Alternatively, we could use simulations of different kinds to gain further knowledge. This is done by many research groups across the globe. A comprehensive and general treatment with analytic methods, however, has not been developed except for the field theory we introduce in chapter 5. Tackling these issues and finding an analytical description of structure growth also in the nonlinear regime of structure formation will be one of the main motivations for the development of Kinetic Field Theory in chapter 5.

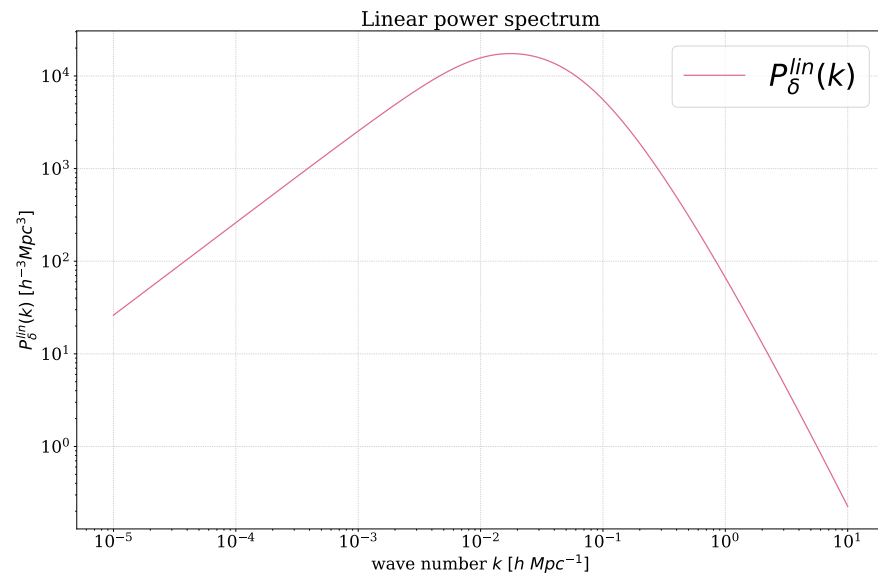


Figure 2.2: Linear density power spectrum. This plot shows the power spectrum of linear structures as derived in Bardeen et al. [3]. This illustration is particularly helpful to visualise the behaviour of the power spectrum as described in 2.33, where the power spectrum grows linear with k up to the turning point k_{eq} , when it starts decreasing with k^{-3} .

GRAVITATIONAL LENSING

Gravitational lensing is a phenomenon which allows to probe the distribution of (mostly dark) matter in the universe and its evolution through time. The effect is a particularly interesting one as it enables us to probe matter on both very small and very large scales. It describes the deflection of light by overdensities in the matter distribution along the line of sight.

The effect was predicted by Einstein's theory of General Relativity in 1915 and proposed as a possibility to probe the theory. Although it was expected to be very hard to measure the effect with the lens being a single star, [51] already realised that the effect must be strong enough for a deflector consisting of a *nebula* (galaxy).

The phenomenon of gravitational lensing shows three different categories: strong, weak and micro-lensing. Strong lensing shows when observer, lens and light source are in near-perfect alignment and the mass density of the lens exceeds a certain threshold (called the critical mass density). The shape of the source is strongly distorted leading to observable phenomena like Einstein rings or multiple images of the very same source. Microlensing on the other hand is a method to observe objects using the magnification of light curves of sources behind by the otherwise unobservable lens.

Weak lensing describes the systematic distortion of light sources due to various structures along the line of sight between the observer and the light source. These distortions, however, are too small to be observed directly. They therefore can only be detected and measured by statistically correlating large samples of sources which are typically galaxies. This is discussed in Section 3.6.

The first detection of strong gravitational lensing effects was made by [18]. The first strong lensing system outside the Solar System, however, was only observed in 1979 by [49] and it proved to be even more challenging to probe weak gravitational lensing for the first time. The effect, called *cosmic shear*, induced by the inhomogeneous matter distribution in the universe was then detected and presented by four independent groups [2, 23, 46, 50] in the same year.

The foundation of the lensing formalism and the most important quantities are shown in many different textbooks and articles, however in order to introduce the formalism of gravitational lensing needed we closely follow [4].

3.1 JACOBI EQUATION

For all calculations following we assume that the universe is described by a Friedmann-Lemaître-Robertson-Walker (FLRW) cosmological model. Furthermore, we assume General Relativity [45] to be valid throughout. We assume the gravitational potential to be weak ($\Phi \ll c^2$) and the peculiar velocity of the sources of gravitation to be slow with respect to the mean background. Gravitational lensing describes the bending of light due to the influence of a gravitational field. We therefore start by considering a bundle of light rays, written in general relativity as null geodesics. For our first step, we pick out a single fiducial ray. Its tangent vector is given by:

$$k^\mu = \frac{dx^\mu}{d\lambda}, \quad (3.1)$$

with λ an affine parameter parametrising the light ray and k normalised such that its projection to the four-velocity of a freely falling observer equals one:

$$\langle k, u_{obs} \rangle = 1. \quad (3.2)$$

This normalisation determines the choice of the affine parameter λ : A wave vector \tilde{k} projected onto the velocity of a freely falling observer returns the light ray's frequency measured by the very same observer. Therefore, the affine parameter must be chosen such, that $k = \tilde{k}/\omega_{obs} = \tilde{k}/|\langle \tilde{k}, u_{obs} \rangle|$.

We now consider a neighbouring ray of the chosen one and the tangent vector v of the curve connecting both rays considered. We call this connection curve γ . The tangent vector is modified by the influence of a curvature field characterised by $R = R(k, v)$ according to the *equation of geodesic deviation* (Jacobi equation):

$$\nabla_k^2 v = R(k, v)k. \quad (3.3)$$

∇_k denotes the covariant derivative with respect to the wave vector k and $R(k, v)$ describes the curvature as in equation 1.10. One can now evaluate this equation by introducing a (two-dimensional) screen perpendicular to our light-ray within the

observer's three-space spanned by vectors E_1 and E_2 . Both vectors are parallelly transported along the fiducial light ray. The projection of the vector v on the screen is described by vector components $v_{1,2}$ and 3.3 can be rewritten as:

$$\nabla_k^2 \begin{pmatrix} v_1 \\ v_2 \end{pmatrix} = \mathcal{T} \begin{pmatrix} v_1 \\ v_2 \end{pmatrix}, \quad (3.4)$$

where we introduce the optical tidal matrix:

$$\mathcal{T} = \begin{pmatrix} \mathcal{R} + \text{Re}(\mathcal{F}) & \text{Im}(\mathcal{F}) \\ \text{Im}(\mathcal{F}) & \mathcal{R} - \text{Re}(\mathcal{F}) \end{pmatrix}. \quad (3.5)$$

$\text{Re}(X)$ and $\text{Im}(X)$ denote the real and imaginary parts of the variable X and the components of the optical tidal matrix \mathcal{T} are given by:

$$\begin{aligned} \mathcal{F} &= \frac{1}{2} C_{\alpha\beta\gamma\delta} \epsilon^\alpha k^\beta k^\gamma \epsilon^\delta, \\ \mathcal{R} &= \frac{1}{2} R_{\alpha\beta} k^\alpha k^\beta + \frac{1}{2} C_{\alpha\beta\gamma\delta} \epsilon^\alpha k^\beta k^\gamma \epsilon^{*\delta}, \end{aligned} \quad (3.6)$$

with the Weyl tensor $C_{\alpha\beta\gamma\delta}$ [defined e.g. in 45, eq. 15.110 and below in 3.23] and the vector $\epsilon := E_1 + iE_2$. It is now assumed, that one can split the contribution from the background and the contribution from *clumps* of matter as additional sources of gravity to the light rays' behaviour in the influence of the total gravitational field:

$$\mathcal{T} = \mathcal{T}_{bg} + \mathcal{T}_{cl}. \quad (3.7)$$

3.2 THE TIDAL MATRIX

3.2.1 Tidal Matrix: Background

We will now consider both contributions separately, starting with the contribution from the background in a freely expanding FLRW-universe, described by the Friedmann-Lemaitre-Robertson-Walker metric [e.g. 6, eq. 1.11]:

$$ds^2 = a^2(\eta) \left[-d\eta^2 + dw^2 + f_K^2(w) d\Omega^2 \right], \quad (3.8)$$

where by η we denote the conformal time, related to cosmic time t by $d\eta = \frac{c}{a} dt$. $d\Omega$ is the solid angle element, w the (comoving) radial distance w and $f_K(w)$ the comoving angular-diameter distance (cf. eq. 1.16). This metric is equivalent to 1.17. Assuming

the background to be symmetric the Weyl curvature tensor $C_{\alpha\beta\gamma\delta}$ in eq. 3.6 vanishes. With k being a null vector the contraction of the Ricci-Tensor with k can be rewritten as $R_{\alpha\beta}k^\alpha k^\beta = G_{\alpha\beta}k^\alpha k^\beta = \frac{8\pi G}{c^4}T_{\alpha\beta}k^\alpha k^\beta$ using Einstein's field equations 1.7. For an ideal fluid with negligible pressure we insert $T_{\alpha\beta}k^\alpha k^\beta = \rho c^2 \langle u, k \rangle^2$ for the stress-energy-tensor 1.18. Having normalised the wave vector before, it turns out that the projection $|\langle k, u \rangle|$ equals:

$$|\langle k, u \rangle| = 1 + z, \quad (3.9)$$

where we introduce the redshift z (cf. section 1.5) of the fluid with respect to the observer. Knowing, that the density of pressure-less, non-relativistic matter evolves with $\rho = \rho_0(1+z)^3$ the total expression for \mathcal{R} is given by:

$$\mathcal{R} = -\frac{4\pi G}{c^2}\rho_0(1+z)^5, \quad (3.10)$$

leading to the optical tidal matrix for the background contribution:

$$\mathcal{T}_{bg} = \mathcal{R}\mathcal{I}_2, \quad (3.11)$$

with the two-dimensional unit matrix \mathcal{I}_2 .

In order to continue with our description of the background contribution we now analyse the equation of motion 3.3. First, we have to choose an affine parameter. Ignoring peculiar velocities again we write:

$$\langle k, u \rangle = \left\langle \frac{dx}{d\lambda}, u \right\rangle = \frac{dx^0}{d\lambda} = \frac{cdt}{d\lambda}, \quad (3.12)$$

knowing that $u^\mu = \delta_0^\mu$. This must be equal to $1+z = 1/a$. Therefore,

$$d\lambda = ac dt = a^2 d\eta. \quad (3.13)$$

By remembering that the screen (and therefore its basis vectors) are parallelly transported with k we rewrite the left hand side of the Jacobi equation:

$$\nabla_k^2 v^i = \frac{d^2 v^i}{d\lambda^2}, \quad (3.14)$$

and replace the affine parameter with the comoving radial distance:

$$d\lambda = a^2 dw. \quad (3.15)$$

One can now introduce *co-moving bundle dimensions* v^i/a and analyse their propagation with w by using the relation of w and

the affine parameter λ and making use of the first Friedmann equation in order to find:

$$\left(\frac{d}{dw^2} + K\right) \frac{v^i}{a} = 0. \quad (3.16)$$

We introduced the curvature K when we inserted Friedmann's equation. Equation 3.16 describes the propagation of the comoving bundle dimensions in the homogeneous and isotropic universe, i.e. in the background.

3.2.2 Tidal Matrix: Clumps

Having determined the equation of motion describing the propagation of the comoving light-bundle dimension in the background we continue by describing the influence of overdensities in the universe called *clumps*. The name also reflects their property of being smaller in spatial terms than the curvature scale of the background universe. Those clumps' Newtonian potential $\Phi = \phi c^2 \ll c^2$ perturbs the FLRW metric such as:

$$ds^2 = a^2(\eta) \left[-(1 + 2\phi)d\eta^2 + (1 - 2\phi) \left(dw^2 + f_K^2(w)d\Omega^2 \right) \right]. \quad (3.17)$$

In a locally flat space we approximate $f_K(w) \approx w$ and start by looking at the light in the comoving Newtonian environment with:

$$d\bar{s}^2 = -(1 + 2\phi)d\eta^2 + (1 - 2\phi)d\bar{w}^2. \quad (3.18)$$

We introduce the dual basis

$$\begin{aligned} \theta^0 &= (1 + \phi)d\eta \\ \theta^i &= (1 - \phi)dw^i \end{aligned} \quad (3.19)$$

in terms of which the metric 3.18 looks Minkowskian. For the following considerations we neglect terms of higher order than linear in ϕ and time derivatives of the potential. The latter terms become negligible, since they get damped by a factor of c^{-1} as we convert them to derivatives with respect to the coordinate x^0 . We introduce the shorthand $A_j := \partial_j A$ and calculate the components of the Riemann tensor in order to be able to calculate the Weyl curvature tensor later on. We find:

$$\begin{aligned} R_{0i0j} &= \phi_{ij}, & R_{ijij} &= \phi_{ii} + \phi_{jj}, \\ R_{1213} &= \phi_{23}, & R_{1223} &= -\phi_{13}, \\ R_{1323} &= \phi_{12}, \end{aligned} \quad (3.20)$$

while all the other elements vanish. This enables us to calculate the Ricci tensor $R_{jl} = R^i_{jil}$ and the Ricci scalar $R = R^i_i$, i.e. the trace of the tensor with the same name,

$$R_{\alpha\beta} = \nabla^2 \phi \mathcal{I}_4, \quad R = 2\nabla^2 \phi. \quad (3.21)$$

Based on that we can calculate the Einstein tensor in this setup:

$$G_{\alpha\beta} = R_{\alpha\beta} + \frac{R}{2} g_{\alpha\beta} = \nabla^2 \phi \delta^0_\alpha \delta^0_\beta, \quad (3.22)$$

where we also insert the stress-energy tensor 1.18. The Weyl curvature is defined as:

$$C_{\alpha\beta\gamma\delta} = R_{\alpha\beta\gamma\delta} - g_{\alpha[\gamma} R_{\delta]\beta} + g_{\beta[\gamma} R_{\delta]\alpha} + \frac{R}{3} g_{\alpha[\gamma} g_{\delta]\beta}, \quad (3.23)$$

and we use the shorthand notation for antisymmetrising $A_{\alpha[\beta} B_{\gamma]\delta} = \frac{1}{2} (A_{\alpha\beta} B_{\gamma\delta} - A_{\alpha\gamma} B_{\beta\delta})$ as it is defined, e.g., in [48, p. 26]. Plugging in numbers, we find the only non-zero components to be:

$$\begin{aligned} C_{0i0j} &= \phi_{ij} - \frac{1}{3} \nabla^2 \phi \eta_{ij}, & C_{ijij} &= \phi_{ii} + \phi_{jj} - \frac{2}{3} \nabla^2 \phi, \\ C_{12113} &= \phi_{23}, & C_{1223} &= -\phi_{13}, & C_{1323} &= \phi_{12}. \end{aligned} \quad (3.24)$$

We can now calculate both components of the tidal matrix for clump contribution with:

$$\mathcal{R}_{cl} = -\nabla^2 \phi \quad (3.25)$$

$$\mathcal{F}_{cl} = -(\phi_{11} - \phi_{22}) - 2i\phi_{12} \quad (3.26)$$

and find the tidal matrix:

$$\mathcal{T}_{cl} = -2 \begin{pmatrix} \phi_{11} & \phi_{12} \\ \phi_{12} & \phi_{22} \end{pmatrix}. \quad (3.27)$$

If we call the specific potential which is passed by the light ray $\phi^{(0)}$ and expand the gradient of the potential as:

$$\partial_i(\phi - \phi^{(0)}) := \partial_i \delta\phi = \partial_j \partial_i \phi|_0 x^j = -\frac{1}{2} (\mathcal{T}_{cl})_{ij} x^j, \quad (3.28)$$

we can rewrite the geodesic deviation equation as:

$$\frac{d^2 x^i}{d\lambda^2} = \frac{d^2 x^i}{dw^2} = -2\partial^i \delta\phi, \quad (3.29)$$

where we use the fact that in the local Newtonian metric $d\lambda = dw$. Since only potential differences have physical importance, but not absolute potential values, we reset the potential $\phi := \delta\phi$ and notice that the x^i in the local frame are *comoving* bundle dimensions v^i/a which are subject to cosmic expansion as well. Altogether, the equivalent to eq. 3.16 including clumps is given by:

$$\left(\frac{d}{dw^2} + K \right) x^i + 2\partial^i \phi = 0. \quad (3.30)$$

3.3 LENSING POTENTIAL AND LENSING EQUATION

In order to solve equation 3.30 and proceed with the definition of the lensing potential, a key quantity for the central object of this thesis which is the weak (gravitational) lensing power spectrum, we start by solving the inhomogeneous oscillator equation 3.30. We find the appropriate Green's function to be:

$$\begin{aligned} G(w, w') &= \frac{1}{\sqrt{K}} \sin\left(\sqrt{K}(w - w')\right) \Theta(w - w') \\ &= f_K(w - w') \Theta(w - w'), \end{aligned} \quad (3.31)$$

where f_K is again the comoving angular diameter distance (cf. eq. 3.8). For the solution we furthermore need appropriate boundary conditions which we find to be provided by:

$$x^i \Big|_{w=0} = 0, \quad (3.32)$$

$$\frac{dx^i}{dw} \Big|_{w=0} = \theta^i. \quad (3.33)$$

Since this might not be trivial to understand at this stage we want to elaborate on this in greater detail. It is worth recalling that $x^i = v^i/a$ is the local description of the tangent vector connecting the light rays considered. The first condition therefore describes that the x^i of all rays considered at $w = 0$, i.e. at the observer's position, are vanishing since we consider rays starting there. We do, however, consider rays which may start in different directions θ^i which is described by the second condition. This is schematically illustrated in Fig. 3.1. The solution of eq. 3.30 with boundary conditions 3.32 and 3.33 is given by:

$$x^i(w) = f_K(w) \theta^i - 2 \int_0^w dw' f_K(w - w') \partial^i \phi(x^j(w'), w'). \quad (3.34)$$

For the rest of this calculation we shall assume very small deflection angles and use Born's approximation for the integration along the unperturbed light path $x^i(w') \approx f_K(w') \theta^i$. The application of this widely used approximation is very well justified by numerical simulations [e.g. 33, 43].

Considering gravitational lensing as the phenomenon of light coming from a distant source being deflected by a deflector closer to the observer we only integrate from the observer (at $w = 0$) to the comoving radial distance of the source w_s . We define the angle $\beta^i := x^i(w_s)/f_K(w_s)$ and find:

$$\beta^i = \theta^i - 2 \int_0^{w_s} dw' \frac{f_K(w_s - w')}{f_K(w_s)} \partial^i \phi(f_K(w') \theta^j, w'). \quad (3.35)$$

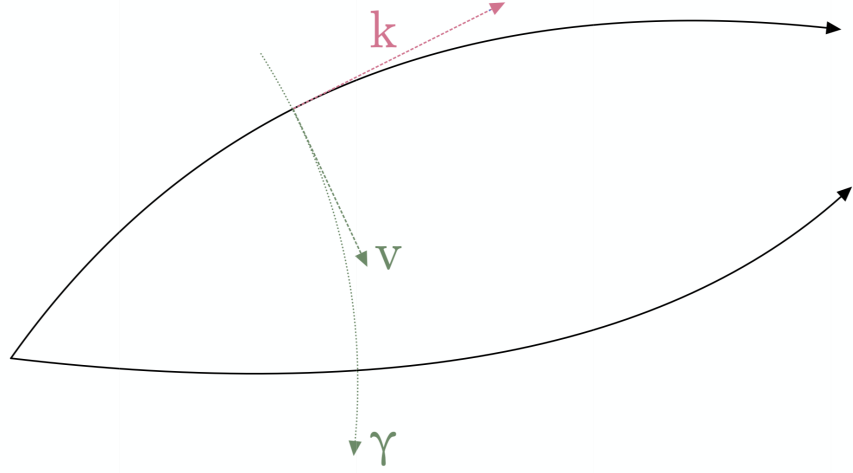


Figure 3.1: A bundle of light rays (null geodesics, continuous black). The light ray is characterised by its tangent vector k (pink, dashed) connected to its neighbours by the curve γ (green, dotted) with the associated tangent vector v (green, dashed). Dashed lines indicate tangent vectors, whereas the dotted line describes the constructed connection of the two rays (continuous lines).

If we rename the subtrahend of this equation,

$$\alpha^i(\theta^j) := 2 \int_0^{w_s} dw' \frac{f_K(w_s - w')}{f_K(w_s)} \partial^i \phi(f_K(w') \theta^j, w'),$$

and call it *reduced deflection angle* we can write down the *lensing equation*:

$$\beta^i = \theta^i - \alpha^i(\theta^j). \quad (3.36)$$

This equation is schematically elaborated in Fig. 3.2 We then define a derivative with respect to angular coordinates $\partial_\theta = f_K(w) \partial_x$ which enables us to write down the reduced deflection angle as angular gradient of a newly introduced *effective lensing potential*:

$$\psi(\theta^j) = 2 \int_0^{w_s} dw' \frac{f_K(w_s - w')}{f_K(w_s) f_K(w')} \phi(f_K(w') \theta^j, w'). \quad (3.37)$$

3.4 COSMIC SHEAR AND CONVERGENCE

In this section we introduce two central quantities of weak gravitational lensing: *shear* and *convergence*. These will not only be important in the light of the weak lensing power spectrum, the central object of this thesis, but also when relating this to

and V (with $\phi(p) \in V$) in S^2 to a neighbourhood U', V' in \mathbb{R}^2 and call them h_1 and h_2 :

$$\begin{aligned} h_1 &: U \rightarrow U', \\ h_2 &: V \rightarrow V'. \end{aligned}$$

We can then span U' and V' with coordinate pairs (θ^1, θ^2) and (β^1, β^2) , respectively and – in the cartesian vector spaces – finally express the Jacobian matrix $D\zeta$ by partial derivatives:

$$(D\zeta)_j^i = \frac{\partial \beta^i}{\partial \theta^j} = \frac{\partial(\theta - \alpha)^i}{\partial \theta^j} = \delta_j^i - \frac{\partial^2 \psi}{\partial \theta_i \partial \theta^j} = \delta_j^i - \psi_j^i, \quad (3.40)$$

where by the first symbol in the last term we denote the common Kronecker-delta:

$$\delta_{ij} = \begin{cases} 1 & i = j \\ 0 & i \neq j \end{cases}, \quad (3.41)$$

and for the last part we made use of the common shorthand for derivatives $A_j^i := \partial^i \partial_j A$ for an arbitrary variable A . One now separates this differential into its trace and the trace-free part:

$$(D\zeta)_j^i = \begin{pmatrix} 1 - \kappa & 0 \\ 0 & 1 - \kappa \end{pmatrix} - \begin{pmatrix} \gamma_1 & \gamma_2 \\ \gamma_2 & -\gamma_1 \end{pmatrix}, \quad (3.42)$$

where we introduce and define the convergence:

$$\kappa := \frac{1}{2} \psi_i^i \quad (3.43)$$

as well as the two components of the cosmic shear γ :

$$\gamma := \gamma_1 + i\gamma_2 \quad (3.44)$$

$$\gamma_1 := \frac{1}{2} (\psi_1^1 - \psi_2^2) \quad (3.45)$$

$$\gamma_2 := \psi_1^2 = \psi_2^1. \quad (3.46)$$

While the convergence κ is responsible for an enlargement of the objects on the sky, isotropically, due to the lens mapping, the shear components elliptically distort the image. This is being exploited in order to detect gravitational lensing.

In order to further investigate the meaning of the convergence we plug the definition of the lensing potential into the expression for the convergence in the locally Cartesian environment:

$$\kappa(x^j) = \int_0^{w_s} dw' \frac{f_K(w') f_K(w_s - w')}{f_K(w_s)} \partial_{x^i} \partial^{x^i} \phi(x^j, w'), \quad (3.47)$$

and find with

$$\nabla^2 \phi = \frac{4\pi G}{c^2} \rho$$

that the convergence is a suitably weighed surface-mass-density of the matter inhomogeneities which cause lensing:

$$\kappa(\theta^i) = \frac{4\pi G}{c^2} \int_0^{w_s} dw' \frac{f_K(w') f_K(w_s - w')}{f_K(w_s)} \rho(f_K(w') \theta^i, w'). \quad (3.48)$$

The simplified Poisson equation (eq. 3.43) holds due to the fact that the partial derivatives ∂_i are taken with respect to coordinates orthogonal to the line of sight (i.e. the integration variable). The third derivative in direction of the line of sight vanishes after the integration into the very same direction, if the potential is localised.

3.5 THE WEAK LENSING POWER SPECTRUM

Having introduced the lensing potential in eq. 3.37 we are ready to develop the *weak lensing power spectrum*. Writing down the angular correlation function of the effective lensing potential we find:

$$\begin{aligned} \langle \psi(\vec{\theta}) \psi(\vec{\theta}') \rangle &= \int_0^{w_s} dw \int_0^{w_s} dw' \frac{w_s - w}{w_s w} \frac{w_s - w'}{w_s w'} \\ &\cdot \int \frac{d^3 q}{(2\pi)^3} P_\phi(q) e^{i\vec{q} \cdot (\vec{x} - \vec{x}')}. \end{aligned} \quad (3.49)$$

As this is not trivial to see, we shall have a look at the correlation function of the gravitational potential.

$$\langle \phi(\vec{x}) \phi^*(\vec{x}') \rangle = \int \frac{d^3 q}{(2\pi)^3} \int \frac{d^3 q'}{(2\pi)^3} \langle \hat{\phi}(\vec{q}) \hat{\phi}^*(\vec{q}') \rangle e^{i(\vec{q} \cdot \vec{x} - \vec{q}' \cdot \vec{x}')} \quad (3.50)$$

$$= \int \frac{d^3 q}{(2\pi)^3} \int \frac{d^3 q'}{(2\pi)^3} P_\phi(q) \delta(\vec{q} - \vec{q}') (2\pi)^3 e^{i(\vec{q} \cdot \vec{x} - \vec{q}' \cdot \vec{x}')} \quad (3.51)$$

$$= \int \frac{d^3 q}{(2\pi)^3} P_\phi(q) e^{i\vec{q} \cdot (\vec{x} - \vec{x}')}, \quad (3.52)$$

where we abbreviate $\vec{x} := (w\theta, w)$ and expand the gravitational potential in Fourier modes for the first equality:

$$\phi(\vec{x}) = \int \frac{d^3 q}{(2\pi)^3} \hat{\phi}(\vec{q}) e^{i\vec{q} \cdot \vec{x}}, \quad (3.53)$$

and insert the definition of the potential power spectrum:

$$\langle \hat{\phi}(q)\hat{\phi}^*(q') \rangle = (2\pi)^3 \delta(q - q') P_\phi(|q|), \quad (3.54)$$

in order to get to the second line. We perform an integration over q' using the Dirac- δ -function in order to find the final result. For the average $\langle \hat{\phi}(q)\hat{\phi}^*(q') \rangle$ we take all Fourier modes with wave number q which are contained in the volume.

The Fourier basis can now be expanded once more into spherical harmonics:

$$e^{i\vec{q}\vec{x}} = 4\pi \sum_{lm} i^l j_l(qw) Y_{lm}^*(\vec{\theta}_x) Y_{lm}(\vec{\theta}_q), \quad (3.55)$$

and we use this expansion in order to further manipulate the three-dimensional integral in eq. 3.49:

$$\begin{aligned} \int \frac{d^3q}{(2\pi)^3} P_\phi(q) e^{i\vec{q}(\vec{x}-\vec{x}')} &= \int \frac{d^3q}{(2\pi)^3} 16\pi^2 P_\phi \left(\sum_{lm} i^l j_l(qw) Y_{lm}^*(\vec{\theta}_x) Y_{lm}(\vec{\theta}_q) \right) \\ &\quad \cdot \left(\sum_{l'm'} -i^{l'} j_{l'}(qw') Y_{l'm'}^*(\vec{\theta}'_x) Y_{l'm'}(\vec{\theta}'_q) \right) \end{aligned} \quad (3.56)$$

$$\begin{aligned} &= \frac{2}{\pi} \int q^2 dq P_\phi(q) \int d\Omega \sum_{lm} \sum_{l'm'} -i^{l+l'} \\ &\quad \cdot j_l(qw) j_{l'}(qw') \\ &\quad \cdot Y_{lm}^*(\vec{\theta}_x) Y_{l'm'}(\vec{\theta}'_x) Y_{lm}(\vec{\theta}_q) Y_{l'm'}^*(\vec{\theta}'_q) \end{aligned} \quad (3.57)$$

$$\begin{aligned} &= \frac{2}{\pi} \int q^2 dq P_\phi(q) \sum_{lm} \sum_{l'm'} -i^{l+l'} j_l(qw) \\ &\quad \cdot j_{l'}(qw') Y_{lm}^*(\vec{\theta}_x) Y_{l'm'}(\vec{\theta}'_x) \delta_{ll'} \delta_{mm'} \end{aligned} \quad (3.58)$$

$$\begin{aligned} &= \frac{2}{\pi} \int q^2 dq P_\phi(q) \sum_{lm} -i^{2l} j_l(qw) j_l(qw') \\ &\quad \cdot Y_{lm}^*(\vec{\theta}_x) Y_{lm}(\vec{\theta}'_x). \end{aligned} \quad (3.59)$$

Plugging this into the expression 3.49 and providing boundaries for the integral in 3.49 we find:

$$\begin{aligned} \langle \psi(\vec{\theta}) \psi(\vec{\theta}') \rangle &= \frac{2}{\pi} \sum_{lm} \int_0^{w_s} dw \int_0^{w_s} dw' \frac{w_s - w}{w_s w} \frac{w_s - w'}{w_s w'} \\ &\quad \cdot \int_0^\infty q^2 dq P_\phi(q) j_l(qw) j_l(qw') Y_{lm}^*(\vec{\theta}_x) Y_{lm}(\vec{\theta}'_x). \end{aligned} \quad (3.60)$$

For the only angles left as arguments in the expression on the right hand side are θ_x we abbreviate $\theta = \theta_x$. We now expand the constituents of the left hand side of this equation into spherical harmonics as well:

$$\psi(\vec{\theta}_x) = \sum_{lm} \psi_{lm} Y_{lm}, \quad (3.61)$$

with coefficients

$$\psi_{lm} = \int d\vec{\theta} \psi(\vec{\theta}) Y_{lm}^*(\vec{\theta}), \quad (3.62)$$

and define the angular power spectrum by

$$\langle \psi_{lm} \psi_{l'm'}^* \rangle = \delta_{ll'} \delta_{mm'} C_\ell^\psi. \quad (3.63)$$

We use the expanded lensing potential in the description of the angular correlation function

$$\langle \psi(\vec{\theta}) \psi(\vec{\theta}') \rangle = \sum_{lm} \sum_{l'm'} \langle \psi_{lm} \psi_{l'm'}^* \rangle Y_{lm} Y_{l'm'}^* \quad (3.64)$$

$$= \sum_{lm} Y_{lm} Y_{lm}^* C_\ell^\psi. \quad (3.65)$$

Comparing both terms leads to:

$$C_\ell^\psi = \frac{2}{\pi} \int_0^{w_s} dw \int_0^{w_s} dw' \frac{w_s - w}{w_s w} \frac{w_s - w'}{w_s w'} \int_0^\infty q^2 dq P_\phi(q) \cdot j_l(qw) j_l(qw'). \quad (3.66)$$

Assuming that typical scales considered here, $2\pi/q$, are much smaller than the cosmological distances w, w' we conclude that $qw \gg 2\pi$. The spherical Bessel functions $j_l(qw)$ are then varying much faster than the potential power spectrum. We can evaluate this power spectrum of the lensing potential at $q = l/w$ using that the spherical Bessel functions peak there, additionally use the fact:

$$\int_0^\infty q^2 dq j_l(qw) j_l(qw') = \frac{\pi}{2w^2} \delta(w - w'), \quad (3.67)$$

and find:

$$C_\ell^\psi = \int_0^{w_s} dw \left(\frac{w_s - w}{w_s w^2} \right)^2 P_\phi \left(\frac{l}{w} \right) \quad (3.68)$$

for the angular power spectrum depending on the gravitational potential power spectrum. One can then replace the gravitational

potential power spectrum P_ϕ by the density power spectrum P_δ , since ϕ and δ are related by the Poisson equation:

$$\nabla^2 \phi = \frac{3}{2a} \frac{H_0^2}{c^2} \Omega_{m0} \delta, \quad (3.69)$$

which translates to:

$$k^2 \hat{\phi} = \frac{3}{2a} \frac{H_0^2}{c^2} \Omega_{m0} \hat{\delta} \quad (3.70)$$

for their respective Fourier transforms and leads to:

$$P_\phi(k) = \frac{9}{4a^2} \frac{H_0^4}{c^4} \Omega_{m0}^2 \frac{P_\delta(k)}{k^4}. \quad (3.71)$$

This transforms the expression for the angular power spectrum to:

$$C_\ell^\psi = \frac{9}{4l^4} \frac{H_0^4}{c^4} \Omega_{m0}^2 \int_0^{w_s} dw \left(\frac{w_s - w}{w_s a(w)} \right)^2 P_\delta \left(\frac{l}{w} \right). \quad (3.72)$$

In order to calculate an angular power spectrum of the convergence (eq. 3.43), we apply two derivatives to the lensing potential in eq. 3.61 and remember that for spherical harmonics

$$\partial^i \partial_i Y_{lm}(\theta) = l(l+1) Y_{lm}(\theta) \approx l^2 Y_{lm} \quad (l \gg 1) \quad (3.73)$$

holds. This, finally, leads to the relation of the angular convergence power spectrum with the power spectrum of the density contrast P_δ :

$$C_\ell^\kappa = \frac{9}{4} \left(\frac{H_0}{c} \right)^4 \Omega_{m0}^2 \int_0^{w_s} dw \left(\frac{w_s - w}{w_s a(w)} \right)^2 P_\delta \left(\frac{l}{w} \right). \quad (3.74)$$

3.6 MEASUREMENT AND UNCERTAINTY

Locally, one can apply the flat-sky approximation assuming again that one can approximate the curved space of the sphere with a two-dimensional Cartesian neighbourhood. We have already introduced the complex shear $\gamma = \gamma_1 + i\gamma_2$. We will also make use of its complex conjugate $\gamma^* = \gamma_1 - i\gamma_2$. In the flat-sky approximation it is possible to calculate the shear's Fourier transform and calculate the power spectrum:

$$C_\ell^\gamma = \langle \hat{\gamma} \hat{\gamma}^* \rangle. \quad (3.75)$$

One can by introducing a differential operator $\tilde{\partial} = \partial_1 + i\partial_2$ and relating convergence and shear to the potential, by $\kappa = \frac{1}{2}\tilde{\partial}^+\tilde{\partial}\psi$ and $\gamma = \frac{1}{2}\tilde{\partial}^2\psi$ respectively, find that

$$C_\ell^\gamma = \langle \hat{\gamma}\hat{\gamma}^* \rangle = \left\langle \frac{l^4}{4}\hat{\psi}\hat{\psi}^* \right\rangle = \langle \hat{\kappa}\hat{\kappa}^* \rangle = C_\ell^\kappa. \quad (3.76)$$

We thereby related the convergence power spectrum, as given in 3.74 to the same quantity for the cosmic shear. For completeness, we also mention the fact that the shear power spectrum is related to the two-point correlation function of shear by the Fourier transform as is the density power spectrum,

$$\tilde{\xi}_\kappa(\theta) = \int_0^\infty \frac{ldl}{2\pi} C_\ell^\kappa J_0(l\theta) = \tilde{\xi}_\gamma(\theta). \quad (3.77)$$

Given a smooth and continuous shear field one could measure this quantity directly. The shear field, however, is not directly measurable. We therefore will sketch in chapter 7 methods to measure cosmic shear and show how [22] suggests to calculate the shear power spectrum from a discrete set of shear values.

MODEL INDEPENDENT COSMOLOGY

INTRODUCTION

In chapter 1 we introduced the function $E(a)$. Being the dynamic part of the Hubble function $H(a) = H_0 E(a) = \frac{\dot{a}}{a}$ it describes the universe's expansion in time and is therefore central for our understanding of the cosmos' history. However, the quantity as given before in eq. 1.27 relies on a certain theoretical framework based on a particular cosmological model. The expansion function for the Λ CDM-universe, for example:

$$E(a) = \sqrt{\Omega_{m0}a^{-3} + \Omega_{r0}a^{-4} + \Omega_{\Lambda0} + \Omega_{K0}a^{-2}}, \quad (4.1)$$

requires a Friedmann universe, i.e. a universe following Friedmann's equations of expansion (eq. 1.19-1.20).

Even more assumptions were made when we wrote down an approximation for the linear growth function $D_+(a)$ which describes the density contrast's (growing) evolution during the linear phase of cosmic structure formation:

$$\delta(a) = D_+(a)\delta_0. \quad (4.2)$$

There we referred to [6, pp. 131-133] who had a close look at different stages of the universe's evolution considering different eras.

Supernovae of type Ia (SNe Ia) are known to be of very high luminosity making them easily observable even at large distances [e.g. 17, 28]. With SNe Ia as standard candles [27] invented a method to determine the expansion solely from observations. [21] then simplified it and applied the new formalism to [39], a large set of SNe-Ia data. They proceeded to derive the linear growth factor $D_+(a)$ by using their own model-independent analysis of $E(a)$. This function is completely parameter-free as well, except for one last remaining degree of freedom: the present-day matter density Ω_{m0} .

In this chapter, we introduce the method of [21] to derive the expansion function $E(a)$ and the linear growth factor $D_+(a)$ purely from observations of SNe Ia [39] with only the basic assumption of spatial symmetries and the current matter density Ω_{m0} as free parameter. This will become essential in order to derive the

central piece of this thesis, a model-independent weak lensing power spectrum.

4.1 DERIVING THE EXPANSION FUNCTION $E(a)$

The aim of this section is to explain how [21] derives $E(a)$ from the sample of supernovae type Ia [39].

We start with a definition of the normalised Chebyshev polynomials T_n :

$$T_n(x) := \begin{cases} \frac{1}{\sqrt{\pi}} & (n = 0) \\ \sqrt{\frac{2}{\pi}} \cos(n \cdot \arccos x) & (n > 0) \end{cases}. \quad (4.3)$$

The Chebyshev polynomials are defined on $[-1, 1]$. Looking to investigate $E(a)$ and $D_+(a)$ with $a \in [0, 1]$ we want to shift the Chebyshev polynomials to the scale factor's domain. The polynomials get shifted to $[0, 1]$ by:

$$T_n^*(x) = T_n(2x - 1). \quad (4.4)$$

These modified Chebyshev polynomials will supply an orthonormal basis system in which we will expand a modified, inverse expansion function. We start by converting measured distance moduli μ_i which are defined as the difference between the apparent magnitude m and the absolute magnitude M , $\mu = m - M$ and related to the distance d by $\mu = 5(\log_{10}(d) - 1)$ to luminosity distances:

$$D_{l,i} = 10^{1+0.2\mu_i} \text{pc} \quad (4.5)$$

and introduce the quantity x :

$$x_i := \frac{a_i - a_{min}}{1 - a_{min}}, \quad (4.6)$$

depending on the scale factor a . We introduce this quantity in order to operate on the same unit interval where the Chebyshev polynomials are normalised. The scale factor is given as discrete a_i in the measurement set. a_{min} refers to the smallest scale factor in the sample corresponding to the farthest object. The *scaled luminosity distance* which we will need later on in equation 4.12, is introduced as:

$$d_i = a_{min}^2 (1 + \delta a \cdot x_i) D_{l,i}, \quad (4.7)$$

where we also defined $\delta a := (1 - a_{min})/a_{min}$.

The application of both transformations provide us with a nicely

scaled set of data. Expressing the radial comoving distance (1.35) in terms of those new coordinates x we find:

$$\begin{aligned} w(x) &= \int_t^{t_0} \frac{cdt'}{a(t')} = \int_x^1 \frac{cdx'}{a(x')\dot{x}'} \\ &= \frac{c}{H_0} \int_x^1 \frac{dx' e(x')}{a_{min}}. \end{aligned} \quad (4.8)$$

In the last step we introduce:

$$e(x) := [\dot{x}(1 + \delta a \cdot x)]^{-1}. \quad (4.9)$$

Rewriting

$$\begin{aligned} \dot{x}_i &= \dot{a}/(1 - a_{min}) = \dot{a}/(a_{min}\delta a) \\ &= H(a) \frac{a}{a_{min}\delta a} = H_0 E(a) \frac{1 + x \cdot \delta a}{\delta a}, \end{aligned} \quad (4.10)$$

we can write the luminosity distance in a new form:

$$D_l(x) = \frac{w(x)}{a(x)} = \frac{1}{a_{min}^2(1 + x \cdot \delta a)} \int_x^1 dx' e(x'). \quad (4.11)$$

The first equality is of course only possible for vanishing curvature (cf. section 1.6.3). Rescaling by the factor $\frac{1}{a_{min}^2(1+x \cdot \delta a)}$ we find the scaled luminosity distance:

$$d(x) = \int_x^1 dx' e(x'), \quad (4.12)$$

or, similarly,

$$e(x) = -d'(x). \quad (4.13)$$

We can now write the scaled luminosity distance in terms of the shifted Chebyshev polynomials defined earlier:

$$d(x) = \int_x^1 dx' e(x') = \sum_{j=1}^M c_j p_j(x) \quad (4.14)$$

with $p_j(x) := \int_x^1 dx' T_j^*(x')$. Defining $P = (P_{ij})$ with $P_{ij} = p_j(x_i)$ we introduce the vector of coefficients, \vec{c} by:

$$\vec{d} = P\vec{c}. \quad (4.15)$$

By \vec{d} we denote the data vector consisting of our data points d_i . We furthermore define a covariance matrix of the data vector by $C = \langle \vec{d} \otimes \vec{d} \rangle$. Then the maximum likelihood solution for \vec{c} is given as:

$$\vec{c} = \left(P^T C^{-1} P \right)^{-1} \left(P^T C^{-1} \right) \vec{d}. \quad (4.16)$$

These components of \vec{c} can then be converted to the expansion function via 4.10-4.14.

4.1.1 Errors $\Delta E(a)$

Before we introduce the method from [21] for calculating D_+ , we turn to the calculation of the uncertainties of the expansion function.

We write down the Fisher matrix:

$$F = P^T C^{-1} P, \quad (4.17)$$

which is then rotated into its eigenframe by an appropriate matrix R resulting in a diagonal matrix F' :

$$F' = R^T F R. \quad (4.18)$$

The eigenvalues of this matrix, i.e. its diagonal entries, give rise to a vector of uncertainties:

$$\Delta c'_i = \sigma'_i. \quad (4.19)$$

Rotating the vector $\Delta \vec{c}' = (\Delta c'_i)$ back into the original frame we arrive at:

$$\Delta \vec{c} := R^T \Delta \vec{c}'. \quad (4.20)$$

These errors propagate via 4.10-4.14 to the uncertainties to $E(a)$ providing us with estimates for $\Delta E(a)$.

4.2 THE LINEAR GROWTH FUNCTION $D_+(a)$

We also want to present the second part of [21] which is the derivation of a model-independent $D_+(a)$ which we will use in chapter 5 for the calculation of the power spectrum. In order to understand the growth function properly we turn again to the solution of eq. 2.21 for vanishing pressure reading:

$$\ddot{\delta} + 2H\dot{\delta} = 4\pi G\rho_0\delta. \quad (4.21)$$

The solution to this equation can be written as:

$$\delta(\vec{x}, t) = f(\vec{x}) \cdot D(t) \quad (4.22)$$

as there are no mixed spatial and temporal derivatives in 4.21 which is homogeneous in δ . There are two solutions $D_{\pm}(t)$ to this differential equation of second order of which we only shall consider the growing one named D_+ as the decreasing one is not

relevant for our purpose. We transform the differential equation 4.21 from time t to the scale factor a and find with:

$$\frac{d}{dt} = aH_0E(a)\frac{d}{da}, \quad (4.23)$$

$$\frac{d^2}{dt^2} = aH_0^2E(a) \left[(E(a) + aE'(a)) \frac{d}{da} + aE(a) \frac{d^2}{da^2} \right], \quad (4.24)$$

that 4.21 translates to:

$$D_+'' + \left(\frac{3}{a} + \frac{E'(a)}{E(a)} \right) D_+ = \frac{3}{2} \frac{\Omega_m}{a^2} D_+, \quad (4.25)$$

where we again used the density parameter $\Omega_m = \rho/\rho_{\text{crit}}$ as defined in 1.25. In order to solve this equation we set the initial condition for the linear growth function to be:

$$D_+(a_{\text{min}}) = 1. \quad (4.26)$$

We assume that the linear growth factor follows a power law in this early stages of cosmic expansion:

$$D_+(a) = a^n. \quad (4.27)$$

Plugging this ansatz into the differential equation for D_+ two solutions for the exponent n arise:

$$n_{\pm} = \frac{1}{4} \left(-1 - \epsilon \pm \sqrt{(1 + \epsilon)^2 + 24(1 - \omega)} \right). \quad (4.28)$$

Here, we introduced the two parameters:

$$\begin{aligned} \epsilon &:= 3 + 2 \frac{d \log E}{d \log a} = 3 + 2 \frac{a}{E(a)} \frac{dE(a)}{da}, \\ \omega &:= 1 - \Omega_m(a). \end{aligned} \quad (4.29)$$

We choose the positive, growing solution, abbreviate $n := n_+$ and find for small parameters ϵ, ω in the matter-dominated era:

$$n \approx 1 - \frac{\epsilon + 3\omega}{5}. \quad (4.30)$$

The first parameter ϵ can be fixed knowing $E(a)$ and the second one can be determined by choosing the only remaining free parameter Ω_{m0} , knowing that the time-dependent matter density parameter behaves like:

$$\Omega_m(a) = \Omega_{m0} E^{-2}(a) a^{-3}. \quad (4.31)$$

Knowing both parameters, we can deduce n and are able to calculate the growth function when considering the second initial condition:

$$\begin{aligned} D'_+(a)|_{a=a_{min}} &= \left. \frac{d}{da} a^n \right|_{a=a_{min}} = n \cdot a^{n-1} \Big|_{a=a_{min}} \\ &= n \cdot \frac{a^n}{a} \Big|_{a=a_{min}} = \left\{ \frac{n}{a} D_+(a) \right\} \Big|_{a=a_{min}} = \frac{n}{a_{min}}. \end{aligned} \quad (4.32)$$

After solving the equation 4.25 with the two boundary conditions for D_+ and D'_+ at $a = a_{min}$ we can renormalise (which we can do because equation 4.25 is homogeneous):

$$D_+(a = 1) := 1. \quad (4.33)$$

In order to determine the uncertainty of the growth function we consider the uncertainty of the expansion function propagating to the growth function. We realise that the uncertainty gets smaller towards $a = 1$. [21] traces this behaviour of $\Delta D_+(a)$ back to the choice of normalisation 4.33. As in [21] we will give the $D_+(a)$ for a realistic matter density parameter $\Omega_{m0} = 0.3$ in the next section together with the results for the expansion function $E(a)$.

4.3 RESULTS FROM HAUDE ET AL. [21]

In this section, we present the expansion function $E(a)$ as given in [21] and compare it to the expansion function as derived from a standard Λ CDM-model cosmology from eq. 1.27. The SNe Ia sample [39] covers supernovae in a range of redshifts corresponding to scale factors from 0.31 to 1. By applying the method described in 4.1 they derive both the expansion function as well as its uncertainty with 3 significant coefficients, i.e. coefficients satisfying:

$$|c_j| \geq \Delta c_j. \quad (4.34)$$

[21] explain the small uncertainties by the fact of the entire information of SNe data being compressed into the three coefficients. They find an expansion function which would be best fitted by a very simple Λ CDM-Model with:

$$E(a) = \sqrt{\Omega_{m0} a^{-3} + 1 - \Omega_{m0}}, \quad (4.35)$$

where the best-fit present-day matter density Ω_{m0} is given by $\Omega_{m0} = 0.324 \pm 0.002$. We show both the curve derived by [21]

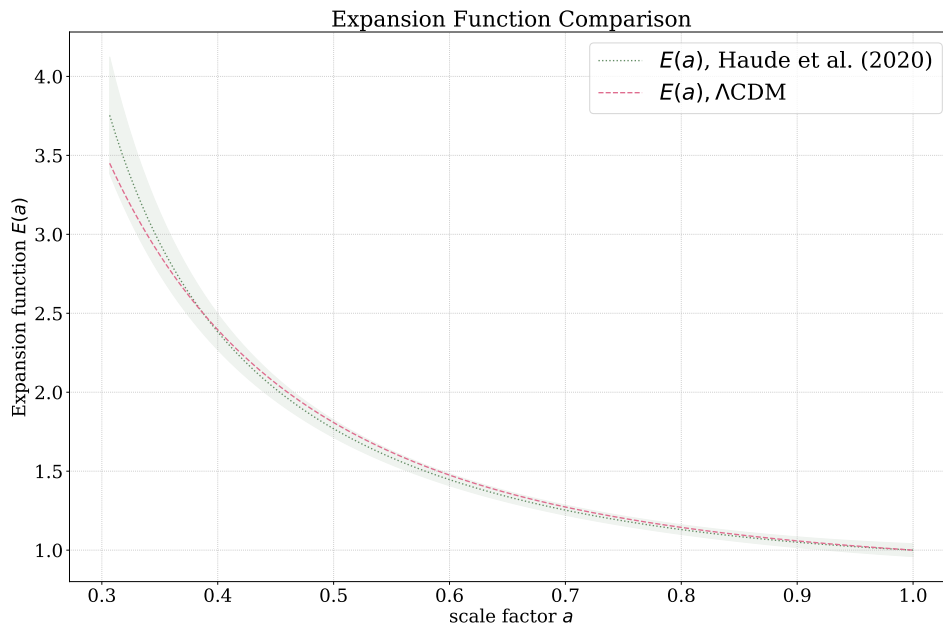


Figure 4.1: Expansion function. We show the expansion function provided by [21] from their method of model-independent cosmology. This curve, a dotted line here, is shown with its uncertainty in green. In order to compare the curve to an expansion function (eq. 4.35) in a Λ CDM universe we show this one as well as a dashed line in pink, using the value for Ω_{m0} as provided by [21]. As the SNe Ia sample [39] used by [21] only provides data within a scale factor range $a \in [0.3067, 1]$ we also choose to show the Λ CDM-curve only in this range for there is no possibility to compare it to the model-independent results elsewhere.

as well as the curve obtained by their fitting function with their best-fit 4.35 with $\Omega_{m0} = 0.324$ in Fig. 4.1.

Analysing the growth of cosmic structures we also want to discuss their findings for the linear growth function $D_+(a)$, describing the growth of structures in the linear phase of structure formation. We compare the curve obtained with the method of [21] to the one obtained with the standard theory of a Λ CDM cosmology (eq. 2.27) in Fig. 4.2, again using the same parameter for the present-day matter density.

CONCLUDING REMARKS

In this chapter, we demonstrated how [21] improved the method of [27] to infer a parameter-free expansion function $E(a)$ from a

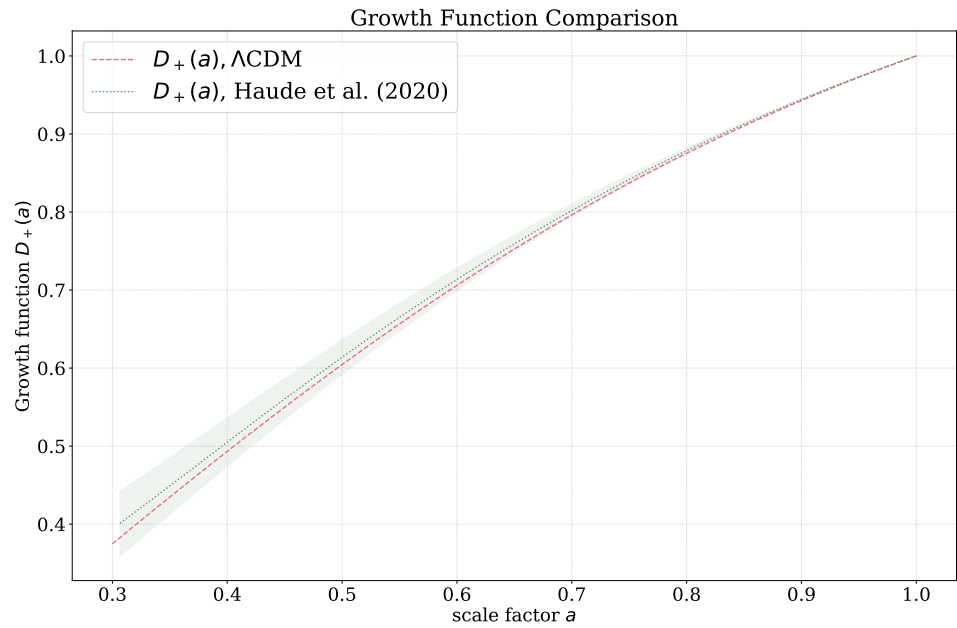


Figure 4.2: Linear growth function $D_+(a)$. We show the growth function provided by [21] derived by the method discussed in 4.2. The only parameter used is $\Omega_{m0} = 0.3$. The result is shown as a dashed green line together with its uncertainty. In order to compare their result to a growth function in the standard model of cosmology we also show a growth function obtained by a classical approximation as dotted pink line.

large set of supernovae measurements [39] and used this result to further calculate a model-independent growth factor $D_+(a)$ leaving the present-day matter density as the only parameter to be fixed. Both results are essential for our aim of building a model-independent weak lensing power spectrum as we will discuss later on in chapter 6.

The comparison of both quantities $E(a)$ and $D_+(a)$ with predictions from theory in the cosmological standard model Λ CDM shows good agreement of the model-independent and the theory-predicted curves in both cases well within the uncertainties of the model-independent expansion and growth functions.

The best fit matching the expansion function alone is found for $\Omega_{m0} = 0.324$ which is a value for the present-day matter density parameter only slightly larger than the one measured by [35] ($\Omega_{m0} = 0.3147 \pm 0.0074$).

In this chapter we introduce the Kinetic Field Theory (KFT) as developed and explained in [5, 8, 10, 11, 20, 47]. KFT was developed in order to apply a formalism of statistical field theories to classical particles with a focus on calculating key quantities in cosmology. In particular, a closed, analytic, non-perturbative and parameter-free equation for the non-linear density fluctuation power spectrum (cf. chapter 2, eq. 2.28) was derived. As we need this power spectrum for our calculation of the angular weak lensing power spectrum (as discussed in chapter 3, eq. 3.74) we will introduce KFT only to the point where we will be able to compute the density fluctuation power spectrum. We want to mention, however, that KFT has been used for further analyses explaining the density profile of dark matter haloes, computing velocity power spectra and even in applications to cold Rydberg atoms. As the latter one is a system quite different to cosmological applications the variety of applications is rather remarkable. For those and other applications of KFT we refer to the review [11]. It is also this review which we will *closely* follow in order to present KFT in this chapter. We will however extend our discussion of KFT by some parts we took from [10].

We start by introducing the *generating functional* of KFT (5.1), the central object of the theory and continue by extracting information from this functional in the next section (5.3). We will then adapt and use the formalism developed so far for applications in cosmology (5.4-5.7) and elaborate on how to derive both the free density fluctuation power spectrum (5.8) as well as an approximate expression for the non-linear density fluctuation power spectrum including particle interactions (5.9).

5.1 THE GENERATING FUNCTIONAL

The first and central mathematical object of Kinetic Field Theory is the generating functional Z , defined as:

$$Z = \int \mathcal{D}\phi(\mathbf{x}) P[\phi(\mathbf{x})] \exp \left\{ i \int d\mathbf{x} \langle O(\mathbf{x}), \phi(\mathbf{x}) \rangle \right\}, \quad (5.1)$$

where $P(\phi)$ is the probability distribution of states ϕ . We furthermore introduced a source field O . We will elaborate on the purpose of such source fields later on.

It can be very helpful to think of this generating functional as a modification of the partition sum from statistical mechanics as it incorporates a probability distribution $P(\phi)$ and integrates over all states ϕ . If however the state space is a function space rather than ordinary phase space, it generalises to a path integral which is reflected in the definition 5.1.

Considering a canonical ensemble of N classical particles the state space is given by the phase space Γ of the particles with trajectories (q_j, p_j) with $q \in \mathbb{R}^3$ and $p \in \mathbb{R}^3$, the position and momentum of a particle which is labelled by j . We define this tuple as $x_j := (q_j, p_j)$. We furthermore introduce the tensorial object:

$$\mathbf{x} = x_j \otimes e_j. \quad (5.2)$$

Again, the summation over repeated indices is implied, $x_j \otimes e_j = \sum_j x_j \otimes e_j$. We want to point out that $\mathbf{x} = \mathbf{x}(t)$ is a time-dependent variable although we will not always write down the time dependence explicitly. The unit vector e_j has nonvanishing components only at j -th position, $(e_j)_i = \delta_{ij}$, where we use the Kronecker delta. For the newly introduced tensor we define a scalar product:

$$\langle \mathbf{x}, \mathbf{y} \rangle = x_j \cdot y_j. \quad (5.3)$$

This implies that the vector x of particle j is multiplied only with the vector y of the very same particle.

The generating functional can be written down as an ordinary integral over the phase space of the N particles considered. This is possible as the integral over trajectories turns into an (ordinary) integral over possible starting points since the trajectories of the particles (which are described with Dirac delta functions) are deterministic.

In order to – in analogy to a quantum field theory – extract cumulants from the generating functional later on we start introducing *auxiliary generator fields*. In order to obtain the average position of a particle j , for example, we introduce the conjugate field \mathbf{J} into the generating functional:

$$Z[\mathbf{J}] = \int d\mathbf{x} P(\mathbf{x}) \exp \left\{ i \int_0^\infty dt' \langle \mathbf{J}(t'), \mathbf{x}(t') \rangle \right\} \quad (5.4)$$

and apply a functional derivative with respect to J_j before setting $\mathbf{J} = 0$ again:

$$\langle x_j(t) \rangle = -i \frac{\delta}{\delta J_j(t)} Z[\mathbf{J}] \Big|_{\mathbf{J}=0}. \quad (5.5)$$

The tensor \mathbf{J} itself has components J_{q_j}, J_{p_j} and is constructed similarly to the tensor \mathbf{x} via:

$$\mathbf{J} = \begin{pmatrix} J_{q_j} \\ J_{p_j} \end{pmatrix} \otimes e_j. \quad (5.6)$$

In a next step, the probability $P(\mathbf{x})$ is split up into the probability of the ensemble occupying an initial state $P(\mathbf{x}^{(i)})$ and the corresponding conditional transition probability $P(\mathbf{x}|\mathbf{x}^{(i)})$:

$$P(\mathbf{x}) = \int d\mathbf{x}^{(i)} P(\mathbf{x}|\mathbf{x}^{(i)}) P(\mathbf{x}^{(i)}). \quad (5.7)$$

The transition probability $P(\mathbf{x}|\mathbf{x}^{(i)})$ for trajectories in classical mechanics can be described by a functional delta distribution with the Hamiltonian flow $\Phi_{cl}(\mathbf{x}^{(i)})$:

$$P(\mathbf{x}|\mathbf{x}^{(i)}) = \delta_D[\mathbf{x} - \Phi_{cl}(\mathbf{x}^{(i)})]. \quad (5.8)$$

With the equation of motion written as $E(\mathbf{x}) = 0$ the Hamiltonian flow is given by all solutions of this equation for initial points within a given domain of phase space Γ . The solutions of the classical equation of motion with initial points at $\mathbf{x}^{(i)}$ can be written as $E(\mathbf{x}, \mathbf{x}^{(i)}) = 0$. The former transition probability (eq. 5.8) is then given by:

$$P(\mathbf{x}|\mathbf{x}^{(i)}) = \delta_D[E(\mathbf{x}, \mathbf{x}^{(i)})]. \quad (5.9)$$

This singles out the solutions of the equations of motion as the only possible trajectories which is a sensible statement for classical mechanics.

5.2 EQUATIONS OF MOTION

We now want to solve the equations of motion. With the symplectic matrix:

$$\mathcal{I} := \begin{pmatrix} 0 & \mathcal{I}_3 \\ -\mathcal{I}_3 & 0 \end{pmatrix}, \quad (5.10)$$

we can write down the equation of motion for a single particle as:

$$\dot{x} - \mathcal{I}\nabla_x H = 0, \quad (5.11)$$

with the Hamiltonian H which will be specified for our purpose later on and three-dimensional unit matrices \mathcal{I}_3 . For non-interacting particles the Hamiltonian equations are linear, allowing for a solution using a Green's function $G(t, t')$. In order to prepare for interactions, however, we can amend the equation 5.11 by a source term K leading to solutions:

$$\bar{x}(t) = G(t, 0)x^{(i)} + \int_0^t dt' G(t, t')K(t'). \quad (5.12)$$

Assuming that the interactions between particles can be characterised with a potential V the source term is:

$$K(t') = (0, -\nabla V(t'))^T. \quad (5.13)$$

As x is a six-dimensional vector G must be a 6×6 matrix consisting of three blocks $g_{qq}\mathcal{I}_3$, $g_{qp}\mathcal{I}_3$ and $g_{pp}\mathcal{I}_3$. The g_{ij} -propagators can themselves be interpreted as a measure of time. In order to write down a solution for all ensemble particles \bar{x} we need to construct both a Green's function $\mathbf{G}(\mathbf{t}, \mathbf{t}') = G(t, t') \otimes \mathcal{I}_N$ and a suitable source field $\mathbf{K} := K_j \otimes e_j$ for *all* of the N particles. Then, we can write:

$$E(\mathbf{x}, \mathbf{x}^{(i)}) = \mathbf{x}(t) - \bar{\mathbf{x}}(t) = 0. \quad (5.14)$$

This allows for a reformulation of the generating functional:

$$\begin{aligned} Z[\mathbf{J}] &= \int d\mathbf{x}^{(i)} \int d\mathbf{x} \delta_D(\mathbf{x} - \bar{\mathbf{x}}) P(\mathbf{x}^{(i)}) \cdot \exp \left\{ i \int_0^\infty dt' \langle \mathbf{J}(t'), \mathbf{x}(t') \rangle \right\} \\ &= \int d\mathbf{x}^{(i)} P(\mathbf{x}^{(i)}) \exp \left\{ i \int_0^\infty dt' \langle \mathbf{J}(t'), \bar{\mathbf{x}}(t') \rangle \right\} \\ &:= \int d\Gamma \exp \left\{ i \int_0^\infty dt' \langle \mathbf{J}(t'), \bar{\mathbf{x}}(t') \rangle \right\}, \end{aligned} \quad (5.15)$$

where we introduce $d\Gamma := d\mathbf{x}^{(i)} P(\mathbf{x}^{(i)})$.

5.3 DENSITY

In order to obtain the cosmic density which we will need for the calculation of the density fluctuation power spectrum (cf.

eq. 2.28) from the generating functional we define a density operator. The cosmic number density at a given time is:

$$\rho(q, t_1) = \sum_{j=1}^N \delta_D(q - q_j(t_1)). \quad (5.16)$$

Here, we again used that the system consists of N particles at their respective positions q_j . After a Fourier transformation we find for Fourier mode k_1 :

$$\tilde{\rho}(k_1, t_1) = \sum_{j=1}^N \exp \{ -ik_1 \cdot q_j(t_1) \}. \quad (5.17)$$

The tilde indicates the Fourier representation of the density. We shall henceforth omit the tilde and assume operations in Fourier space from now on. For further analysis we start to abbreviate the arguments $(1) = (k_1, t_1)$ and $(-1) = (-k_1, t_1)$.

The position q_j contained in the expression for the density can now be substituted by a functional derivative with respect to the q_j -th component of the auxiliary field \mathbf{J} at time t_1 :

$$\hat{\rho}_j(1) := \exp \left\{ -k_1 \frac{\delta}{\delta J_{q_j}(t_1)} \right\}. \quad (5.18)$$

Summing up those operators for single particles we find the density operator:

$$\hat{\rho}(1) = \sum_{j=1}^N \hat{\rho}_j(1), \quad (5.19)$$

leading to a density of the form 5.17 when applied. Noticing, that the one-particle operator 5.18 contains a functional derivative in the exponential we realise that the application of this operator corresponds to a shift of the generator field. This shift amounts after r applications of the density operator to:

$$\Delta \mathbf{J} = - \sum_{j=1}^r \delta_D(t' - t_j) \cdot \begin{pmatrix} k_j \\ 0 \end{pmatrix} \otimes e_j. \quad (5.20)$$

The generating functional can then, after setting $\mathbf{J} = 0$ again, be written as:

$$Z[\mathbf{L}] = \int d\Gamma \exp \{ i \langle \mathbf{L}_q, \mathbf{q} \rangle + i \langle \mathbf{L}_p, \mathbf{p} \rangle + i S_I \}, \quad (5.21)$$

where we introduce a shift vector \mathbf{L} with:

$$\mathbf{L}_q = - \sum_{j=1}^r k_j \otimes e_j, \quad (5.22)$$

and

$$\mathbf{L}_p = - \sum_{j=1}^r k_j g_{qp}(t_j) \otimes e_j, \quad (5.23)$$

as well as the interaction term:

$$S_I = \sum_{j=1}^r k_j \int_0^{t_j} dt' g_{qp}(t_j, t') \nabla_j V(t'). \quad (5.24)$$

Comparing the generating functional 5.21 with the former expression, we must stress that the given positions and momenta \mathbf{q}, \mathbf{p} correspond to the components of the *initial* phase space tensor $\mathbf{x}^{(i)}$. It is also worth mentioning that up to this point the formalism has not been specified for a particular application except for the assumption that we can trace back any interaction to an interaction potential.

Assuming that the potential V can be expressed as a linear superposition of potential contributions by different particles we can further develop an interaction operator \hat{S}_I in order to separate the interaction part of 5.21 from the *free* generating functional Z_0 :

$$Z[\mathbf{L}] = \exp \{i\hat{S}_I\} Z_0[\mathbf{L}], \quad (5.25)$$

where we defined

$$Z_0[\mathbf{L}] = \int d\Gamma \exp \{i \langle \mathbf{L}_q, \mathbf{q} \rangle + i \langle \mathbf{L}_p, \mathbf{p} \rangle\}. \quad (5.26)$$

5.4 COSMOLOGICAL APPLICATIONS

Contrary to our choice in chapter 1 we choose to normalise the scale factor to unity, $a(0) = 1$, at the initial time $t = 0$. As we can renormalise later on this is merely a convenient choice. In comoving coordinates we can write the Lagrangian of a particle of mass m as:

$$L(q, \dot{q}, t) = \frac{m}{2} a^2 \dot{q}^2 - m\Phi. \quad (5.27)$$

The gravitational potential Φ is again connected to the surrounding density via the Poisson equation:

$$\nabla^2 \Phi = 4\pi G a^2 (\rho - \rho_0). \quad (5.28)$$

With an expression for the mean cosmic density ρ_0 early in the matter-dominated epoch, implying $\Omega_{m,i} = 1$, which we want to choose as initial time, one can reformulate the Poisson equation in terms of the density contrast δ (cf. eq. 2.13):

$$\nabla^2 \Phi = \frac{3}{2} H_i^2 \frac{\delta}{a}. \quad (5.29)$$

In chapters 2 and 4 (e.g. eq. 2.26), we introduced and discussed the linear growth-factor D_+ . This function can also be used as a measure of cosmic time. Before we are able to introduce an appropriate Lagrange function for the system we introduce the two functions:

$$g(t) := a^2 D_+ f H, \quad f := \frac{d \log D_+}{d \log a}, \quad (5.30)$$

as well as a modified potential $\bar{\Phi}$ by:

$$\nabla^2 \bar{\Phi} = \frac{3a}{2g} \delta. \quad (5.31)$$

We introduce the new time coordinate D_+ , which we get from $t \rightarrow D_+(t) - D_+(0)$ with $t = 0$ corresponding to an initial time 0 at a moment in the matter dominated epoch where the density fluctuations are sufficiently small for us to remain in the linear phase. Typically, one chooses the time of recombination.

Using the gauge invariance of classical mechanics and by recalling the action principle to find an appropriate transformation to the new time coordinate we can find a *modified* Lagrangian for the newly introduced coordinate of time:

$$\bar{L} = \frac{g}{2} \dot{q}^2 - \bar{\Phi}. \quad (5.32)$$

By defining a reduced potential $\phi = \bar{\Phi}/g$ obeying $\nabla^2 \phi = \frac{3a}{2g^2} \delta$ the equation of motion is given by:

$$\ddot{q} + \frac{\dot{g}}{g} \dot{q} + \nabla \phi = 0. \quad (5.33)$$

With the generalised momentum $p = \frac{\partial}{\partial \dot{q}} \bar{L} = g \dot{q}$ we find the Hamiltonian \bar{H} as Legendre transform of \bar{L} :

$$\begin{aligned} \bar{H} &= \dot{q} p - \bar{L}(q, \dot{q}, t) \\ &= \frac{p^2}{g} - \frac{g}{2} \frac{p^2}{g^2} + \bar{\Phi} \\ &= \bar{\Phi} + \frac{p^2}{2g}, \end{aligned} \quad (5.34)$$

which leads to the Hamiltonian equations of motion:

$$\begin{aligned} \dot{q} &= \partial_p \bar{H} \\ &= \frac{p}{g}, \end{aligned} \quad (5.35)$$

$$\begin{aligned} \dot{p} &= -\partial_q \bar{H} \\ &= -\nabla \bar{\Phi}. \end{aligned} \quad (5.36)$$

The equations of motion can be solved by using the Green's function \bar{G} :

$$\begin{pmatrix} q(t) \\ p(t) \end{pmatrix} = \bar{G}(t, t_0) \begin{pmatrix} q_0 \\ p_0 \end{pmatrix} + \int_{t_0}^t \bar{G}(t, t') \begin{pmatrix} 0 \\ -\nabla \bar{\Phi} \end{pmatrix} dt', \quad (5.37)$$

with

$$\begin{aligned} \bar{G}(t, t') &= \begin{pmatrix} \mathcal{I}_3 & \bar{g}_{qp} \\ 0 & \mathcal{I}_3 \end{pmatrix}, \text{ and} \\ \bar{g}_{qp}(t, t') &= \int_{t'}^t \frac{d\bar{f}}{g(\bar{f})}. \end{aligned} \quad (5.38)$$

This propagator $\bar{g}_{qp}(t, t')$ turns out to be limited from above due to cosmic expansion with the result that the description of trajectories with this solution deviates from the *true* trajectories which must include all interactions. In order to account for those, at least in part, one has to introduce more sophisticated propagators like the improved Zel'dovich propagator [4] leading to:

$$\bar{q}^0(t) = \bar{q}^{(i)} + g_{qp}(t, 0) \cdot \bar{p}^{(i)}, \quad (5.39)$$

where the superscript (i) refers to the *initial* position and momentum.

The corresponding propagator is given by:

$$g_{qp}(t, t') = H_i \int_{a'}^a \frac{d\tilde{a}}{\tilde{a}^3 H(\tilde{a})}. \quad (5.40)$$

Here, H_i denotes the Hubble parameter at initial time t_i . We will use this propagator for our calculation of a density fluctuation power spectrum later on.

5.5 INITIAL PROBABILITY DISTRIBUTION

In order to evaluate the generating functional in 5.21 we need to specify the probability distribution $P(\mathbf{x}^{(i)})$ in $d\Gamma$. Recalling the Helmholtz decomposition theorem, a look at the peculiar particle velocities reveals that the decomposition of the velocity field into a curl-free field and a divergence-free field allows us to introduce a velocity potential. The divergence-free component of the field quickly decays due to cosmic expansion and momentum conservation. Calling the velocity potential Ψ we can derive from the linearised continuity equation 2.1:

$$\partial_t \delta + \nabla \cdot \vec{u} = 0, \quad (5.41)$$

that, at early times when $D_+ = 1 = \partial_t D_+$ holds after introducing D_+ as measure of cosmic time ($D_+ = t$) we get:

$$\delta + \nabla^2 \Psi = 0. \quad (5.42)$$

As we assume the initial density fluctuation field δ to be of Gaussian nature, the continuity equation implies the same for the velocity potential Ψ . The same equation enables us to relate the power spectra of both quantities as well. In Fourier space the equation reads:

$$\delta_k + k^2 \Psi_k = 0 \quad (5.43)$$

for the k -th mode, leading to $P_\Psi = k^{-4} P_\delta$. We again used the notation $\delta_k = \delta(\vec{k})$. After drawing particle positions with a probability proportional to δ and choosing momenta for each particle proportional to $\nabla \Psi$ the initial probability distribution is given by:

$$P(\mathbf{x}^{(i)}) = \frac{V^{-N}}{\sqrt{(2\pi)^{3N} \det C_{pp}}} \mathcal{C}(\mathbf{p}) \exp \left\{ \frac{-1}{2} \mathbf{p}^T C_{pp}^{-1} \mathbf{p} \right\}. \quad (5.44)$$

For a derivation of this probability as well as the momentum covariance matrix C_{pp} we refer to [10]. For late times we can set $\mathcal{C}(\mathbf{p}) = 1$ [10, 11]. Defining the variance:

$$\sigma_1^2 = \int_k k^{-2} P_\delta(k) \quad (5.45)$$

we can write down a momentum correlation matrix as sum of the momentum dispersion and of the momentum correlation of particles j and k at a distance $q_{jk} = |q_j - q_k|$:

$$C_{pp} = \frac{\sigma_1^2}{3} \mathcal{I}_3 \otimes \mathcal{I}_N + C_{p_j p_k} \otimes E_{jk}. \quad (5.46)$$

We can trace back the dependence on the *distance* rather than on absolute positions to the cosmological principle introduced earlier (1.1). The expression for momentum dispersion is due to the Gaussian nature of the velocity field where the momenta are drawn from.

5.6 SIMPLIFYING Z_0

In order to further evaluate the free generating functional we use the expression from 5.26 and provide the probability distribution 5.44 to the differential element $d\Gamma$. We perform the \mathbf{p} -integration:

$$\int d\mathbf{p} \exp \left\{ \frac{-1}{2} \mathbf{p}^T C_{pp}^{-1} \mathbf{p} + i \langle \mathbf{L}_p, \mathbf{p} \rangle \right\}, \quad (5.47)$$

change into a coordinate system in which the correlation matrix C_{pp} is diagonal and rewrite the integral as:

$$\int d\mathbf{b} \exp \left\{ \sum_i \frac{-1}{2} b_i^2 \sigma_i^{-2} + i k_i x_i \right\}, \quad (5.48)$$

where the σ_i are the eigenvalues of the correlation matrix and with b_i we denote the elements of the rotated momentum \mathbf{p} . The sum $\sum_i k_i b_i$ is the equivalent of $\langle \mathbf{L}_p, \mathbf{p} \rangle$ in the rotated system. In order to complete the square we add and subtract $0 = \frac{1}{2}(k_i^2 \sigma_i^2 - k_i^2 \sigma_i^2)$ transforming the integral to:

$$\int d\mathbf{b} \prod_i \exp \left\{ \frac{1}{\sigma_i^2} \left(\frac{i}{\sqrt{2}} b_i + \frac{k_i}{\sqrt{2}} \sigma_i^2 \right)^2 - \frac{1}{2} k_i^2 \sigma_i^2 \right\}. \quad (5.49)$$

Since the second argument of the exponential, $-\frac{1}{2} k_i^2 \sigma_i^2$, does not depend on \mathbf{b} any longer, we can pull it out of the integral and solve the remaining integration. The integral then becomes:

$$\begin{aligned} & \exp \left\{ \frac{-1}{2} \sum_i k_i^2 \sigma_i^2 \right\} (2\pi)^{N/2} \sqrt{\prod_i \sigma_i^2} \\ &= \exp \left\{ \frac{-1}{2} \sum_i k_i^2 \sigma_i^2 \right\} (2\pi)^{N/2} \sqrt{\det C_{pp}}. \end{aligned} \quad (5.50)$$

Transforming back to the old coordinate system, we finally find:

$$\begin{aligned} & \int d\mathbf{p} \exp \left\{ \frac{-1}{2} \mathbf{p}^T C_{pp}^{-1} \mathbf{p} + i \langle \mathbf{L}_p, \mathbf{p} \rangle \right\} \\ &= \exp \left\{ \frac{-1}{2} \mathbf{L}_p^T C_{pp} \mathbf{L}_p \right\} (2\pi)^{3N/2} \sqrt{\det C_{pp}}. \end{aligned} \quad (5.51)$$

For the factors conveniently cancel with those in 5.44 the free generating functional reduces to:

$$Z_0[\mathbf{L}] = V^{-N} \int d\mathbf{q} \exp \left\{ \frac{-1}{2} \mathbf{L}_p^T C_{pp} \mathbf{L}_p + i \langle \mathbf{L}_q, \mathbf{q} \rangle \right\}. \quad (5.52)$$

5.7 THE FACTORISED $Z_0[\mathbf{L}]$

This expression can now be factorised [10, section 2.3, App. B]. We will not derive the factorisation in detail as it was laid out beautifully in [10]. The result of the factorisation is:

$$Z_0[\mathbf{L}, 0] = V^{-l} (2\pi)^3 \delta_D \left(\sum_{j=1}^l \vec{L}_{q_j} \right) \cdot \exp \left\{ -\frac{1}{2} (Q_0 - Q_D) \right\} \prod_{2 \leq b < a}^l \int_{k_{ab}} \prod_{1 \leq k < j}^l (\Delta_{jk} + \mathcal{P}_{jk}), \quad (5.53)$$

with:

$$k = 1 \dots (l-1), \quad j = (k+1) \dots l, \quad (5.54)$$

$$b = 2 \dots (l-1), \quad a = (b+1) \dots l, \quad (5.55)$$

and:

$$\begin{aligned} \mathcal{P}_{jk} &= \mathcal{P}(\vec{k}_{jk}, \tau) \\ &= \int_q \left(\exp \left\{ g_{qp}^2(\tau, 0) k_{jk}^2 \left(a_{\parallel} \lambda_{jk}^{\parallel} + a_{\perp} \lambda_{jk}^{\perp} \right) \right\} - 1 \right) e^{i\vec{k}_{jk}\vec{q}}, \end{aligned} \quad (5.56)$$

which is a nonlinearly time-evolved density fluctuation power spectrum. This interpretation of \mathcal{P} will arise when we consider the simplest possible case, $l = 2$. Then the free generating functional contains the information on the two-point correlator, i.e. the density fluctuation power spectrum. We will discuss this in section 5.8. We abbreviated the damping terms in Z_0 by:

$$Q_0 := \frac{\sigma_1^2}{3} \left(\sum_j \vec{L}_{p_j} \right)^2, \quad \text{and} \quad (5.57)$$

$$Q_D := \frac{\sigma_1^2}{3} \sum_{j \neq k} \vec{L}_{p_j} \cdot \vec{L}_{p_k}. \quad (5.58)$$

Furthermore, we abbreviated:

$$\Delta_{jk} := (2\pi)^3 \delta_D(\vec{k}_{jk}), \quad (5.59)$$

and defined the wave vectors:

$$\vec{k}_{jk} := \begin{cases} \vec{L}_{q_j} - \sum_{b=2}^{j-1} \vec{k}'_{jb} + \sum_{a=j+1}^l \vec{k}'_{aj} & k = 1 \\ \vec{k}'_{jk} & k > 1. \end{cases} \quad (5.60)$$

A few more definitions are needed in order to calculate the above quantities. The λ factors are defined as:

$$\lambda_{jk}^{\parallel} := \frac{\vec{L}_{p_j}^T \pi_{jk}^{\parallel} \vec{L}_{p_k}}{g_{qp}^2(\tau, 0) k_{jk}^2}, \quad (5.61)$$

$$\lambda_{jk}^{\perp} := \frac{\vec{L}_{p_j}^T \pi_{jk}^{\perp} \vec{L}_{p_k}}{g_{qp}^2(\tau, 0) k_{jk}^2}, \quad (5.62)$$

and the projectors π are

$$\pi_{jk}^{\parallel} = \hat{k} \otimes \hat{k}, \quad (5.63)$$

$$\pi_{jk}^{\perp} = \mathcal{I}_3 - \pi_{jk}^{\parallel}. \quad (5.64)$$

5.8 THE KFT MATTER DENSITY FLUCTUATION POWER SPECTRUM

For a simple two-point-function the factorised, free generating functional reduces to:

$$Z_0[\mathbf{L}] = (2\pi)^3 \delta_D(k_1 + k_2) V^{-2} \exp\{-Q_0\} \mathcal{P}(k_1, t). \quad (5.65)$$

Having applied the two density-operators the functional must contain the information on the evolution of the density - fluctuation power spectrum without considering interaction. For the two particle case, the non-linearly evolved power spectrum \mathcal{P} appearing in the free generating functional is:

$$\mathcal{P}(k_1, t) := \int_q \left(e^Q - 1 \right) \exp\{ik_1 \cdot q\}. \quad (5.66)$$

Here:

$$Q_0 := \frac{\sigma_1^2}{3} g_{qp}^2(t) k_1^2, \quad Q := -g_{qp}^2(t) k_1^2 a_{\parallel}(q), \quad (5.67)$$

Q_0 in particular acts as a damping term originating in momentum dispersion (hence the factor $\sigma_1^2/3$). The correlation function a_{\parallel} is in turn defined as:

$$a_{\parallel}(q) := a_1(q) + \mu^2 a_2(q), \quad (5.68)$$

and depends on the distance q and the separation angle $\mu = \cos(\alpha)$ with α being the angle enclosed by k_1 and q . The function a_{\parallel} is a function correlating those components of the momentum

which are parallel (\parallel) to the connecting line of both particle positions, q_{12} . The two auxiliary functions a_i are given by:

$$a_1(q) = \frac{-1}{2\pi^2} \int_0^\infty dk P_\delta(k) \frac{j_1(kq)}{kq}, \quad (5.69)$$

$$a_2(q) = \frac{1}{2\pi^2} \int_0^\infty dk P_\delta(k) j_2(kq). \quad (5.70)$$

As usual, the j_i denote spherical Bessel functions [e.g. 16]. Considering the exponential only up to linear order and considering the small- q limits for a_\parallel we arrive at a linearly evolving power spectrum:

$$\mathcal{P}(k, t) \approx g_{qp}^2(t) P_\delta(k), \quad (5.71)$$

which we will show in Fig. 5.1.

5.9 A NOTE ON INTERACTIONS

There are different methods to account for particle interactions in the generating functional discussed, e.g., in [11]. A possible path is to use the *Born approximation* [9]. Another way is to average the interaction term in 5.25 [7]. We will use the results of the Born approximation in order to have access to a fully nonlinear power spectrum. By considering 5.25, we can see that it is possible to write the power spectrum with interactions like:

$$\bar{\mathcal{P}} = \exp \{-Q_0 + iS_I\} \mathcal{P}(k, t). \quad (5.72)$$

Considering particle trajectories [6] introduced an effective force $f(t)$ [6, eq. 62] in order to write down the interaction term as:

$$S_I(t) = -k_1 \cdot \int_0^t dt' g_{qp}(t, t') (f_1(t') - f_2(t')), \quad (5.73)$$

where f_j denotes the force $f(t)$ acting on particle j . The force terms can then be re-written as:

$$f_1(t) - f_2(t) = f_{12} - f_{21} + \sum_{j=3}^N (f_{1j} - f_{2j}), \quad (5.74)$$

and f_{ij} is the force $f(t)$ on particle i exerted by particle j . Considering those particles, we know that $f_{ij} = -f_{ji}$ and thus $f_{ij} - f_{ji} = 2f_{ij}$. Using the argument of isotropy and neglecting higher-order correlations [11] omit the sum $\sum_{j=3}^N (f_{1j} - f_{2j})$ on the right hand side of the equation 5.74 as the forces exerted by particles 3 to N will cancel on average. This leads to:

$$S_I(t) = -2k_1 \cdot \int_0^t dt' g_{qp}(t, t') f_{12}(t'). \quad (5.75)$$

When we introduced the growth factor as measure of time we also introduced a reduced potential $\phi = \bar{\Phi}/g$.

The potential v of a unit point mass in the considered system can in Fourier-space be written by:

$$\tilde{v}(t) = \frac{-3a}{2\rho_0 k^2 g^2}. \quad (5.76)$$

We look at the gradient of the potential of a particle j at the position of particle i which of course constitutes the force term f_{ij} . This force term is needed for the description of the action. The potential gradient is given by:

$$\nabla_i \phi_j(t) = \frac{-3ia}{2\rho_0 g^2} \int_k \frac{k}{k^2} \exp(ik \cdot (q_i(t) - q_j(t))). \quad (5.77)$$

It is quite complicated to evaluate this potential gradient. The Born approximation replaces:

$$q_j(t) \rightarrow q_j^{(i)} + g_{qp}(t)p_j^{(i)}. \quad (5.78)$$

This allows to find an approximate expression for the force f_{ij} . We will however not give this derivation, but refer to [11] for a detailed expression of both the derivation and the discussion of the evaluated force term.

We show the comparison of a numerically emulated power spectrum [44], the nonlinear power spectrum from KFT and the linearly evolved power spectrum in Fig. 5.1, finding large deviations only on very small scales, whereas the shape of the power spectra show remarkable resemblance.

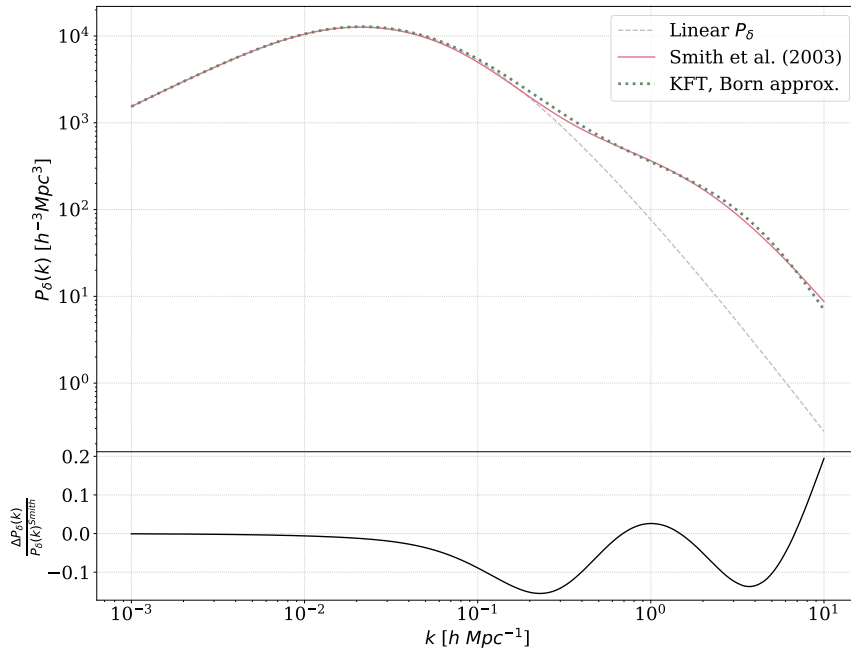


Figure 5.1: Comparing matter density fluctuation power spectra. The linearly evolved power spectrum (silver, dashed line) is compared to the numerically obtained nonlinear power spectrum (green, dotted line) as well as to the analytically calculated nonlinear power spectrum from Kinetic Field theory (pink continuous line) in the upper panel. The lower panel shows the relative difference $\frac{p_\delta^{\text{Smith}} - p_\delta^{\text{KFT}}}{p_\delta^{\text{Smith}}}$ of the two nonlinear power spectra.

Part II

WEAK LENSING POWER SPECTRA

THE PARAMETER-FREE WEAK LENSING POWER SPECTRUM

INTRODUCTION

It is still difficult to use observational methods in order to directly prove or disprove theories addressing the problem of structure formation, let alone to investigate the nature and behaviour of the cosmic dark sector. Measuring the density power spectrum for example, being a central object of statistical structure formation theory, proves to be challenging and must often be evaluated via biased tracers, such as galaxies or with numerical simulations.

Gravitational lensing however is a well-tested method to observe the distribution of matter, independent of its nature, being sensitive to gravity only. The angular weak lensing power spectrum C_l^γ introduced in chapter 3 in particular provides us with a method to observe a two-point correlator $\langle \bar{\gamma} \bar{\gamma}^* \rangle$. This in turn, by its relation to the matter density power spectrum $P_\delta(k)$, allows to test predictions of structure formation theories without relying on either numerical simulations or biased tracers.

By calculating the angular power spectrum of weak gravitational lensing from the Kinetic Field Theory we provide a method to probe this new theory of cosmic structure formation with a quantity which can be obtained from new large field surveys like *Euclid* [1] which will provide an extensive dataset for lensing analyses.

The theoretical expression for the angular weak lensing power spectrum, as defined in eq. 3.74, however, does depend on a specific cosmological model when making use of a specific distance measure and a particular form of the density power spectrum. This introduces a further source of possible errors. The issue can be addressed by providing the quantities needed, in our case the expansion function and the power spectrum obtained with as little assumptions on the cosmology as possible.

With a well-calibrated measured lensing power spectrum (which we will discuss in chapter 7) this allows us to test and improve the theory behind the theoretical prediction, whenever we have a nicely calibrated set of lensing data at hand.

According to our own derivation, based on the review [4], in chapter 3, equation 3.74, the angular lensing power spectrum $C_l^\kappa = C_l^\gamma$ is defined as:

$$C_l^\gamma = \frac{9}{4} \left(\frac{H_0}{c} \right)^4 \Omega_{m0}^2 \int_0^{w_s} dw \left(\frac{w_s - w}{w_s a(w)} \right)^2 P_\delta \left(\frac{l}{w}, a \right). \quad (6.1)$$

In order to calculate a model-independent angular power spectrum we need to understand how the function is affected by different parameters and models. Apart from H_0, c and Ω_{m0} there are two major constituents in the integral above: The cosmic matter density power spectrum $P_\delta(k)$ and the comoving distance line element dw . Both quantities were discussed independently in chapters 1 (w) and 2 (P_δ). Looking at the major components separately in the following sections we will discuss the influence of specific cosmological models and parameters.

6.1 ANALYSING THE INGREDIENTS WITH SCHMIDT AND BARTELMANN [38]

6.1.1 The Comoving Distance $w(a)$

Recalling the definition of the comoving distance from eq. 1.35:

$$w(a) = \int_{t(a)}^{t_0} \frac{dt'}{a(t')} = \int_a^1 \frac{da'}{a'^2 H(a')}, \quad (6.2)$$

as well as the definition of the Hubble function (eq. 1.27):

$$H(a) = H_0 E(a), \quad (6.3)$$

we can write:

$$w(a) = H_0^{-1} \int_a^1 \frac{da'}{a'^2 E(a')}. \quad (6.4)$$

The influence of any cosmological model on the comoving distance is caused by the nature of the cosmic expansion function $E(a)$. This function normally requires a specific cosmological model with parameters behaving in a particular way in time. The expression for the comoving distance as function of cosmic scale factor leads to the differential:

$$dw = \frac{-da}{H_0 a'^2 E(a)}, \quad (6.5)$$

and allows to reformulate the lensing power spectrum in terms of an integral over scale factor rather than comoving distance:

$$\begin{aligned} C_l^\gamma &= \frac{9}{4} \left(\frac{H_0}{c} \right)^4 \Omega_{m0}^2 \int_1^{a_s} \frac{-da}{a^4 E(a)} \left(\frac{w_s - w(a)}{w_s} \right)^2 P_\delta \left(\frac{l}{w(a)} \right) \\ &= \frac{9}{4} \left(\frac{H_0}{c} \right)^4 \Omega_{m0}^2 \int_{a_s}^1 \frac{da}{a^4 E(a)} \left(\frac{w_s - w(a)}{w_s} \right)^2 P_\delta \left(\frac{l}{w(a)} \right), \end{aligned} \quad (6.6)$$

where we flip the integration boundaries in order to eliminate the minus sign. It is now straightforward to observe the expansion function's influence on the power spectrum at three different points. First, it acts as direct constituent in the integral, second it is part of the remaining comoving distances in the weight function:

$$W(a, a_s) := \left[\frac{w(a_s) - w(a)}{w(a_s)} \right]^2, \quad (6.7)$$

a definition we took from [38], and at a third instance it is present in the argument of the density power spectrum. As discussed in chapter 1 the classical definition of the function in the standard model of cosmology is given by:

$$E(a) = \sqrt{\Omega_{m0} a^{-3} + \Omega_{r0} a^{-4} + \Omega_\Lambda + \Omega_K a^{-2}}, \quad (6.8)$$

for our Λ CDM cosmology.

[38] has extensively analysed the influence of a change in $E(a)$ on the weak lensing power spectrum. In our analysis, we will discuss their findings and extend or modify their investigation wherever needed. We begin by following [38] in calculating the variance of the comoving (radial) distance:

$$\begin{aligned} \frac{\delta w(a)}{\delta E(x)} &= \frac{\delta}{\delta E(x)} \int_a^1 \frac{da'}{a'^2} \frac{1}{E(a')} \\ &= \int_a^1 \frac{da'}{a'^2} \frac{1}{E^2(a')} \delta_D(a' - x) \Theta(x - a) \Theta(1 - x) (-1) \\ &= \frac{-\Theta(x - a) \Theta(1 - x)}{x^2 E^2(x)}, \end{aligned} \quad (6.9)$$

where we used that the functional derivative and the integration commute in this case and that for functions $f(x)$:

$$\frac{\delta f(a)}{\delta f(b)} = \delta_D(a - b). \quad (6.10)$$

The Heaviside step functions:

$$\Theta(x) := \begin{cases} 1 & (x \geq 0) \\ 0 & (x < 0) \end{cases}, \quad (6.11)$$

ensure, that a change in the expansion function $E(a)$ does not influence the scale factor at earlier times.

Instead of plotting the function $\frac{\delta w(a)}{\delta E(x)}$ we decided to plot $w(a)$ for the two particular expansion functions $E(a)$, which we consider in the scope of our work. These are the Λ CDM expansion function and the model-independent expansion function [21]. We show both expansion functions in Fig. 6.1. We decided to do so because on the one hand we do not consider plots of those functional derivatives illustrative in our case, but also because we only analyse the two named cases allowing for an easy comparison of the discussed effects.

6.1.2 The Density Power Spectrum P_δ

Returning to the weak lensing power spectrum C_l we also must analyse the expression 6.6 for the empirical expansion function with a density power spectrum based on the changed comoving distance. This again is worked out by [38] analytically who analyses each part of the integral for its variation with respect to $E(a)$ separately. It is mainly a masterpiece of functional analysis which is why we refer the ambitious reader to the work itself for a detailed discussion and will ourselves only give a quick and comprehensive overview of their results. We will again refrain from illustrating their results in form of functional derivative figures, but will give the results obtained both with Λ CDM and [21]-expansion functions for all the results similar to the illustrations in Fig. 6.1.

Considering the weak lensing power spectrum one can identify three parts which will also give rise to the three analyses [38] performs. The integral in 6.6 is renamed as:

$$I := \int_{a_s}^1 W^2(a, a_s) P_\delta \left(\frac{l}{w(a)} \right) \frac{da}{a^4 E(a)} \quad (6.12)$$

with $W(a, a_s)$ defined already. In order to proceed, they define an uncertainty distribution:

$$R(x, a_s, l) = \frac{\Delta I}{I} = \left| \frac{\delta \log I}{\delta E} \right| \Delta E, \quad (6.13)$$

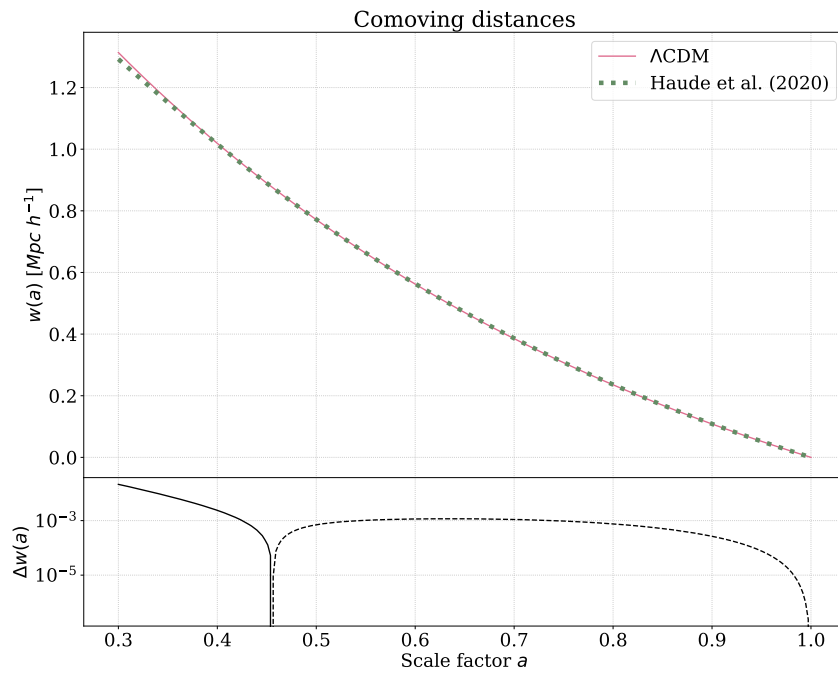


Figure 6.1: Comparing comoving distances. We show both the comoving distance using the standard expansion function of Λ CDM cosmology (pink straight line) as well as the comoving distance obtained with the purely empirical expansion function from [21]. The difference $w^{Haude}(a) - w^{\Lambda CDM}(a)$ is shown in the lower panel where the y-scale is logarithmic and the dashed line indicates a negative value of the difference.

and calculate $\frac{\delta \log I}{\delta E}$, finding:

$$\frac{\delta \log I}{\delta E} = \int_{a_s}^1 \frac{da}{a^4 E} \Theta(x - a_s) \Theta(1 - x) \left\{ W^2 P_\delta \cdot \left(2 \frac{\delta \log W}{\delta E} + \frac{\delta \log P_\delta}{\delta E} + \frac{-\delta_D(x - a)}{E} \right) \right\}, \quad (6.14)$$

where the product rule is applied and the Dirac-distribution in the last summand is the result of the functional derivative $\frac{\delta E(a')}{\delta E(x)}$. We now follow [38] analysing each single part of the variational integral 6.14:

(i)

$$\frac{\delta \log W}{\delta E} = \frac{\Theta(1 - x) \Theta(x - a_s)}{w(a_s) x^2 E^2(x)} \left(1 - \frac{\Theta(a - x)}{W(a, a_s)} \right), \quad (6.15)$$

where the results from $\frac{\delta w}{\delta E}$ are extended and the product rule is applied.

(ii)

$$\frac{\delta \log P}{\delta E} = \frac{\Theta(1 - x) \Theta(x - a)}{w(a) x^2 E(x)} \varkappa(k, a) + \frac{\delta \log D_+(a)}{\delta E(x)} \alpha(k, a), \quad (6.16)$$

where:

$$\varkappa(k, a) := \frac{\partial}{\partial \log k} \log P_\delta(k, a), \quad (6.17)$$

is the change of matter density power spectrum with a changed wave number k which one can trace back to the change in the comoving distance. We also define:

$$\begin{aligned} \alpha(k, a) &= \frac{\partial}{\partial \log D_+} \log P_\delta(k, a) \\ &= \begin{cases} 2 & \text{(linear)} \\ \Omega_m^{-\gamma}(a) \frac{\partial}{\partial \log a} P_\delta(a) & \text{(nonlinear)} \end{cases}, \end{aligned} \quad (6.18)$$

where a case distinction is made for the linear and nonlinear part of the power spectrum. Ω_m^γ is determined by the logarithmic derivative $\frac{d \log D_+}{d \log a} = \Omega_m^\gamma$. It is worth stressing that a functional derivative term arises here which has not been part of our first expression $\frac{\delta I}{\delta E}$.

Before we follow [38] in analysing this expression $\frac{\delta D_+}{\delta E}$, we want not to miss mentioning that the k -derivative of P_δ originates from the derivative $\frac{\delta}{\delta E} P_\delta(l/w)$ with w being a function of the expansion function.

(iii)

$$\frac{\delta}{\delta E} \left(\frac{D_+(a)}{D_+(1)} \right) = D_+(a) g(x) \{ \Xi(x-a) - \Xi(x,1) \}, \quad (6.19)$$

where

$$g(x) := x D_+^2(x) \Omega_m(x) \left(\Omega_m^{2\gamma-1} - \frac{3}{2} \right), \quad (6.20)$$

and

$$\Xi(x,a) := \Theta(a-x) \int_x^a \frac{dy}{y^3 D_+^2(y) E(y)}. \quad (6.21)$$

The last function Ξ is renamed from [38], where it is referred to as Γ .

By inserting all of these results one can obtain the full expression for $\frac{\delta \log I}{\delta E}$ and the uncertainty distribution $R(x, a_s, l)$ (eq. 6.13). We however will instead of illustrating this functional derivative show all the ingredients discussed, W^2 and $P_\delta(l/w)$ for both cases considered as well as the final product C_l^γ , where we used the model-independent expansion function. For a model density power spectrum we use the nonlinear power spectrum of [44], as it was done in [10].

6.2 A NEW P_δ FOR THE LENSING POWER SPECTRUM

After we already replaced the expansion function with a model-independent version we now exchange the second major model-dependent component P_δ which we formerly described by, e.g., [3, 36, 44] with the power-spectrum from KFT.

In order to isolate the influence of the exchange of power spectra in a first step we reset the expansion function to the expansion function 1.27 of Λ CDM cosmology.

We deduced a power spectrum with KFT in section 5.8. There, we used the factorised form of the free generating functional (cf. section 5.7) with two applied density operators in order to calculate the two-point correlation of cosmic density. This happening in Fourier space we can easily identify this result with the correlator which constitutes the cosmic density power spectrum, cf. eq. 2.28.

The generating functional for two applied density operators in the factorised case reads:

$$\begin{aligned} Z_0[\mathbf{L}, 0] = & V^{-2} (2\pi)^3 \delta_D(\vec{L}_{q_1} + \vec{L}_{q_2}) \\ & \cdot \exp \left\{ -\frac{1}{2} (Q_0 - Q_D) \right\} (\Delta_{21} + \mathcal{P}_{21}), \end{aligned} \quad (6.22)$$

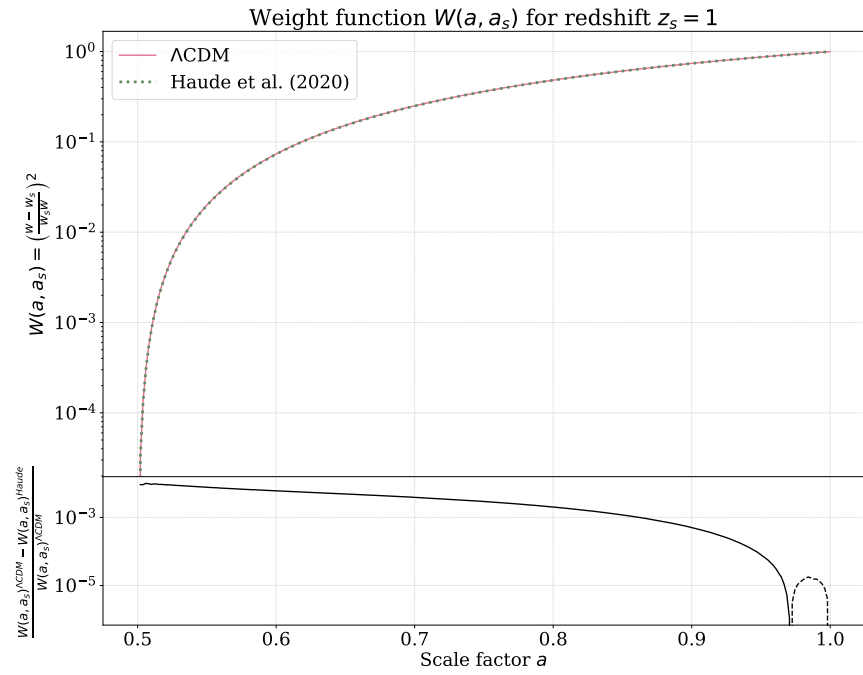


Figure 6.2: Model-independent W^2 , compared to the weight function taken from a Λ CDM model. While the upper panel shows both weight functions in pink (continuous line, Λ CDM) and green (dotted line, Haude et al. [21]) the lower panel shows the relative difference, $\frac{W(a, a_s)^{\Lambda\text{CDM}} - W(a, a_s)^{\text{Haude}}}{W(a, a_s)^{\Lambda\text{CDM}}}$, finding only a very small difference on the sub-percent level between both curves. The redshift of the source was chosen to be $z_s = 1$.

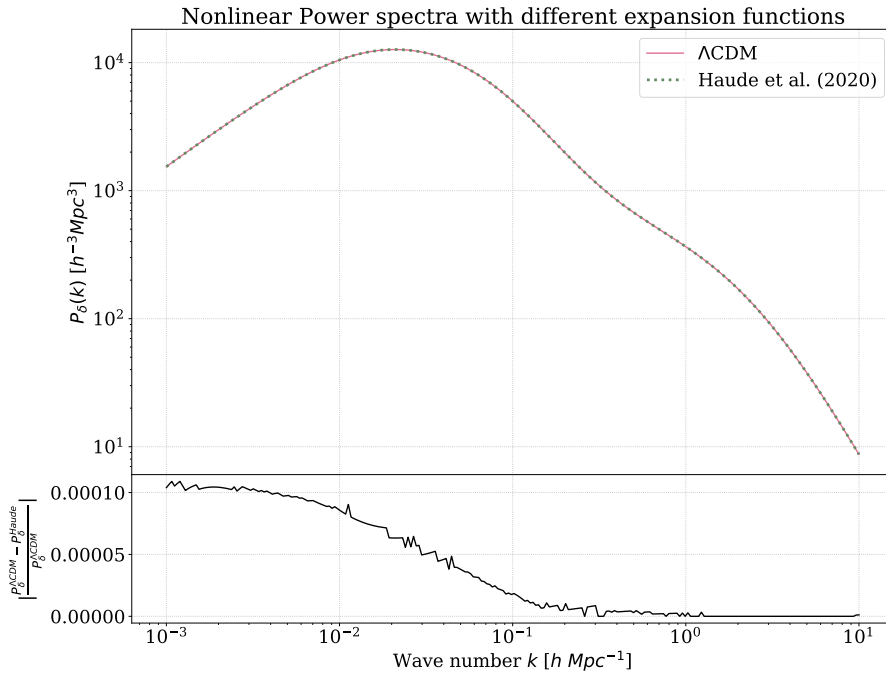


Figure 6.3: Model-independent P_δ . In this plot we compared the density power spectra from Smith et al. [44] for the different expansion functions discussed, i.e. the model-independent cosmology (green, dashed line) as well as the Λ CDM model expansion function 1.27 (pink, continuous line). In the lower panel, showing the reduced difference of both curves, we observe virtually no deviations of the power spectra due to the different choice of underlying cosmologies.

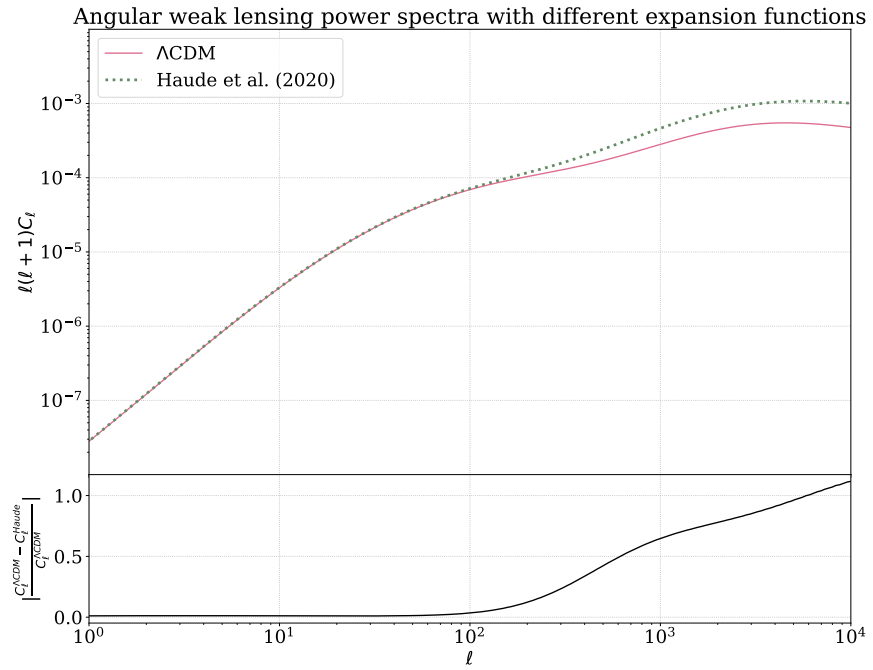


Figure 6.4: Model-independent C_l . In this figure we calculate the weak lensing power spectrum with different expansion functions. In the upper panel, we use the expansion function of Λ CDM for the calculation of the weak lensing spectrum (continuous pink line) as well as the model-independent cosmology from Haude et al. [21] (green dashed line). In the lower panel we observe large deviations only for very high moments ℓ .

with

$$\Delta_{21} = (2\pi)^3 \delta_D(\vec{k}_{21}), \quad (6.23)$$

$$\begin{aligned} \mathcal{P}_{21} &= \int_q \left(\exp \left\{ g_{qp}^2(\tau, 0) k_{21}^2 \left(a_{\parallel} \lambda_{21}^{\parallel} + a_{\perp} \lambda_{21}^{\perp} \right) \right\} - 1 \right) e^{i\vec{k}_{21}\vec{q}} \\ &= \mathcal{P}(\vec{k}_{21}). \end{aligned} \quad (6.24)$$

We already defined the other constituents of these elements in section 5.7. We then rename:

$$\vec{L}_{q_1} = \vec{k}_{21} =: \vec{k}. \quad (6.25)$$

With the Dirac-distribution in 6.22 we know that there can only be one independent wave vector which we already know for power spectra. Calculating the λ factors we find

$$\lambda_{21}^{\parallel} = -1, \quad (6.26)$$

$$\lambda_{21}^{\perp} = 0. \quad (6.27)$$

We are then left with the short expression for the cosmic density power spectrum

$$\mathcal{P}(\vec{k}, \tau) = \int_q \left(e^Q - 1 \right) e^{i\vec{k}\vec{q}}, \quad (6.28)$$

where we introduced the shorthand $Q := -g_{qp}^2(\tau) k^2 a_{\parallel}(q)$. For small k or early times, i.e. small g_{qp} , we can linearise the exponential and will find the *linearly* evolved power-spectrum

$$\mathcal{P}^{lin}(k, t) \approx g_{qp}^2(\tau) P_{\delta}(k). \quad (6.29)$$

Referring to 6.28 as \mathcal{P}^{KFT} we can now use this for the calculation of the weak lensing power spectrum:

$$C_l^{\gamma} = \frac{9}{4} \left(\frac{H_0}{c} \right)^4 \Omega_{m0}^2 \int_{a_s}^1 \frac{da}{a^4 E(a)} \left(\frac{w_s - w(a)}{w_s} \right)^2 \mathcal{P}_{\delta}^{\text{KFT}} \left(\frac{l}{w(a)} \right), \quad (6.30)$$

and compare it to the C_l obtained with a model P_{δ} (e.g. [3]) in Fig. 6.5.

6.3 A MODEL-INDEPENDENT WEAK LENSING SPECTRUM

In order to calculate a fully model-independent power spectrum for the weak lensing effect we now use both the parameter-free power spectrum from KFT (eq. 6.28) as well as the model-independent expansion function from [21], chapter 4 to calculate

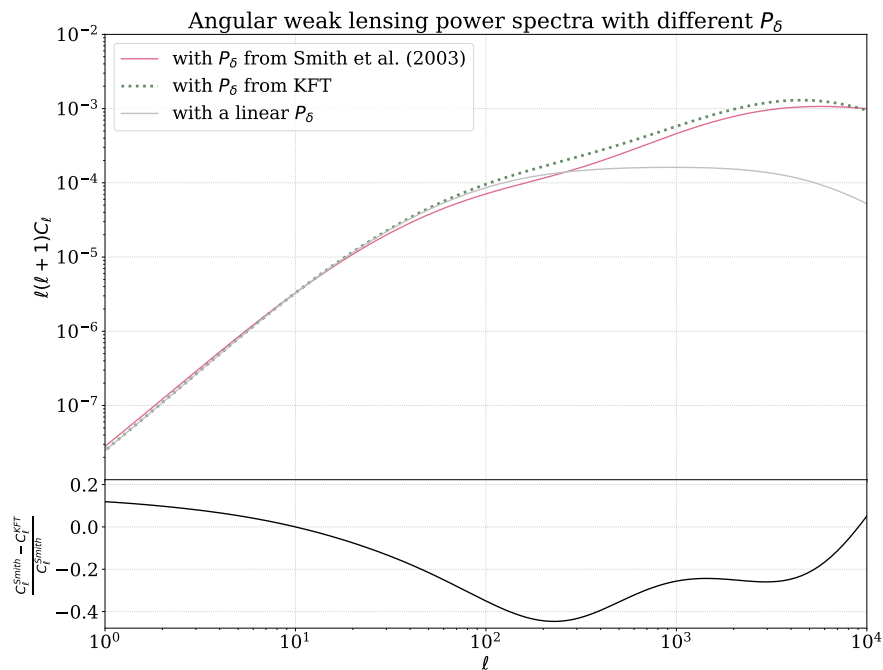


Figure 6.5: Comparing weak lensing power spectra for a Λ CDM universe. Here, we compared the lensing spectrum calculated with a density fluctuation power spectrum from Smith et al. [44] (straight, pink line) on the one hand and from Kinetic Field Theory (dashed, green line) on the other hand. Furthermore, we show as a silver line the weak lensing spectrum as obtained when using a *linear* density power spectrum. In the lower panel of the figure we observe the difference of the two which indicates maximal deviation at the same point when the linear power spectrum starts deviating from the nonlinear one, marking the onset of nonlinear structure formation.

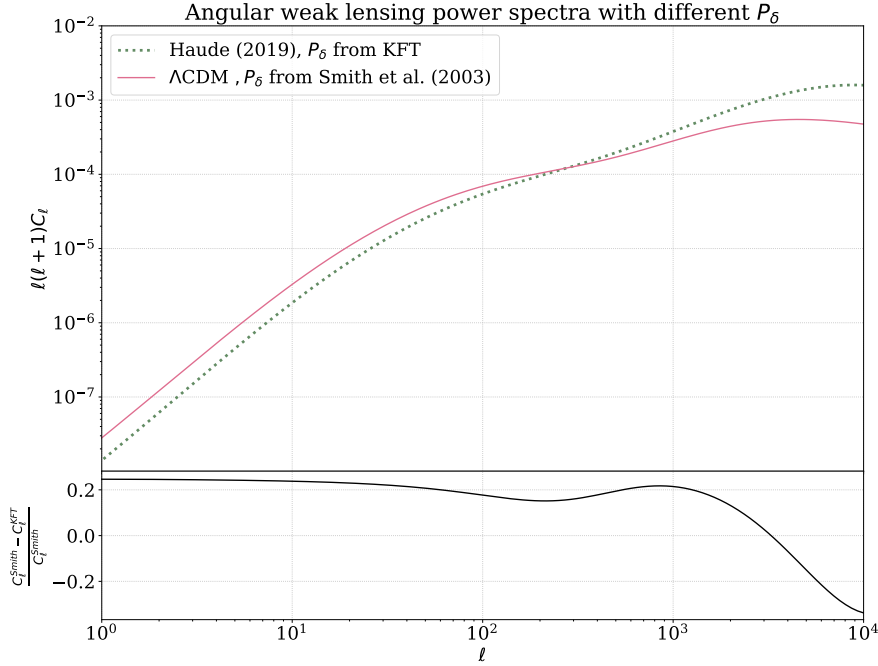


Figure 6.6: Comparing the fully model-independent lensing power spectrum by using the KFT density power spectrum as well as the purely observational expansion function from [21] to a power spectrum obtained with a Λ CDM expansion function and a modeled density power spectrum. Both for the very large and in the very small moments we recognise substantial deviations when directly comparing the power spectrum based on a model cosmology and numerical simulations to a power spectrum obtained by using model-independent cosmology and Kinetic Field Theory.

C_l .

After we replace the weight function and the power spectrum, the only parameters left are H_0, c and Ω_{m0} . We compare the model-independent angular power spectrum and the difference remaining between both curves. In order to not only compare our findings to established models we also want to compare them to a different C_l -calculation from numerical cosmology. There, we use the data obtained from the code UFALCON [41, 42], a highly efficient alternative to conventional N -body simulations. We choose this data set in order to get a value for the lensing power spectrum from a present-day numerical approach for

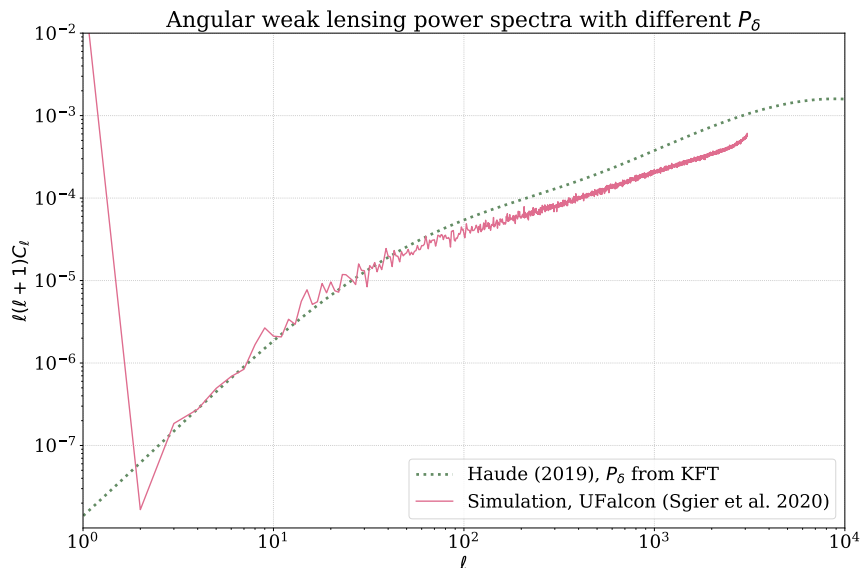


Figure 6.7: Comparing our model-independent weak lensing power spectrum to the power spectrum from the N-body like simulation scheme UFALCON. While both curves agree reasonably well up to $\ell \approx 100$, a deviation starts to evolve and grow similar to the deviation in Fig. 6.6 growing towards high l .

nonlinear cosmic structure formation analysis. We show this comparison in Fig. 6.7.

CONCLUDING REMARKS

In this chapter, we introduced the weak lensing power spectrum in a way which is parameter-free and model-independent to the greatest possible extent. To our knowledge this is the weak lensing power spectrum with the least assumptions on specific cosmological models and parameters so far. We achieved that by incorporating both an expansion function which was obtained from observations only [21] as well as a power spectrum which only assumes a probability distribution as an initial condition which can be measured to great accuracy at the time of recombination and develops this in time by using fundamental laws of physics only. Both model-independent ingredients $E(a)$ and P_δ are tested against well-established models and compared to results from numerical simulations.

For all comparisons we found that the combination of the ap-

plication of model-independent cosmology and Kinetic Field Theory led to substantial deviations of our weak lensing spectra from the weak lensing spectra with well-established models. These could be traced back to deviations of the density fluctuation power spectra when one uses the expansion and growth-functions of model-independent cosmology for the Kinetic Field Theory Framework. Calculating the angular weak lensing spectrum then leads to a deviation of approximately 20 percent from the modelled lensing spectra.

INTERMISSION: OBSERVING C_ℓ

As we discussed before (chapters 3, 6), the weak lensing power spectrum can be a central piece in testing structure formation theories and probing the cosmic dark sector. The measurement of expression 3.75, linking the theoretically predicted power spectrum, from which we derived our model-independent lensing power spectrum, $C_\ell^\gamma[P_\delta, w]$, to a correlator of measurable observables, $C_\ell^\gamma = \langle \tilde{\gamma} \tilde{\gamma}^* \rangle$, however required a smooth shear field $\gamma = \gamma(\vec{\theta}) \forall \vec{\theta} \in \mathbb{S}^2$ to be (directly) observable in order to calculate the power spectrum.

Observing the sky, however, no complex scalar field with shear values at every single point presents itself, ready to be evaluated by cosmologists eager to calculate the power spectrum. What we can however observe are stars and galaxies with measurable shapes which are deformed by the gravitational lensing effect with respect to their intrinsic source shapes. In this brief intermission chapter, we want to explain which steps are needed to obtain a weak lensing power spectrum from a survey, i.e. from an image, often poor in resolution, of the sky.

7.1 FROM OBSERVATIONS TO SHEAR DATA

The first step is to analyse every single astronomical object in the image for its character, size and shape (whereby we shall refer to ellipticity values and not to the size from now on). Thankfully, there is software well-tested which analyses large field surveys in a reasonable amount of time and provides us with a detailed list of the objects contained in the image [e.g. 12].

As these object parameters are subject to observational problems, a proper calibration must then follow allowing to recover an object's properties as they would be detected with perfect cameras. One of the main challenges, for example, is to deconvolve the image with the instrument's own point spread function (PSF). While there are many methods to perform a calibration like this we only name the one of [25] where we suggested a method to use strong lensing analyses for calibration purposes. This however requires a large set (~ 50) of strong lensing systems with a remarkable image quality (comparable to the quality of

the COSMOS survey [40]). In the same paper, however, we also presented a method named cloning, invented by [13–15], which can be used for calibration of weak lensing data on its own without the need of analysing strong lensing systems.

Having achieved a set of properly calibrated observations one can continue to calculate the cosmic shear in selected regions. We therefore assume that the ellipticities of galaxies are randomly distributed. This is actually a rather bold claim. In order to account for intrinsic and extrinsic alignments of galaxies due to gravitational potential fields of large scale structure sophisticated methods have been developed. We however shall stick to the idealising assumption of randomly distributed galaxy ellipticities. One can justify this approximation for sufficiently large regions where even the effects of alignments might vanish when being averaged over.

By averaging over $N \gg 1$ galaxies and their intrinsic (source) ellipticities ϵ_α^s we find:

$$\langle \epsilon_\alpha^s \rangle_N = 0, \quad (7.1)$$

where $\langle \cdot \rangle_N$ denotes the arithmetic mean of the N galaxy ellipticities considered.

As the weak lensing effect leads to an additional deformation of the shapes observed, we add this to the source ellipticity and write:

$$\epsilon_\alpha = \epsilon_\alpha^s + \gamma(\theta). \quad (7.2)$$

In order to prevent confusion we want to stress here that the α refers to the *component* of the ellipticity and does not enumerate the galaxies considered. Averaging over N galaxies again the shear (averaged over the region of the N galaxies) remains, while the source ellipticities cancel again:

$$\langle \epsilon_\alpha \rangle_N = \langle \gamma(\theta) \rangle_{A_N}, \quad (7.3)$$

where A_N is the area enclosing the N galaxies considered. This shear can then be again calibrated [e.g. 25, eq. 2.5].

7.2 FROM REAL-SPACE SHEAR TO THE LENSING POWER SPECTRUM

Having obtained a set of calibrated ellipticity data we can proceed to calculate the weak lensing power spectrum. As the data set will be discrete for any observation, consisting of the stars' and galaxies' ellipticities, we have to introduce a formalism to

calculate the weak lensing power spectrum from this discrete set. Here, we will follow the method and introduce the estimators invented by [22] for the remainder of this chapter.

The N galaxies of our calibrated measurement data set are at positions $\vec{\theta}_i$ and have shape parameters $\epsilon_{1,2}$ which we combine to the complex ellipticity:

$$\epsilon_i = \epsilon_{1,i} + i\epsilon_{2,i}, \quad (7.4)$$

similar to the complex shear we introduced earlier (eq. 3.44). Here, the index i enumerates the galaxies considered. After the calibration process the stars are not being considered any longer and only the galaxies are taken into account for the calculation of the cosmic shear. These galaxy ellipticities are Fourier-transformed:

$$\tilde{\epsilon}_\alpha(\vec{\ell}) = \sum_{i=1}^N \exp(i\vec{\ell} \cdot \vec{\theta}_i) \cdot \epsilon_{\alpha,i}, \quad (7.5)$$

before we start splitting up the measured ellipticity into intrinsic galaxy shape and ellipticity contributions from shear deformations:

$$\begin{aligned} \tilde{\epsilon}_\alpha &= \sum_{i=1}^N \left\{ \epsilon_{\alpha,i}^s \exp(i\vec{\ell} \cdot \vec{\theta}_i) \right\} \\ &+ \int d\vec{\theta} \left\{ \exp(i\vec{\ell} \cdot \vec{\theta}) \gamma(\vec{\theta}) \sum_i \delta_D(\vec{\theta} - \vec{\theta}_i) \right\}. \end{aligned} \quad (7.6)$$

Here and in the remainder of this chapter, we use the tilde sign to mark Fourier-transformed quantities. In order to make the notation easier, we define

$$n(\vec{\theta}) = \sum_i \delta_D(\vec{\theta} - \vec{\theta}_i). \quad (7.7)$$

We operate in the two dimensions we can observe on $\mathbb{S}^2 \simeq \mathbb{R}^2$ (cf. section 3.4) in the whole chapter. Therefore, $\delta_D(\vec{\theta}) = \delta_D^{(2)}(\vec{\theta})$. We continue defining:

$$\tilde{n}(\vec{\ell}) = \int d\vec{\theta} e^{i\vec{\ell} \cdot \vec{\theta}} n(\vec{\theta}), \quad (7.8)$$

and turn to the first major approximation, where we replace the newly defined $n(\vec{\theta})$ term by:

$$\prod_{j=1}^N \left(\frac{1}{A} \int d\vec{\theta}_j \right) (n(\vec{\theta})) = \tilde{n} \Pi(\vec{\theta}), \quad (7.9)$$

with the aperture function:

$$\Pi(\vec{\theta}) = \begin{cases} 1 & \vec{\theta} \text{ in survey area} \\ 0 & \text{otherwise} \end{cases}, \quad (7.10)$$

the survey area:

$$A = \int d\vec{\theta} \Pi(\vec{\theta}), \quad (7.11)$$

and

$$\bar{n} = \frac{N}{A}, \quad (7.12)$$

the mean number density of galaxies in the field. This replacement of $n(\vec{\theta})$, is, however small, an essential approximation since the Dirac delta-distributions in $n(\vec{\theta})$ would prevent further progress. We can further abbreviate:

$$\tilde{n}(\vec{\ell}) = (2\pi)^2 \bar{n} \Delta(\vec{\ell}), \quad (7.13)$$

when we define:

$$\Delta(\vec{\ell}) = \int \frac{d\vec{\theta}}{(2\pi)^2} e^{i\vec{\ell} \cdot \vec{\theta}} \Pi(\vec{\theta}). \quad (7.14)$$

This Δ is different from the Δ_{jk} used in chapter 5 as it defines a $(2\pi)^2$ -scaled Fourier transform of the aperture function $\Pi(\vec{\theta})$. With a sufficiently large field, i.e. a field of a size much larger than the (squared) mean separation of galaxies, $|A| \gg |\vec{\theta}|^2$, which is simply connected (which should hold for most surveys large enough to perform weak lensing analyses), we can set $\Pi(\vec{\theta}) \approx 1$ and $\Delta(\vec{\ell}) \approx \delta_D(\vec{\ell})$. Carrying out the δ_D -integral in 7.6 then leaves us with:

$$\tilde{\epsilon}_\alpha(\vec{\ell}) = \bar{n} \tilde{\gamma}_\alpha(\vec{\ell}) + \sum_{i=1}^N \left\{ \epsilon_{\alpha,i}^s \cdot \exp(i\vec{\ell} \cdot \vec{\theta}_i) \right\}. \quad (7.15)$$

[22] introduces the convergence power spectrum as:

$$\begin{aligned} \left\langle \tilde{\kappa}_E(\vec{\ell}) \tilde{\kappa}_E^*(\vec{\ell}') \right\rangle &= (2\pi)^2 \delta_D(\vec{\ell} - \vec{\ell}') C_\ell \\ &=: \langle \tilde{\kappa} \tilde{\kappa}^* \rangle \\ &= \langle \tilde{\gamma} \tilde{\gamma}^* \rangle. \end{aligned} \quad (7.16)$$

The subscript E refers to the distinction of modes in analogy to electrodynamics (E and B) where fields get decomposed into curl- and divergence free parts. For a *pure* lensing signal, which is curl-free, the divergence-free B -mode will vanish. In the following, we shall ignore the B modes which are however present

in real-world data from shear surveys (e.g. the Dark Energy Survey [30] or the surveys [40], [1] mentioned earlier). We abbreviated $\kappa := \kappa_E$ as we do not investigate the divergence-free B -modes and will only need κ_B one more time. Before defining the estimator from [22] we will give the shear-convergence relation they gave (equations 5,8 therein):

$$\gamma(\vec{\theta}) = \pi^{-1} \int d\vec{\theta}' \mathcal{D}(\vec{\theta} - \vec{\theta}') \kappa(\vec{\theta}'), \quad (7.17)$$

with:

$$\mathcal{D}(\vec{\theta}) = \frac{\theta_2^2 - \theta_1^2 - 2i\theta_1\theta_2}{|\theta|^4}, \quad (7.18)$$

and:

$$\tilde{\gamma}(\vec{\ell}) = \exp(2i\beta) \tilde{\kappa}(\vec{\ell}), \quad (7.19)$$

where by β we denote the polar angle of the argument $\vec{\ell}$. This definition 7.19 at hand we can easily see the equality of the convergence and shear power spectra: $\langle \tilde{\kappa} \tilde{\kappa}^* \rangle = \langle \tilde{\gamma} \tilde{\gamma}^* \rangle$. The power spectrum estimator in [22] is defined:

$$\hat{C}_{\vec{\ell}} := \left(\bar{n}^2 A_r(\vec{\ell}) A \right)^{-1} \cdot \int_{A_r(\vec{\ell})} d\vec{\ell} \left| \tilde{\epsilon}_1(\vec{\ell}) \cos(2\beta) + \tilde{\epsilon}_2(\vec{\ell}) \sin(2\beta) \right|^2 - \frac{\sigma_{\epsilon}^2}{2\bar{n}}, \quad (7.20)$$

as band power for disjunct bins at $\vec{\ell}$. $A_R(\vec{\ell}) = 2\pi\bar{\ell}\Delta\ell$ is the approximate area of the annulus with mean radius $\bar{\ell}$ which is the area we average over for our band power estimator.

The estimator is shown to be unbiased. This proof starts by again splitting intrinsic ellipticities from shear contributions:

$$\begin{aligned} & \left| \tilde{\epsilon}_1(\vec{\ell}) \cos(2\beta) + \tilde{\epsilon}_2(\vec{\ell}) \sin(2\beta) \right|^2 \\ = & \left| \sum \epsilon_1^s(\vec{\ell}) \cos(2\beta) + \gamma_1 \bar{n} \cos(2\beta) + \epsilon_2^s(\vec{\ell}) \sin(2\beta) + \gamma_2 \bar{n} \sin(2\beta) \right|^2. \end{aligned} \quad (7.21)$$

We ignore terms with mixed γ and ϵ (for we still consider them to be uncorrelated and ignore alignment effects). With:

$$\left\langle \epsilon_i^s \epsilon_j^{s*} \right\rangle = \delta_{ij} \sigma_{\epsilon}^2, \quad (7.22)$$

$$\left\langle \epsilon_i^s \epsilon_j^s \right\rangle = 0, \quad (7.23)$$

from the definition of the intrinsic ellipticity dispersion, we find:

$$\left\langle \epsilon_{\alpha,i}^s \epsilon_{\beta,j}^{s*} \right\rangle = \delta_{ij} \delta_{\alpha\beta} \frac{\sigma_{\epsilon}^2}{2}. \quad (7.24)$$

The persistent application of these equations to the power spectrum estimator results, after a rather lengthy calculation, in:

$$\begin{aligned} \langle \hat{C}_\ell \rangle = (A_R(\bar{\ell})A)^{-1} \int_{A_R(\bar{\ell})} \left\langle \tilde{\gamma}_1^2 \cos^2(2\beta) + \tilde{\gamma}_2^2 \sin^2(2\beta) + \right. \\ \left. (\tilde{\gamma}_1 \tilde{\gamma}_2^* + \tilde{\gamma}_1^* \tilde{\gamma}_2) \sin(2\beta) \cos(2\beta) \right\rangle. \end{aligned} \quad (7.25)$$

With:

$$\frac{\tilde{\kappa}_F + \tilde{\kappa}_F^*}{2} = \tilde{\gamma}_1 \cos(2\beta) + \tilde{\gamma}_2 \sin(2\beta) = \tilde{\kappa}(\ell), \quad (7.26)$$

where we introduce κ_F as the convergence containing also the divergence-free B -modes $\tilde{\kappa}_F = \tilde{\kappa}_E + i\tilde{\kappa}_B$. We find:

$$\begin{aligned} \langle \hat{C}_\ell \rangle &= \frac{1}{A_R(\bar{\ell})A} \int_{A_R(\bar{\ell})} d\vec{\ell} \langle \kappa \kappa^* \rangle \\ &= \frac{1}{A_R(\bar{\ell})A} \int_{A_R(\bar{\ell})} d\vec{\ell} (2\pi)^2 \delta_D(0) C_\ell. \end{aligned} \quad (7.27)$$

Remembering our approximation $\Delta(\vec{\ell}) \approx \delta_D(\vec{\ell})$ we now introduce an approximation for the second order:

$$|\Delta(\vec{\ell})|^2 \approx \delta_D(\vec{\ell}) \Delta(\vec{\ell}) = \delta_D(\vec{\ell}) \Delta(0) = \delta_D(\vec{\ell}) \frac{A}{(2\pi)^2}. \quad (7.28)$$

The application of this identity finally leads to:

$$\begin{aligned} \langle \hat{C}_\ell \rangle &= \frac{1}{A_R A} \int_{A_R} \int_{A_R} d\vec{\ell} (2\pi)^2 \Delta(0) C_\ell \\ &= \frac{1}{A_R A} \int_{A_R} \int_{A_R} d\vec{\ell} C_\ell = C_{\bar{\ell}}. \end{aligned} \quad (7.29)$$

[22] generalises this for $\Delta(\ell)$ without the named approximation. We recommend to read this as well, but we will not repeat this here, since it will not be used in the scope of this thesis.

UNCERTAINTIES

In the last and final chapter of this thesis, we want to extend our calculation of the lensing power spectrum by an estimation of the uncertainties connected with our signal. This estimate provides us with a range in which we can expect deviations when actually using large field surveys to explore the sky and to probe the weak lensing power spectrum 7. The same principle applies if we want to compare our result to results differently obtained in general, e.g. from numerical simulations (cf. chapter 6).

While [38] evaluated the effect of a variation of the expansion function on the weak lensing power spectrum we aim at deriving an expansion of the uncertainty from the variance of the KFT power spectrum and, later on, for a description of the power spectrum uncertainty as a natural consequence of the measurement process.

8.1 A NAIVE APPROACH TO THE VARIANCE

The first possibility coming to mind when we want to measure the weak lensing spectrum signal's uncertainty is to consider the variance of the same:

$$\begin{aligned}\text{Var}(C_\ell) &= \langle C_\ell C_\ell \rangle - \langle C_\ell \rangle^2 \\ &= \langle C_\ell C_\ell \rangle - C_\ell^2.\end{aligned}\quad (8.1)$$

The second term is rather trivial to evaluate, as we only have to square our results from 6. The correlator, however, is more interesting to investigate. We consider:

$$\begin{aligned}\langle C_\ell C_\ell \rangle &= \left\langle \frac{9}{4} \left(\frac{H_0}{c} \right)^4 \Omega_{m0} \int d\tau w W^2 P_\delta \left(\frac{\ell}{w} \right) \right. \\ &\quad \left. \cdot \frac{9}{4} \left(\frac{H_0}{c} \right)^4 \Omega_{m0} \int d\tau' W'^2 P_\delta \left(\frac{\ell}{w'} \right) \right\rangle.\end{aligned}\quad (8.2)$$

We abbreviate:

$$\zeta^2 := \left(\frac{9}{4} \left(\frac{H_0}{c} \right)^4 \Omega_{m0} \right)^2 \quad (8.3)$$

and simplify the slightly modified expression $\langle C_\ell C_{\ell'} \rangle$:

$$\langle C_\ell C_{\ell'} \rangle = \zeta^2 \int dw \int dw' W^2 W'^2 \left\langle P_\delta \left(\frac{\ell}{w} \right) P_\delta \left(\frac{\ell'}{w'} \right) \right\rangle. \quad (8.4)$$

As we already know from the definition of the matter density power spectrum, the power spectrum can be identified with a two-point-correlator:

$$\langle \delta_k \delta_k^* \rangle = \delta_D(k - k') (2\pi)^3 P_\delta(k), \quad (8.5)$$

where δ_k is to be understood as Fourier-mode of the density contrast δ , $\tilde{\delta}(k) =: \delta_k$. By inserting this in the $\langle C_\ell C_{\ell'} \rangle$ correlator, we get

$$\begin{aligned} \langle C_\ell C_{\ell'} \rangle &\sim \iint_{w, w'} W^2 W'^2 \langle \delta \delta \rangle \langle \delta' \delta' \rangle \\ &\sim \iint_{w, w'} W^2 W'^2 \langle \delta \delta \delta' \delta' \rangle. \end{aligned} \quad (8.6)$$

We therefore see, that the computation of the signal's variance requires the evaluation of a four-point correlator of cosmic density. As the density contrast is only a scaled and shifted version of cosmic density:

$$\delta = \frac{\rho - \rho_0}{\rho_0} = \frac{\rho}{\rho_0} - 1, \quad (8.7)$$

we calculate $\langle \rho \rho \rho' \rho' \rangle$, instead, in order to make the connection to KFT clearer.

8.2 A 4TH-ORDER CORRELATOR WITH KFT

The calculation of the correlator we need in order to calculate the variance of the weak lensing power spectrum seems straightforward with the fully factorised expression (section 5.7) for the generating functional after the application of $n = 4$ density operators:

$$\hat{\rho} \hat{\rho} \hat{\rho} \hat{\rho} Z_0[\mathbf{J}, \mathbf{K}]|_{\mathbf{J}, \mathbf{K}=0} =: Z_0[\mathbf{L}]. \quad (8.8)$$

This free generating functional reads:

$$\begin{aligned} Z_0[\mathbf{L}] &= V^{-4} (2\pi)^3 \delta_D \left[\vec{L}_{q_1} + \vec{L}_{q_2} + \vec{L}_{q_3} + \vec{L}_{q_4} \right] \\ &\cdot \exp \left\{ -\frac{1}{2} (Q_0 - Q_D) \right\} \prod_{2 \leq b < a}^4 \int_{k_{int}} \prod_{1 \leq k < j}^4 (\Delta_{jk} + \mathcal{P}_{jk}) \end{aligned} \quad (8.9)$$

where by k_{int} we refer to the so-called *internal* wave vectors \vec{k}_{jk} with $k \geq 2$, whereas the \vec{k}_{jk} with $k = 1$ are called *external* for they contain the shift vectors (cf. section 5.7):

$$\vec{k}_{jk; k=1} := \vec{L}_{q_j} - \sum_{b=2}^{j-1} \vec{k}_{jb} + \sum_{a=j+1}^l \vec{k}_{aj}. \quad (8.10)$$

Considering the expression 8.9 for the fully factorised generating functional we find that the integral

$$I_4 = \int_{k_{int}} \prod_{1 \leq k < j}^4 (\Delta_{jk} + \mathcal{P}_{jk}) \quad (8.11)$$

is similar to:

$$\begin{aligned} \int_{k_{int}} \Delta_{jk}^6 + 6\Delta_{jk}^5 \mathcal{P}_{jk} + 15\Delta_{jk}^4 \mathcal{P}_{jk}^2 + 20\Delta_{jk}^3 \mathcal{P}_{jk}^3 \\ + 15\Delta_{jk}^2 \mathcal{P}_{jk}^4 + 6\Delta_{jk} \mathcal{P}_{jk}^5 + \mathcal{P}_{jk}^6. \end{aligned} \quad (8.12)$$

We then enumerate the terms in descending order of Δ_{jk} and start calculating. Many terms will look rather similar as only the indices of their components are permuted. We will show one example with term II ($\int 6\Delta_{jk}^5 \mathcal{P}_{jk}$) and abbreviate the other cases by simply indicating that there's a number of permutation terms giving this number in brackets.

As one can read off from eq. 8.12 there are $20 + 2 \cdot 15 + 2 \cdot 6 + 2 = 64$ terms in the end. These can be calculated:

I

$$\int_{k_{int}} \Delta_{jk}^6 = (2\pi)^{18} \left(\delta_D(\vec{L}_{q_2}) \cdot \delta_D(\vec{L}_{q_3}) \cdot \delta_D(\vec{L}_{q_4}) \right),$$

II

$$\begin{aligned} \int_{k_{int}} \Delta_{jk}^5 \mathcal{P}_{jk} &= (2\pi)^{15} \delta_D(\vec{L}_{q_2}) \delta_D(\vec{L}_{q_3}) \mathcal{P}(\vec{L}_{q_4}) + [2^*] \\ &+ (2\pi)^{15} \delta_D(\vec{L}_{q_4}) \mathcal{P}(\vec{L}_{q_3}) \delta_D(\vec{L}_{q_3} + \vec{L}_{q_2}) + [2^{**}]. \end{aligned}$$

The two permutation terms in the first line are:

$$\begin{aligned} [2^*] &= (2\pi)^{15} \delta_D(\vec{L}_{q_3}) \delta_D(\vec{L}_{q_4}) \mathcal{P}(\vec{L}_{q_2}) \\ &+ (2\pi)^{15} \delta_D(\vec{L}_{q_2}) \delta_D(\vec{L}_{q_2}) \mathcal{P}(\vec{L}_{q_3}), \end{aligned}$$

the permutations in the second line are:

$$\begin{aligned} [2^{**}] &= (2\pi)^{15} \delta_D(\vec{L}_{q_2}) \mathcal{P}(\vec{L}_{q_4}) \delta_D(\vec{L}_{q_4} + \vec{L}_{q_3}) \\ &+ (2\pi)^{15} \delta_D(\vec{L}_{q_3}) \mathcal{P}(\vec{L}_{q_2}) \delta_D(\vec{L}_{q_2} + \vec{L}_{q_4}), \end{aligned}$$

III

$$\begin{aligned}
\int_{k_{int}} \Delta_{jk}^4 \mathcal{P}_{jk}^2 &= (2\pi)^{12} \delta_D(\vec{L}_{q_2}) \mathcal{P}(\vec{L}_{q_4}) \mathcal{P}(\vec{L}_{q_3}) + [2] \\
&+ (2\pi)^{12} \delta_D(\vec{L}_{q_4}) \mathcal{P}(\vec{L}_{q_3}) \mathcal{P}(\vec{L}_{q_3} + \vec{L}_{q_2}) + [5] \\
&+ (2\pi)^{12} \mathcal{P}(\vec{L}_{q_4}) \mathcal{P}(\vec{L}_{q_3}) \delta_D(\vec{L}_{q_3} + \vec{L}_{q_2}) + [2] \\
&+ (2\pi)^{12} \mathcal{P}(-\vec{L}_{q_2}) \mathcal{P}(-\vec{L}_{q_3}) \delta_D(\vec{L}_{q_2} + \vec{L}_{q_3} + \vec{L}_{q_4}) + [2],
\end{aligned}$$

IV

$$\begin{aligned}
\int_{k_{int}} \Delta_{jk}^3 \mathcal{P}_{jk}^3 &= (2\pi)^9 \delta_D \left(\sum_{j=2}^4 L_{q_j} \right) \\
&\cdot \int d\mathbf{k}_{43} \mathcal{P}(\vec{L}_{q_3} + \vec{k}_{43}) \mathcal{P}(-\vec{L}_{q_2} - \vec{L}_{q_3} - \vec{k}_{43}) \mathcal{P}(\vec{k}_{43}) \\
&+ (2\pi)^9 \mathcal{P}(\vec{L}_{q_3}) \mathcal{P}(-\vec{L}_{q_2} - \vec{L}_{q_3}) \mathcal{P}(\vec{L}_{q_4} + \vec{L}_{q_2} + \vec{L}_{q_3}) + [5] \\
&+ (2\pi)^9 \mathcal{P}(\vec{L}_{q_3}) \mathcal{P}(\vec{L}_{q_4}) \mathcal{P}(\vec{L}_{q_2} + \vec{L}_{q_3} + \vec{L}_{q_4}) + [2] \\
&+ (2\pi)^9 \mathcal{P}(\vec{L}_{q_3}) \mathcal{P}(\vec{L}_{q_2} + \vec{L}_{q_3}) \mathcal{P}(\vec{L}_{q_2}) + [5] \\
&+ (2\pi)^9 \delta_D(\vec{L}_{q_4}) \mathcal{P}(\vec{k}_{32}) \mathcal{P}(\vec{L}_{q_2} + \vec{k}_{32}) \mathcal{P}(\vec{L}_{q_3} - \vec{k}_{32}) + [2] \\
&+ (2\pi)^9 \mathcal{P}(\vec{L}_{q_2}) + \mathcal{P}(\vec{L}_{q_3}) + \mathcal{P}(\vec{L}_{q_4}),
\end{aligned}$$

V

$$\begin{aligned}
\int_{k_{int}} \Delta_{jk}^2 \mathcal{P}_{jk}^4 &= (2\pi)^6 \int d\mathbf{k}_{32} \mathcal{P}(\vec{k}_{32}) \mathcal{P}(\vec{L}_{q_4} - \vec{L}_{q_3} - \vec{k}_{32}) \mathcal{P}(\vec{k}_{32} - \vec{L}_{q_3}) \\
&\quad \cdot \mathcal{P}(\vec{L}_{q_3} + \vec{L}_{q_4} - \vec{L}_{q_3}) + [2] \\
&+ (2\pi)^6 \int d\mathbf{k}_{42} \mathcal{P}(\vec{L}_{q_2} - \vec{k}_{42}) \mathcal{P}(\vec{k}_{42}) \mathcal{P}(\vec{L}_{q_2} + \vec{L}_{q_3} + \vec{k}_{42}) \\
&\quad \cdot \mathcal{P}(\vec{L}_{q_4} - \vec{k}_{42}) + [2] \\
&+ (2\pi)^6 \int d\mathbf{k}_{32} \mathcal{P}(\vec{k}_{32}) \mathcal{P}(\vec{L}_{q_4}) \mathcal{P}(\vec{L}_{q_2} + \vec{L}_{q_4} + \vec{k}_{32}) \\
&\quad \cdot \mathcal{P}(\vec{L}_{q_3} - \vec{k}_{32}) + [5] \\
&+ (2\pi)^6 \int d\mathbf{k}_{32} \mathcal{P}(\vec{k}_{32}) \mathcal{P}(\vec{L}_{q_4}) \mathcal{P}(\vec{L}_{q_2} + \vec{L}_{q_4} + \vec{k}_{32}) \\
&\quad \cdot \mathcal{P}(\vec{L}_{q_3} - \vec{k}_{32}) + [2],
\end{aligned}$$

VI

$$\begin{aligned}
\int_{k_{int}} \Delta_{jk} \mathcal{P}_{jk}^5 &= (2\pi)^3 \int d\mathbf{k}_{32} d\mathbf{k}_{42} \mathcal{P}(\vec{k}_{32}) \mathcal{P}(\vec{k}_{42}) \mathcal{P}(\vec{L}_{q_4} - \vec{k}_{42}) \\
&\quad \cdot \mathcal{P}(\vec{L}_{q_2} + \vec{k}_{32} + \vec{k}_{42}) \\
&\quad \cdot \mathcal{P}(\vec{L}_{q_3} - \vec{k}_{32} - \vec{k}_{42} + \vec{L}_{q_4}) + [2] \\
&+ (2\pi)^3 \int d\mathbf{k}_{32} d\mathbf{k}_{42} \mathcal{P}(\vec{k}_{32}) \mathcal{P}(\vec{k}_{42}) \mathcal{P}(\vec{L}_{q_2} + \vec{k}_{32} + \vec{k}_{42}) \\
&\quad \cdot \mathcal{P}(\vec{L}_{q_3} - \vec{k}_{32}) \mathcal{P}(\vec{L}_{q_4} - \vec{k}_{42}) + [2],
\end{aligned}$$

VII

$$\int_{k_{int}} \mathcal{P}_{jk}^6 = \int dk_{32} dk_{42} dk_{43} \mathcal{P}(\vec{k}_{32}) \mathcal{P}(\vec{k}_{42}) \mathcal{P}(\vec{k}_{43}) \mathcal{P}(\vec{L}_{q_2} + \vec{k}_{32} + \vec{k}_{42}) \\ \cdot \mathcal{P}(\vec{L}_{q_3} - \vec{k}_{32} + \vec{k}_{43}) \mathcal{P}(\vec{L}_{q_4} - \vec{k}_{42} - \vec{k}_{43}),$$

The integrations of course are meant to range over all three dimension of the k_{ij} and we abbreviated $\int dk_{ij} := \int d\vec{k}_{ij}$ for simplicity. While the first term can be quashed for it sets $\vec{L}_{q_j} = 0 \forall j$ the other terms might lead to nonzero contributions for nonvanishing \vec{L}_{q_j} as well. It however proved impossible for us to finally *evaluate* convolved terms as they appear in (IV) to (VII) numerically. We want to reassure the reader that we tried.

8.2.1 Encountering Numerical Problems

To explain this, we start by rewriting the expression \mathcal{P} as in [24, eq.7.7]:

$$\mathcal{P}_{21}(\vec{L}_{p_1}, \vec{L}_{p_2}, \vec{L}_{q_1}) = \frac{(\vec{L}_{p_1} \cdot \vec{L}_{q_1})(\vec{L}_{p_2} \cdot \vec{L}_{q_1})}{L_{q_1}^4} P_\delta^{(i)}(L_{q_1}) + \\ + \int_q \left(e^{-\vec{L}_{p_1}^T C_{pp} \vec{L}_{p_2}} - 1 + \vec{L}_{p_1}^T C_{pp} \vec{L}_{p_2} \right) e^{i\vec{L}_{q_1} \cdot \vec{q}}, \quad (8.13)$$

and stress that the expression depends on \vec{L}_{p_1} and \vec{L}_{p_2} . [24] found that for the currently existing integration routine to be successful the alignment of those two vectors \vec{L}_{p_j} is crucial. The integration is possible for, e.g., ordinary power spectra where $\vec{L}_{p_1} = -\vec{L}_{p_2}$. [24] analysed the \vec{L}_{p_j} in a plane (Fig. 7.1 therein) and found that the critical points strongly depend on the angle $2\theta'$ enclosed by both considered \vec{L}_{p_j} . If however the angle starts to decrease from π (i.e. the antiparallel alignment for the power spectrum) the critical point [24, point 1 in Fig. 7.1] starts to degenerate and moves into both directions of the z -axis [24, points 4 in Fig. 7.1]. Thus, our integration method, a saddle-point approximation around the origin, will simply *miss* the critical point leading to invalid results.

It is precisely this property of the system which hinders progress in the evaluation of the terms we needed to evaluate for the four-point correlation function: This function depends, in our notation, on the three shift vectors $\vec{L}_{q_{1,2,3}}$ which add to zero. Recalling that for the case of the power spectrum $\vec{L}_{p_i} = g_{qp}(t, 0) \vec{L}_{q_i}$

holds, we can see that for every possible configuration at least one of the angles enclosed by the $\vec{L}_{p_{1,2,3}}$ will be much smaller than π . Thus, in a convolution integral as encountered in terms (IV) to (VII) the angles will force the critical points of integration to degenerate and move on the z -axis away from our integration origin. In effect, we cannot yet evaluate the integral.

Although this proves that we were not able to evaluate those terms in the scope of this thesis we want to mention that there are promising approaches to fix the problem of integrating terms just like this by bypassing the obstacle with help of the Faddeeva function.

8.3 FINDING AN APPROXIMATION

Having failed in evaluating the four point function from KFT we again turn to [22] for at least an approximation of the uncertainty. The approach of this paper is to use the estimators developed earlier (presented in chapter 7) and derive their variance, originating in the derivation of the shear power spectrum from a discrete set of data instead of a continuous shear field.

We start by calculating the covariance:

$$\text{Cov}(C_{\bar{\ell}}; \bar{\ell}, \bar{\ell}') = \langle C_{\bar{\ell}} C_{\bar{\ell}'} \rangle - C_{\bar{\ell}} C_{\bar{\ell}'}, \quad (8.14)$$

and, as before, especially the first part of the right-hand side. We investigate with the estimators 7.20 inserted,

$$\begin{aligned} \langle \hat{C}_{\bar{\ell}} \hat{C}_{\bar{\ell}'} \rangle &= \int_{A_R(\bar{\ell})} \frac{d\bar{\ell}}{\bar{n}^2 A A_R(\bar{\ell})} \int_{A_R(\bar{\ell}')} \frac{d\bar{\ell}'}{\bar{n}^2 A A_R(\bar{\ell}')} \\ &\quad \left\langle \left| \tilde{\epsilon}_1(\bar{\ell}) \cos(2\beta) + \tilde{\epsilon}_2(\bar{\ell}) \sin(2\beta) \right|^2 \right. \\ &\quad \cdot \left. \left| \tilde{\epsilon}_1(\bar{\ell}') \cos(2\beta') + \tilde{\epsilon}_2(\bar{\ell}') \sin(2\beta') \right|^2 \right\rangle \\ &\quad - \frac{\sigma_\epsilon^2}{2\bar{n}} \left\{ \int_{A_R(\bar{\ell})} \frac{d\bar{\ell}}{\bar{n}^2 A A_R(\bar{\ell})} \left\langle \left| \tilde{\epsilon}_1(\bar{\ell}) \cos(2\beta) + \tilde{\epsilon}_2(\bar{\ell}) \sin(2\beta) \right|^2 \right\rangle \right. \\ &\quad \left. + \int_{A_R(\bar{\ell}')} \frac{d\bar{\ell}'}{\bar{n}^2 A A_R(\bar{\ell}')} \left\langle \left| \tilde{\epsilon}_1(\bar{\ell}') \cos(2\beta') + \tilde{\epsilon}_2(\bar{\ell}') \sin(2\beta') \right|^2 \right\rangle \right\} \\ &\quad + \frac{\sigma_\epsilon^4}{4\bar{n}^2}. \end{aligned} \quad (8.15)$$

If we evaluate the first correlator we will again find four-point correlators. [22] argues that these can be expanded into a sum

of products of two-point correlators for a Gaussian field. They justify the assumption of Gaussian statistics for very large scales, i.e. for a analysis of a field large enough for nonlinear peaks not to play a significant part for the shear estimation. We will for our estimate follow this path keeping in mind that for this approximation we relinquish nonlinear and non Gaussian influences. Ignoring nonlinear effects of course is a painful loss, considering that a central beauty of KFT - and therefore our model-independent power spectrum - is the investigation of nonlinear structure. As we need large scales for the estimation of the weak-lensing signal ([25] uses 100 and 200 galaxies, distributed over a range of several arcminutes), however, this approximation does seem justified.

We now consider the second term:

$$\int_{A_R(\vec{\ell})} \frac{d\vec{\ell}}{\bar{n}^2 A A_R(\vec{\ell})} \left\langle \left| \tilde{\epsilon}_1(\vec{\ell}) \cos(2\beta) + \tilde{\epsilon}_2(\vec{\ell}) \sin(2\beta) \right|^2 \right\rangle, \quad (8.16)$$

and find it to equal

$$C_\ell + \frac{\sigma_\epsilon^2}{2\bar{n}}. \quad (8.17)$$

The same statement holds for the third term when replacing every ℓ by a ℓ' . We then turn to the evaluation of the many four-point correlators appearing in 8.15 after expanding them into the sum of products of two-point correlators. With:

$$\tilde{\epsilon}_\alpha(\vec{\ell}) \approx \bar{n} \gamma_\alpha(\vec{\ell}) + \sum_i \epsilon_{\alpha,i}^s \exp(i\ell\theta_i), \quad (8.18)$$

we find that we can write the correlators as:

$$\begin{aligned} \langle \tilde{\epsilon}_\alpha(\vec{\ell}) \tilde{\epsilon}_\beta(\vec{\ell}') \rangle &= \bar{n}^2 \langle \tilde{\gamma}_\alpha(\vec{\ell}) \tilde{\gamma}_\beta(\vec{\ell}') \rangle \\ &+ \sum_{ij} \langle \epsilon_{\alpha,i}^s \epsilon_{\beta,j}^s \exp(i(\vec{\ell}\vec{\theta}_i - \vec{\ell}'\vec{\theta}_j)) \rangle \\ &= \bar{n}^2 \langle \tilde{\gamma}_\alpha(\vec{\ell}) \tilde{\gamma}_\beta(\vec{\ell}') \rangle \\ &+ \delta_{\alpha\beta} \frac{\sigma_\epsilon^2}{2} \left(\sum_i \exp(i\vec{\theta}_i(\vec{\ell} - \vec{\ell}')) \right), \end{aligned} \quad (8.19)$$

when we recall and apply the definition of the ellipticity dispersion σ_ϵ and assume again that shear and intrinsic ellipticities are not correlated. We furthermore see that:

$$\begin{aligned} \tilde{n}(\vec{\ell}) &= \int d\vec{\theta} \exp(i\vec{\ell}\vec{\theta}) \sum_i \delta_D(\theta - \theta_i) \\ &= \sum_i \exp(i\vec{\ell}\vec{\theta}_i) \end{aligned} \quad (8.20)$$

and:

$$\tilde{n}(\vec{\ell} - \vec{\ell}') = (2\pi)^2 \tilde{n} \delta_D(\vec{\ell} - \vec{\ell}'), \quad (8.21)$$

finding:

$$\langle \tilde{\epsilon}_\alpha(\vec{\ell}) \tilde{\epsilon}_\beta(\vec{\ell}') \rangle = \tilde{n}^2 \langle \tilde{\gamma}_\alpha(\vec{\ell}) \tilde{\gamma}_\beta(\vec{\ell}') \rangle + \delta_{\alpha\beta} \frac{\sigma_\epsilon^2}{2} (2\pi)^2 \tilde{n} \delta_D(\vec{\ell} - \vec{\ell}'). \quad (8.22)$$

We use the relations of $\tilde{\gamma}$ and $\tilde{\kappa}$ to calculate the final form of the correlator:

$$\begin{aligned} \langle \hat{C}_{\vec{\ell}} \hat{C}_{\vec{\ell}'} \rangle &= \int_{A_R(\vec{\ell})} \int_{A_R(\vec{\ell}')} \frac{d\vec{\ell} d\vec{\ell}'}{\tilde{n}^4 A^2 A_R(\vec{\ell}) A_R(\vec{\ell}')} \{ \mathcal{A} + \mathcal{B} + \mathcal{C} \} \\ &\quad - \frac{\sigma_\epsilon^2}{2\tilde{n}} (C_{\vec{\ell}} + C_{\vec{\ell}'}) - \frac{\sigma_\epsilon^4}{4\tilde{n}^2} \end{aligned} \quad (8.23)$$

with the term \mathcal{A} being the *cosmic covariance*, which is a consequence of the field being of finite extent, given as:

$$\mathcal{A} = \tilde{n}^4 \left(A^2 C_\ell C_{\ell'} + 2\delta_D(\vec{\ell} - \vec{\ell}') A (2\pi)^2 C_\ell^2 \right). \quad (8.24)$$

The term \mathcal{C} is *shot noise* from the intrinsic ellipticity dispersion:

$$\mathcal{C} = \frac{\sigma_\epsilon^4}{4} (2\pi)^4 \tilde{n}^2 \left(\frac{A^2}{(2\pi)^4} + 2\delta_D(\vec{\ell} - \vec{\ell}') \frac{A}{(2\pi)^2} \right), \quad (8.25)$$

and the \mathcal{B} is a mix of both:

$$\mathcal{B} = \frac{\sigma_\epsilon^2}{2} (2\pi)^2 \tilde{n}^3 \left(\frac{A^2}{(2\pi)^2} C_\ell + \frac{A^2}{(2\pi)^2} C_{\ell'} + 4\delta_D(\vec{\ell} - \vec{\ell}') A C_\ell \right). \quad (8.26)$$

Returning to the covariance we finally subtract $C_\ell C_{\ell'}$ and find:

$$\begin{aligned} \text{Cov}(C_{\vec{\ell}}; \vec{\ell}, \vec{\ell}') &= 2(2\pi)^2 A \tilde{n}^2 \int_{A_R(\vec{\ell})} \int_{A_R(\vec{\ell}')} \frac{d\vec{\ell} d\vec{\ell}'}{\tilde{n}^4 A^2 A_R(\vec{\ell}) A_R(\vec{\ell}')} \\ &\quad \delta_D(\vec{\ell} - \vec{\ell}') \left[\tilde{n} C_\ell + \frac{\sigma_\epsilon^2}{2} \right]^2. \end{aligned} \quad (8.27)$$

The Dirac distribution sets $\vec{\ell} = \vec{\ell}'$. Integration leads to:

$$\text{Cov}(C_{\vec{\ell}}; \vec{\ell}, \vec{\ell}') = \frac{4\pi}{A \bar{\ell} \Delta \ell} \left(C_{\vec{\ell}} + \frac{\sigma_\epsilon^2}{2\tilde{n}} \right)^2 \delta_{\vec{\ell}\vec{\ell}'}, \quad (8.28)$$

where $\Delta \ell$ is the thickness of the $\vec{\ell}$ -annulus. With our C_ℓ from chapter 6 we can use real-survey parameters and give a realistic estimate of our power spectrum and its uncertainty. We shall do so in Fig. 8.1 where we choose $\Delta \ell = 100$ and σ_E, A and \tilde{n} to be from the Canada-France-Hawaii Telescope (CFHT) survey.

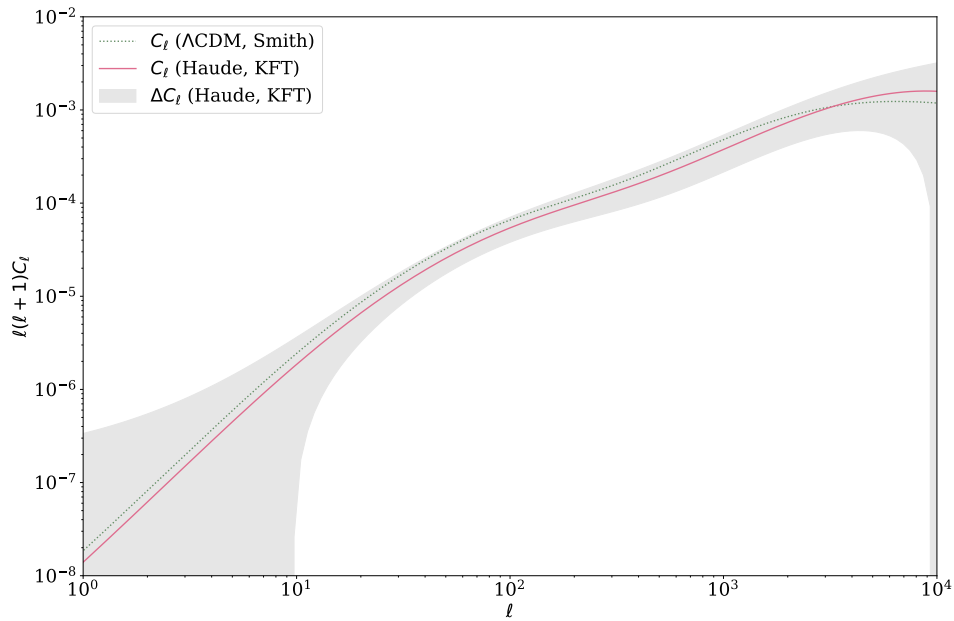


Figure 8.1: The model-independent weak lensing power spectrum and its uncertainty according to Joachimi, Schneider, and Eifler [22] and eq. 8.28. We furthermore showed the same comparison as in Fig. 6.6. Judging from this estimate of the signal's uncertainty it will not be possible to use a CFHT-like survey to determine the power spectrum more accurately.

CONCLUSION

In this thesis we calculated a model-independent angular weak lensing power spectrum. To achieve this we replaced the cosmological model by a set of functions, the expansion function $E(a)$ and the linear growth factor $D_+(a)$, which were derived from observational data only using the method of [21]. Furthermore, we used a parameter-free analytic expression for the cosmic matter density power spectrum P_δ obtained from the Kinetic Field Theory instead of a modelled or a numerically simulated power spectrum.

Both changes yielded an expression for the power spectrum which depended on three remaining parameters only: The speed of light c , the Hubble parameter h and the present-day matter density parameter Ω_{m0} . All of them have been measured to great accuracy by various surveys.

Hence, we extended the wide range of Kinetic Field Theory applications by an application in gravitational lensing adding its key statistical quantity. The lensing effect has been well-tested and measured in various existing surveys. More large-scale surveys are planned and scheduled (e.g. [1]) and the angular power spectrum is investigated with numerical simulations. This allows for another possible source of verification and calibration of our theoretical predictions and measurement effects.

In a second step, we used Kinetic Field Theory in order to calculate an analytical expression for the variance of the power spectrum signal calculated before. We therefore calculated the four-point function of cosmic density with Kinetic Field Theory, but were not able to evaluate this expression numerically.

Looking for another possibility to obtain an estimate of the signal's uncertainty, we found an approximation by ignoring non Gaussian contributions to the shear field which allowed us to expand the four-point functions into a sum of products of two-point correlators. Hence, we were able to express the uncertainty in terms of the weak lensing spectrum and the geometrical parameters of the survey considered.

Having calculated both a fully model-independent power spectrum and a rough estimate of its uncertainty we outlined another possibility for a reliable test of the Kinetic Field Theory using real-world measurement data from upcoming lensing surveys

for comparison. This allows for further improvements of the theories tested, especially since we eliminated further sources of possible errors by replacing influences of particular cosmological models by introducing model-independent cosmology.

We were able to compare the lensing power spectrum from Kinetic Field Theory with its respective counterpart from numerical simulations. We found good accordance of our results, the model-independent weak lensing spectrum, with classically obtained results. While the numeric values of the spectrum showed a clear discrepancy of up to 20 percent, the general shape and order of magnitude of the lensing spectra agreed quite well. This confirms, that Kinetic Field Theory, combined with model-independent cosmology can be a strong tool in order to better understand cosmic structure formation and to calculate central quantities.

We want our results to be pathfinders, integrating the lensing formalism into the framework of Kinetic Field Theory and thus inventing a new instance for a verification of the still rather young, but all the more promising theory.

This finally might lead to new insights about the evolution of the universe, its constituents and cosmic structure – and finally even hint at the nature of the cosmic dark sector.

O.A.M.D.G

Beati pauperes spiritu, quoniam
ipsorum est regnum caelorum.

— [31, Mt 5:3]

GRATIAS AGO

Zuvörderst ist es mir ein Bedürfnis, Matthias Bartelmann ein herzliches *Vergelt's Gott* zu sagen, der mir in den letzten Jahren eine so herausragende Betreuung angedeihen ließ, wie sie manchenorts Neid hervorrufen könnte. Seine Zuversicht, sein Vertrauen in meine Fähigkeiten und besonders seine ansteckende Begeisterung für das Ideal von Bildung und Wissenschaft war inspirierend und über meine Arbeit hinaus bereichernd und wurde mir zum Vorbild.

Für zahlreiche, im Wortsinne erleuchtende Gespräche über oft übersehene Zusammenhänge und die Schönheit des Details – sowie für einen Austausch auf Augenhöhe über schwäbische Sprache und Küche danke ich von Herzen Björn Malte Schäfer.

Auch den anderen Kollegen im Institut, im Besonderen jedoch meinen Bürokollegen Sara Konrad, Carsten Littek und Lukas Heizmann sei an dieser Stelle gedankt. Insbesondere den Letztgenannten verdanke ich nicht nur viel von der Freude, die ich in den Jahren an meinem Arbeitsplatz hatte, sondern auch die geradezu frivole Begeisterung an *knuspriger Kruste*. Den zahlreichen Helfern an der Universität, allen voran Anna Zacheus, danke ich für die zuverlässige und engagierte Hilfe, der *Stiftung der deutschen Wirtschaft* und dort besonders Frau Kilian für die mehr als acht Jahre Unterstützung in Studien- und Promotionsförderung.

Auch jenseits der kosmologischen Sphären gilt es, dankbar zu sein: Meinen Eltern, die mir seit Anbeginn meiner Zeit einen bedingungslosen Großmut in fast allen Belangen menschlichen Daseins zuteil werden lassen – Teresa für alles, besonders jedoch für ihre gnadenlose Geduld – Meinem Firmpaten Fabrizio Campanile für Rat und Unterstützung in mannigfaltiger Form – Meinem besten Freund Steffen für die verlässliche Erdung im Angesicht drohender Höhenflüge – Dem Konvent der Abtei St. Martin in Disentis für ihre großzügige Gastfreundschaft, Abt Winfried sowie Sebastian Feuerstein für die geistige und geistliche Begleitung – Raphaël und Sabrina Sgier für einen ironisch-kollegialen Blick auf das gemeinsame wissenschaftliche Treiben – Veronika Pfeiffer und Simon Dümpelmann für die wirklich schönen Stunden in einer fremden Stadt – und schließlich meinen Zürcher Lebensfreunden für den stets warmen Empfang in der alten Studienheimat.

BIBLIOGRAPHY

- [1] Luca Amendola et al. “Cosmology and Fundamental Physics with the Euclid Satellite.” In: *Living Reviews in Relativity* 16.1, 6 (Sept. 2013), p. 6. DOI: [10.12942/lrr-2013-6](https://doi.org/10.12942/lrr-2013-6). arXiv: [1206.1225](https://arxiv.org/abs/1206.1225) [[astro-ph.CO](#)].
- [2] David J. Bacon, Alexandre R. Refregier, and Richard S. Ellis. “Detection of weak gravitational lensing by large-scale structure.” In: *MNRAS* 318.2 (Oct. 2000), pp. 625–640. DOI: [10.1046/j.1365-8711.2000.03851.x](https://doi.org/10.1046/j.1365-8711.2000.03851.x). arXiv: [astro-ph/0003008](https://arxiv.org/abs/astro-ph/0003008) [[astro-ph](#)].
- [3] J. M. Bardeen, J. R. Bond, N. Kaiser, and A. S. Szalay. “The Statistics of Peaks of Gaussian Random Fields.” In: *ApJ* 304 (May 1986), p. 15. DOI: [10.1086/164143](https://doi.org/10.1086/164143).
- [4] Matthias Bartelmann. “Topical Review: Gravitational lensing.” In: *Classical and Quantum Gravity* 27.23, 233001 (Dec. 2010), p. 233001. DOI: [10.1088/0264-9381/27/23/233001](https://doi.org/10.1088/0264-9381/27/23/233001). arXiv: [1010.3829](https://arxiv.org/abs/1010.3829) [[astro-ph.CO](#)].
- [5] Matthias Bartelmann. “Trajectories of point particles in cosmology and the Zel’dovich approximation.” In: *Phys. Rev. D* 91.8 (2015), p. 083524. DOI: [10.1103/PhysRevD.91.083524](https://doi.org/10.1103/PhysRevD.91.083524). arXiv: [1411.0805](https://arxiv.org/abs/1411.0805) [[gr-qc](#)].
- [6] Matthias Bartelmann. *Das kosmologische Standardmodell*. 2019. DOI: [10.1007/978-3-662-59627-2](https://doi.org/10.1007/978-3-662-59627-2).
- [7] Matthias Bartelmann, Johannes Dombrowski, Sara Konrad, Elena Kozlikin, Robert Lilow, Carsten Littek, Christophe Pixius, and Felix Fabis. “Kinetic field theory: Non-linear cosmic power spectra in the mean-field approximation.” In: *arXiv e-prints*, arXiv:2011.04979 (Nov. 2020), arXiv:2011.04979. arXiv: [2011.04979](https://arxiv.org/abs/2011.04979) [[astro-ph.CO](#)].
- [8] Matthias Bartelmann, Felix Fabis, Daniel Berg, Elena Kozlikin, Robert Lilow, and Celia Viermann. “A microscopic, non-equilibrium, statistical field theory for cosmic structure formation.” In: *New Journal of Physics* 18.4, 043020 (Apr. 2016), p. 043020. DOI: [10.1088/1367-2630/18/4/043020](https://doi.org/10.1088/1367-2630/18/4/043020). arXiv: [1411.0806](https://arxiv.org/abs/1411.0806) [[cond-mat.stat-mech](#)].

- [9] Matthias Bartelmann, Felix Fabis, Sara Konrad, Elena Kozlikin, Robert Lilow, Carsten Littek, and Johannes Dombrowski. “Analytic calculation of the non-linear cosmic density-fluctuation power spectrum in the Born approximation.” In: *arXiv e-prints*, arXiv:1710.07522 (Oct. 2017), arXiv:1710.07522. arXiv: [1710.07522 \[astro-ph.CO\]](#).
- [10] Matthias Bartelmann, Felix Fabis, Elena Kozlikin, Robert Lilow, Johannes Dombrowski, and Julius Mildenerger. “Kinetic field theory: effects of momentum correlations on the cosmic density-fluctuation power spectrum.” In: *New Journal of Physics* 19.8, 083001 (Aug. 2017), p. 083001. DOI: [10.1088/1367-2630/aa7e6f](#). arXiv: [1611.09503 \[astro-ph.CO\]](#).
- [11] Matthias Bartelmann, Elena Kozlikin, Robert Lilow, Carsten Littek, Felix Fabis, Ivan Kostyuk, Celia Viermann, Lavinia Heisenberg, Sara Konrad, and Daniel Geiss. “Cosmic Structure Formation with Kinetic Field Theory.” In: *Annalen der Physik* 531.11 (Nov. 2019), p. 1800446. DOI: [10.1002/andp.201800446](#). arXiv: [1905.01179 \[astro-ph.CO\]](#).
- [12] E. Bertin and S. Arnouts. “SExtractor: Software for source extraction.” In: *A&AS* 117 (June 1996), pp. 393–404. DOI: [10.1051/aas:1996164](#).
- [13] Claudio Bruderer, Chihway Chang, Alexandre Refregier, Adam Amara, Joel Bergé, and Lukas Gamper. “Calibrated Ultra Fast Image Simulations for the Dark Energy Survey.” en. In: *The Astrophysical Journal* 817.1 (Jan. 2016), p. 25. ISSN: 1538-4357. DOI: [10.3847/0004-637X/817/1/25](#). URL: <http://stacks.iop.org/0004-637X/817/i=1/a=25?key=crossref.4e020e7445b6de712c04e93e0252e59a> (visited on 12/06/2019).
- [14] Claudio Bruderer, Andrina Nicola, Adam Amara, Alexandre Refregier, Jörg Herbel, and Tomasz Kacprzak. “Cosmic shear calibration with forward modeling.” en. In: *Journal of Cosmology and Astroparticle Physics* 2018.08 (Aug. 2018). arXiv: 1707.06233, pp. 007–007. ISSN: 1475-7516. DOI: [10.1088/1475-7516/2018/08/007](#). URL: <http://arxiv.org/abs/1707.06233> (visited on 04/29/2020).
- [15] Claudio Bruderer, Justin I. Read, Jonathan P. Coles, Dominik Leier, Emilio E. Falco, Ignacio Ferreras, and Prasenjit Saha. “Light versus dark in strong-lens galaxies: dark matter haloes that are rounder than their stars.” In: *MN-*

- RAS 456.1 (Feb. 2016), pp. 870–884. DOI: [10.1093/mnras/stv2582](https://doi.org/10.1093/mnras/stv2582). arXiv: [1511.01097](https://arxiv.org/abs/1511.01097) [astro-ph.GA].
- [16] Richard Courant and David Hilbert. *Methoden der mathematischen Physik*. 1924. ISBN: 978-3-642-96050-5. DOI: [10.1007/978-3-642-96050-5](https://doi.org/10.1007/978-3-642-96050-5).
- [17] Scott Dodelson. *Modern cosmology*. 2003.
- [18] F. W. Dyson, A. S. Eddington, and C. Davidson. “A Determination of the Deflection of Light by the Sun’s Gravitational Field, from Observations Made at the Total Eclipse of May 29, 1919.” In: *Philosophical Transactions of the Royal Society of London Series A* 220 (Jan. 1920), pp. 291–333. DOI: [10.1098/rsta.1920.0009](https://doi.org/10.1098/rsta.1920.0009).
- [19] Albert Einstein. “Die Feldgleichungen der Gravitation.” In: *Sitzungsberichte der Königlich Preußischen Akademie der Wissenschaften (Berlin)* (Jan. 1915), pp. 844–847.
- [20] Felix Fabis, Elena Kozlikin, Robert Lilow, and Matthias Bartelmann. “Kinetic field theory: exact free evolution of Gaussian phase-space correlations.” In: *Journal of Statistical Mechanics: Theory and Experiment* 4.4 (Apr. 2018), p. 043214. DOI: [10.1088/1742-5468/aab850](https://doi.org/10.1088/1742-5468/aab850). arXiv: [1710.01611](https://arxiv.org/abs/1710.01611) [cond-mat.stat-mech].
- [21] Sophia Haude, Shabnam Salehi, Sofía Vidal, Matteo Maturi, and Matthias Bartelmann. “Model-Independent Determination of the Cosmic Growth Factor.” In: *arXiv e-prints*, arXiv:1912.04560 (Dec. 2019), arXiv:1912.04560. arXiv: [1912.04560](https://arxiv.org/abs/1912.04560) [astro-ph.CO].
- [22] B. Joachimi, P. Schneider, and T. Eifler. “Analysis of two-point statistics of cosmic shear. III. Covariances of shear measures made easy.” In: *A&A* 477.1 (Jan. 2008), pp. 43–54. DOI: [10.1051/0004-6361:20078400](https://doi.org/10.1051/0004-6361:20078400). arXiv: [0708.0387](https://arxiv.org/abs/0708.0387) [astro-ph].
- [23] Nick Kaiser, Gillian Wilson, and Gerard A. Luppino. “Large-Scale Cosmic Shear Measurements.” In: *arXiv e-prints*, astro-ph/0003338 (Mar. 2000), astro-ph/0003338. arXiv: [astro-ph/0003338](https://arxiv.org/abs/astro-ph/0003338) [astro-ph].
- [24] Sara Konrad M.Sc. “Cosmic structure formation in the limit of small scales within Kinetic Field Theory.” Dissertation. Ruprecht-Karls-Universität Heidelberg, 2020.

- [25] Felix Arjun Kuhn, Claudio Bruderer, Simon Birrer, Adam Amara, and Alexandre Réfrégier. “Combining strong and weak lensing estimates in the Cosmos field.” In: *arXiv e-prints*, arXiv:2010.08680 (Oct. 2020), arXiv:2010.08680. arXiv: [2010.08680](https://arxiv.org/abs/2010.08680) [[astro-ph.CO](https://arxiv.org/abs/2010.08680)].
- [26] E Macaulay et al. “First cosmological results using Type Ia supernovae from the Dark Energy Survey: measurement of the Hubble constant.” In: *Monthly Notes of the RAS* 486.2 (Apr. 2019), pp. 2184–2196. ISSN: 0035-8711. DOI: [10.1093/mnras/stz978](https://doi.org/10.1093/mnras/stz978). eprint: <https://academic.oup.com/mnras/article-pdf/486/2/2184/28488227/stz978.pdf>. URL: <https://doi.org/10.1093/mnras/stz978>.
- [27] C. Mignone and M. Bartelmann. “Model-independent determination of the cosmic expansion rate. I. Application to type-Ia supernovae.” In: *A&A* 481.2 (Apr. 2008), pp. 295–303. DOI: [10.1051/0004-6361:20078983](https://doi.org/10.1051/0004-6361:20078983). arXiv: [0711.0370](https://arxiv.org/abs/0711.0370) [[astro-ph](https://arxiv.org/abs/0711.0370)].
- [28] Houjun Mo, Frank C. van den Bosch, and Simon White. *Galaxy Formation and Evolution*. 2010.
- [29] Suvodip Mukherjee, Archisman Ghosh, Matthew J. Graham, Christos Karathanasis, Mansi M. Kasliwal, Ignacio Magaña Hernández, Samaya M. Nissanke, Alessandra Silvestri, and Benjamin D. Wandelt. “First measurement of the Hubble parameter from bright binary black hole GW190521.” In: *arXiv e-prints*, arXiv:2009.14199 (Sept. 2020), arXiv:2009.14199. arXiv: [2009.14199](https://arxiv.org/abs/2009.14199) [[astro-ph.CO](https://arxiv.org/abs/2009.14199)].
- [30] J. Myles et al. “Dark Energy Survey Year 3 Results: Redshift Calibration of the Weak Lensing Source Galaxies.” In: *arXiv e-prints*, arXiv:2012.08566 (Dec. 2020), arXiv:2012.08566. arXiv: [2012.08566](https://arxiv.org/abs/2012.08566) [[astro-ph.CO](https://arxiv.org/abs/2012.08566)].
- [31] Eberhard et Erwin Nestle and Barbara et Kurt Aland, eds. *Novum Testamentum Graece et Latine*. Deutsche Bibelgesellschaft, 1994.
- [32] P. J. E. Peebles. *Principles of Physical Cosmology*. 1993.
- [33] Andrea Petri, Zoltán Haiman, and Morgan May. “Validity of the Born approximation for beyond Gaussian weak lensing observables.” In: *Phys. Rev. D* 95.12, 123503 (June 2017), p. 123503. DOI: [10.1103/PhysRevD.95.123503](https://doi.org/10.1103/PhysRevD.95.123503). arXiv: [1612.00852](https://arxiv.org/abs/1612.00852) [[astro-ph.CO](https://arxiv.org/abs/1612.00852)].

- [34] Planck Collaboration et al. “Planck 2018 results - VI. Cosmological parameters.” In: *A&A* 641 (2020), A6. DOI: [10.1051/0004-6361/201833910](https://doi.org/10.1051/0004-6361/201833910). URL: <https://doi.org/10.1051/0004-6361/201833910>.
- [35] Planck Collaboration et al. “Planck 2018 results. VI. Cosmological parameters.” In: *A&A* 641, A6 (Sept. 2020), A6. DOI: [10.1051/0004-6361/201833910](https://doi.org/10.1051/0004-6361/201833910). arXiv: [1807.06209](https://arxiv.org/abs/1807.06209) [[astro-ph.CO](https://arxiv.org/abs/1807.06209)].
- [36] A. Refregier, L. Gamper, A. Amara, and L. Heisenberg. “PyCosmo: An integrated cosmological Boltzmann solver.” In: *Astronomy and Computing* 25 (Oct. 2018), pp. 38–43. DOI: [10.1016/j.ascom.2018.08.001](https://doi.org/10.1016/j.ascom.2018.08.001). arXiv: [1708.05177](https://arxiv.org/abs/1708.05177) [[astro-ph.CO](https://arxiv.org/abs/1708.05177)].
- [37] Adam G. Riess, Stefano Casertano, Wenlong Yuan, Lucas M. Macri, and Dan Scolnic. “Large Magellanic Cloud Cepheid Standards Provide a 1% Foundation for the Determination of the Hubble Constant and Stronger Evidence for Physics beyond Λ CDM.” In: *The Astrophysical Journal* 876.1 (2019), p. 85. DOI: [10.3847/1538-4357/ab1422](https://doi.org/10.3847/1538-4357/ab1422). URL: <https://doi.org/10.3847/1538-4357/ab1422>.
- [38] Christian F. Schmidt and Matthias Bartelmann. “On the sensitivity of weak gravitational lensing to the cosmic expansion function.” In: *arXiv e-prints*, arXiv:2011.03202 (Nov. 2020), arXiv:2011.03202. arXiv: [2011.03202](https://arxiv.org/abs/2011.03202) [[astro-ph.CO](https://arxiv.org/abs/2011.03202)].
- [39] D. M. Scolnic et al. “The Complete Light-curve Sample of Spectroscopically Confirmed SNe Ia from Pan-STARRS1 and Cosmological Constraints from the Combined Pantheon Sample.” In: *ApJ* 859.2, 101 (June 2018), p. 101. DOI: [10.3847/1538-4357/aab9bb](https://doi.org/10.3847/1538-4357/aab9bb). arXiv: [1710.00845](https://arxiv.org/abs/1710.00845) [[astro-ph.CO](https://arxiv.org/abs/1710.00845)].
- [40] N. Scoville et al. “The Cosmic Evolution Survey (COSMOS): Overview.” In: *ApJS* 172.1 (Sept. 2007), pp. 1–8. DOI: [10.1086/516585](https://doi.org/10.1086/516585). arXiv: [astro-ph/0612305](https://arxiv.org/abs/astro-ph/0612305) [[astro-ph](https://arxiv.org/abs/astro-ph/0612305)].
- [41] R. J. Sgier, A. Réfrégier, A. Amara, and A. Nicola. “Fast generation of covariance matrices for weak lensing.” In: *J. Cosmology Astropart. Phys.* 2019.1, 044 (Jan. 2019), p. 044. DOI: [10.1088/1475-7516/2019/01/044](https://doi.org/10.1088/1475-7516/2019/01/044). arXiv: [1801.05745](https://arxiv.org/abs/1801.05745) [[astro-ph.CO](https://arxiv.org/abs/1801.05745)].

- [42] Raphael Sgier, Janis Fluri, Jörg Herbel, Alexandre Réfrégier, Adam Amara, Tomasz Kacprzak, and Andrina Nicola. “Fast Lightcones for Combined Cosmological Probes.” In: *arXiv e-prints*, arXiv:2007.05735 (July 2020), arXiv:2007.05735. arXiv: [2007.05735 \[astro-ph.CO\]](#).
- [43] Charles Shapiro and Asantha Cooray. “The Born and lens lens corrections to weak gravitational lensing angular power spectra.” In: *J. Cosmology Astropart. Phys.* 2006.3, 007 (Mar. 2006), p. 007. DOI: [10.1088/1475-7516/2006/03/007](#). arXiv: [astro-ph/0601226 \[astro-ph\]](#).
- [44] R. E. Smith, J. A. Peacock, A. Jenkins, S. D. M. White, C. S. Frenk, F. R. Pearce, P. A. Thomas, G. Efstathiou, and H. M. P. Couchman. “Stable clustering, the halo model and non-linear cosmological power spectra.” In: *MNRAS* 341.4 (June 2003), pp. 1311–1332. DOI: [10.1046/j.1365-8711.2003.06503.x](#). arXiv: [astro-ph/0207664 \[astro-ph\]](#).
- [45] Norbert Straumann. *General Relativity*. 2013. ISBN: 978-94-007-5410-2. DOI: [10.1007/978-94-007-5410-2](#).
- [46] L. Van Waerbeke et al. “Detection of correlated galaxy ellipticities from CFHT data: first evidence for gravitational lensing by large-scale structures.” In: *A&A* 358 (June 2000), pp. 30–44. arXiv: [astro-ph/0002500 \[astro-ph\]](#).
- [47] Celia Viermann, Felix Fabis, Elena Kozlikin, Robert Lilow, and Matthias Bartelmann. “Nonequilibrium statistical field theory for classical particles: Basic kinetic theory.” In: *Phys. Rev. E* 91 (6 2015), p. 062120. DOI: [10.1103/PhysRevE.91.062120](#). URL: <https://link.aps.org/doi/10.1103/PhysRevE.91.062120>.
- [48] R. M. Wald. *General relativity*. 1984. DOI: [10.7208/chicago/9780226870373.001.0001](#).
- [49] D. Walsh, R. F. Carswell, and R. J. Weymann. “0957+561 A, B: twin quasistellar objects or gravitational lens?” In: *Nature* 279 (May 1979), pp. 381–384. DOI: [10.1038/279381a0](#).
- [50] David M. Wittman, J. Anthony Tyson, David Kirkman, Ian Dell’Antonio, and Gary Bernstein. “Detection of weak gravitational lensing distortions of distant galaxies by cosmic dark matter at large scales.” In: *Nature* 405.6783 (May 2000), pp. 143–148. DOI: [10.1038/35012001](#). arXiv: [astro-ph/0003014 \[astro-ph\]](#).

- [51] F. Zwicky. "Nebulae as Gravitational Lenses." In: *Phys. Rev.* 51 (4 Feb. 1937), pp. 290–290. DOI: [10.1103/PhysRev.51.290](https://doi.org/10.1103/PhysRev.51.290). URL: <https://link.aps.org/doi/10.1103/PhysRev.51.290>.

